

ABSTRACT

Title of Document: THE NEURAL SUBSTRATES OF
GRAPHOMOTOR SEQUENCE LEARNING.

Bruce A. Swett, PhD 2007

Directed By: Dr. Jose L. Contreras-Vidal, Department of
Kinesiology; Neuroscience and Cognitive
Science and Bioengineering Graduate Programs.

Performing sequences of movements easily and automatically is an integral part of our everyday lives. This dissertation examines how a set of individual movements are assembled into a movement sequence, focusing on the neural regions involved, and the timing of their participation. A second, related question is whether the order of encoding of the individual movements can be detected with kinematic and neuroimaging methods. Understanding how sequences are learned is important for expanding our knowledge of how the brain performs neural computations within healthy persons, and of the alterations of these processes in persons with neurological disorders.

To examine these questions, we combined behavioral, kinematic and neuroimaging methods to examine motor sequence learning in healthy adults. The behavioral task involved subjects learning to copy a novel sequence of line-pairs (a graphomotor trajectory sequence learning paradigm) while blood oxygen level dependent (BOLD) functional magnetic resonance imaging (fMRI) data were simultaneously acquired. This task required the subjects to assemble three sets of line-pairs into a sequence; real-time visual feedback for error correction was provided during production of each line-pair, and subjects were also provided with knowledge of results (their speed and accuracy) after each sequence of line-pairs. Normalized jerk (a kinematic measure of movement smoothness, computed off-line), movement speed and accuracy were used to assess ongoing changes in task performance during the scanning session. The learning curve derived from the normalized jerk scores were used to define five time-bins for analysis of the functional neuroimaging data. Differences in the patterns of BOLD activation during these times were used to characterize the relationship between neural activity and the phases of sequence learning (temporal dynamics). Furthermore, covariance of BOLD responses in selected neural regions, on a per-bin basis, was used to examine the dynamic evolution of functional connectivity between regions during graphomotor sequence learning. Finally, the neural correlates of serial line-pair encoding were evaluated by comparing BOLD responses in candidate brain areas and kinematic measures of learning (normalized jerk and movement time).

Sequence learning, measured by normalized jerk, was best characterized by a curve with a double exponential fit, implying that an early, fast learning process (time-bins 1-2) merged with a slower learning process (bins 3-5). During early learning, the dorsal (superior parietal lobule) and ventral (fusiform gyrus) visual streams, and the dorsal lateral premotor areas were activated (relative to baseline). The inferior parietal lobule was also activated.

An unexpected finding was that portions of the basal ganglia (head of caudate nucleus, anterior putamen) and cerebellum (anterior vermis; dentate nucleus) were deactivated during early learning, relative to baseline. Moreover, the medial prefrontal cortex was activated in bins 1 and 2. In the early portion of the second, slower learning process (bin 3), the dorsal visual stream areas became less active; dorsal lateral premotor cortex activation persisted; and the anterior putamen, head of caudate nucleus and posterior vermis became active for the first time. Ventral visual stream (fusiform gyrus) activation persisted.

In bin 4, activation of the anterior vermis and dentate nucleus continued, along with persisting activation in the posterior vermis. The somatosensory cortex in the hand area became significantly activated in bin 4 only, relative to baseline. In the final time-bin (bin 5), when the subjects reached a plateau in performance, the spatial extent of the anterior putamen and head of the caudate nucleus was reduced, but the anterior vermis increased in activity. Dorsal visual stream activity was significantly lower than baseline, as was activity in the ventral visual stream regions, dorsal lateral

premotor cortex, and inferior parietal lobule. During early learning (bins 1-2), the medial prefrontal cortex was activated; but by the late time-bins (bins 4-5), this region became deactivated, relative to baseline. Limbic regions showed the reverse pattern: they were deactivated in bins 1-2; but became active in bins 4-5.

Covariance analysis (measuring associations between BOLD responses in a selected voxel and all other brain regions) showed positive correlations between activity in primary motor cortex and the anterior, middle, and posterior putamen, and the head of the caudate nucleus. These correlations were manifest during early learning (bin 2) and persisted throughout the late portion of the second learning process (bin 5). Activity in the superior parietal lobule was negatively correlated with activity in the anterior, middle, and posterior putamen, and the head of the caudate nucleus only during early sequence learning (bin 1). These regions were functionally uncoupled during bins 2-5.

Kinematic analysis of the line-pairs showed that the third line-pair was produced more quickly and smoothly than line-pairs 1 and 2. In addition, a greater reduction in normalized jerk and movement time was evident in line-pair 3 than for line-pairs 1 and 2. Significant effects for line-pair, bin and the interaction of line-pair x bin were found for movement time; significant effects for line-pair and the interaction of line-pair x bin, but not bin were found for normalized jerk.

The early portion of the sequence learning process was characterized by dorsal and ventral visual stream activation; dorsal lateral premotor cortical activity; and deactivation of the anterior putamen, head of the caudate nucleus and posterior vermis. This pattern of neural activity in early learning may indicate a relative predominance of visuomotor mapping of the novel sequences. The activation of regions within the ventral visual pathway may indicate either attempts to identify the ideographic characters, or more likely, the classification of the characters as visual objects. The dorsal visual stream areas are involved in visually-guided reaching, and the location of the visual targets and pen position in the work space. The deactivation of portions of the basal ganglia and cerebellum during the early phase of sequence learning may indicate that these regions were being reset, due to the high number of errors being produced.

In the beginning of the second, slower learning process, several changes occurred: the dorsal visual stream areas became less active; the left dorsal premotor cortex activation persisted; and the anterior putamen, head of the caudate nucleus and posterior vermis became active. This pattern of neural activity in the beginning of the second, slower phase of sequence learning suggests that emphasis in the sequence learning process had shifted from visuomotor mapping to improving the kinematic and dynamic motor plans for the new sequences (sequence encoding).

In the final time bin, when the subjects had reached a plateau in performance, the anterior putamen and head of caudate nucleus became less active, but the anterior

vermis increased in activity. This dissociation between activity in specific cerebellar and basal ganglia regions may indicate two distinct learning processes within the latter portion of the second phase of sequence learning. The first may be the encoding of the characters (anterior putamen, head of caudate nucleus), using knowledge of results; the second may involve the improvement of the individual movements and encoding of the line-pairs (anterior vermis), using error feedback correction.

Interestingly, the medial regions involved in the “default mode network” (which have been typically reported as being more active during rest, and deactivated during performance of cognitive or motor tasks) did not become deactivated until later in the task (bins 4-5), but –at least in the case of the medial premotor cortex – were unexpectedly *activated* during early learning, when task demands may be greatest.

The functional connectivity analysis provides an important, alternate method of examining the fMRI data, complementary to the standard contrast methods. These analyses demonstrate, for example that some neural regions (such as the basal ganglia) participate in sequence learning prior to reaching significant levels of activity when compared to baseline.

The significant effects of line-pair in both movement time and normalized jerk indicate that differential effects of sequence order can be detected in the kinematic measures.

Taken together, a model of graphomotor sequence learning emerges, including patterns of neural activation and functional connectivity that correspond to changes in subject performance. This model adds to our current understanding of the neural substrates of graphomotor sequence learning, and may be important in explaining the alterations to these networks in persons with neurodegenerative disorders.

THE NEURAL SUBSTRATES OF GRAPHOMOTOR SEQUENCE LEARNING

By

Bruce A. Swett

Dissertation submitted to the Faculty of the Graduate School of the
University of Maryland, College Park, in partial fulfillment
of the requirements for the degree of
Doctor of Philosophy
2007

Advisory Committee:

Dr. Jose L. Contreras-Vidal, Chair
Dr. Allen Braun, Co-Chair
Dr. Brad Hatfield
Dr. Todd Troyer
Dr. David Poeppel, Dean's Representative

© Copyright by
Bruce A. Swett
2007

Dedication

This dissertation is dedicated to Laura, Christina and Katherine.

Acknowledgements

My deepest thanks go to Jose L. Contreras-Vidal, Allen Braun, Rasmus Birn, Gang Chen, Avis Cohen, Todd Troyer, Brad Hatfield, Feng Rong, Jed Meltzer, Walter Carr, Trent Bradberry, Joe McArdle, Rene Hill, Jeanette Black, Jane Clark, Richard Payne, John Jeka, Sandy Davis, the AFNI team, and the study's participants.

Table of Contents

Dedication.....	i
Acknowledgements.....	ii
Table of Contents.....	iii
List of Tables	vi
List of Figures.....	vii
List of Abbreviations	xviii
Chapter 1: Introduction.....	1
Background and Significance of Sequence Learning	1
Chapter 2: Prior Research on Motor Sequence Learning	6
Neural structures related to visually-guided limb movements	6
Neural structures related to motor sequence learning.....	7
Neurophysiology of motor sequence learning	8
Structural neuroimaging and motor sequence learning in humans.....	10
Functional neuroimaging of motor sequence learning.....	11
Positron Emission Tomography.....	11
Functional Magnetic Resonance Imaging.....	13
Theories of motor sequence learning.....	16
Summary of gaps in our current understanding of motor sequence learning	19
Description of the two current research studies.....	20
Chapter 3: The Neural Substrates of Graphomotor Sequence Learning.....	23
Introduction.....	23
Task analysis of ideographic graphomotor sequence learning task.....	27

Methods.....	32
Subjects.....	34
Procedures.....	35
Data Analysis.....	37
Results.....	41
Discussion.....	51
Chapter 4: Encoding of Graphomotor Sequences.....	59
Introduction.....	59
Research questions.....	61
Methods.....	64
Subjects.....	64
Behavioral task.....	64
Data collection.....	65
Data analysis.....	66
Results.....	68
Discussion.....	70
Order of Encoding of Graphomotor Sequences.....	71
Chapter 5: Conclusions.....	72
Summary of findings.....	72
A model of graphomotor sequence learning.....	73
Functional connectivity and motor sequence learning.....	75
Neural encoding of elements of motor sequences.....	75
Limitations.....	76

Tables.....	81
Figures.....	85
Appendices.....	132
APPENDIX A: Preliminary Experiments.....	133
Bibliography	148

List of Tables

Table 1 Selected Research on Regions of Interest Related to Motor Sequence Learning (p. 82)

Table 2 Regions of Interest with Location, and Percent Signal Change (p. 83)

List of Figures

Figure 1 Frontal-parietal network for reaching (per Bernod, 1999). A. Retinal information (dark blue) represents information about the hand and target location as the monkey moves his hand to the target. Gaze information (light blue) contains information about the direction and movement of eye position (gaze). Arm and hand position and direction are represented in the green. Muscle commands and proprioceptive feedback of arm dynamics. B. The distribution of tuned neuron populations forms a visual to somatic gradient along the parietal to frontal axis. The overlapping regions of tuned neurons create functional domains that combine and distribute signals (page 86)

Figure 2 Multiple, cortico-basal ganglia loops (per Alexander, 1986) (page 87)

Figure 3 Multiple cerebellar output channels from the dentate project to diverse cortical regions, which connect to the same cerebellar area (Middleton and Strick, 1998) (page 88)

Figure 4 Activity of a pre-supplementary motor neuron in monkey during the waiting period before the performance of an incorrect (top) and correct (bottom) sequence of movements (Tanji, et al., 2001) (page 89)

Figure 5 Axonal tract tracing from the cortex to the striatum (modified from Lehericy, et al., 2004) (page 90)

Figure 6 Cortical regions activated during the learning of a graphomotor trajectory sequence under different performance conditions (Seitz, et al., 1997) (page 91)

Figure 7 Cortical regions activated during the learning of a finger movement sequence in the third vs. second learning blocks (adapted from Penhume & Doyon, 2005) (page 92)

Figure 8 Changes in cerebellar activation during the learning of a sequence of finger movements (Doyon & Benali, 2005) (page 93)

Figure 9 Comparison of activations in early vs. late learning, using a modified (explicit) serial reaction time task (Müller, et al., 2002) (page 94)

Figure 10 Hikosaka, et al. model of motor sequence learning (Hikosaka, et al., 2002) (page 95)

Figure 11 Task analysis of the Chinese character sequence learning task: presentation of the target template for first line-pair (A); visuomotor mapping (B); kinematic planning (C); scaling the speed of the motor plan (D); kinematic to dynamic transformation (E); movement execution (F); computation of speed and accuracy

errors (G); knowledge of results (H); modification of DVs in individual line-pairs (I); and modification of DVs for whole character sequence (J) (page 96)

Figure 12 Predicted timing of the elements of the task analysis of the graphomotor sequence learning task. **Note:** all of the elements are involved throughout sequence learning; what is depicted are the relative emphases during the process (page 97)

Figure 13 Model of serial encoding of motor sequences (per Grossberg, 1978) (page 98)

Figure 14 Model of group encoding of motor sequences (per Verwey, et al., 2001, 2003) (page 98)

Figure 15A-C Experimental setup. A. Position of the subject in the scanner –subject views screen through mirror on the head coil. B. The non-ferromagnetic, digitizing tablet mounted on the holder and arm support. C. Example of a Chinese word character (starts from the center) (page 99)

Figure 16 Behavioral time line detail for fMRI study (page 100)

Figure 17A-D The $\{x,y\}$ data from the kinematic data was analyzed per character by computing normalized jerk ($Njerk - B$), which was used as a measure to determine

Learners from Non-Learners with movement time (MT –C). Njerk was also used in a repeated measures ANOVA, to determine if significant learning of the sequences occurred, and if so, to identify a learning period. The timestamps of when the subject wrote each line-pair were transformed into a format for use by AFNI's waver function, to produce a predicted hemodynamic response function (HRF) (page 101)

Figure 18A-D A. The predicted hemodynamic response function (HRF) for writing only for one subject, created by convolving the time series of writing times with a gamma function (AFNI: waver function). B. The predicted HRF for writing times were multiplied by censor files for each time bin within the learning period (C) to produce predicted HRFs for each time bin (page 102)

Figure 19A-B A. The relative composition of the baseline included the fixation screen (a plus sign); complex visual stimuli (performance feedback screen); and a simple hand motion (one inch to the left, then back to the center position). B. Baseline activities as they relate to the overall behavioral paradigm (page 103)

Figure 20 Average normalized Jerk (Njerk), with repeated measures ANOVA (Bonferroni corrected for multiple comparisons). Significant differences between bins 1-2 and bins 20-26 define an average learning period. Errorbars are one standard error; fit is double exponential (adjusted $r^2 = 0.66$) (page 104)

Figure 21 Division of the average learning period into five equal bins (page 104)

Figure 22 Bin 1 of graphomotor sequence learning. All images are functional MRI group statistics (repeated measures ANOVA, $p < 0.01$; with a $p < 0.05$ minimum cluster size threshold to control for type I error, per Monte Carlo simulation), presented over a high-resolution anatomical MRI of one subject from the group. All images are in radiological convention (left =right); coordinates are Talairach-Tournoux, in RAI (right to left; anterior to posterior; inferior to superior) order, and represent the center of maximal activity for that region. Z level is noted on top left of each slice. Area A is left frontal pole [12 -58 -2]; B is left fusiform gyrus [28 68 -12]; C is left inferior parietal lobule [34 45 45]; D is left superior parietal lobule [18 62 55] (page 105)

Figure 23 Bin 2 of graphomotor sequence learning. Area A is bilateral MT / V5 [left=42 62 -2; right=-38 62 -2]; B is bilateral, lateral pre-motor cortex [left=29 5 52;right=-28 6 52]; C is bilateral inferior parietal lobule [left=34 45 45; right=-35 39 46]; D is bilateral superior parietal lobule [left=18 62 55; right=-20 60 56] (page 106)

Figure 24 Bin 3 of graphomotor sequence learning. Area A is bilateral superior parietal lobule [left=18 62 55; right=-20 60 56]; B is the left anterior putamen [28 -5 4]; and C is the medial posterior vermis [5 49 -18] (page 107)

Figure 25 Bin 4 of graphomotor sequence learning. Area A is the right dentate nucleus [-25 45 -26]; B is the subgenual anterior cingulate cortex [0 -32 2]; C is the bilateral anterior putamen [left=28 -5 4; right=-19 -8 0]; area D is the superior medial

gyrus [11 -55 32] and right cuneus [-7 82 32]; E is right primary motor cortex [-56 6 37]; and F is the left primary somatosensory cortex [46 30 49] (page 108)

Figure 26 Bin 5 of graphomotor sequence learning. Area A is the right dentate nucleus [-25 45 -26]; B is the right anterior putamen [-19 -8 0]; C is the subgenual anterior cingulate cortex [0 -32 2]; area D is left frontal pole [12 -58 -2]; left precuneus [2 80 37]; left frontal pole [12 -58 -2]; and the midline dorsal cingulate cortex [2 -5 27]. Area E is left dorso-lateral prefrontal cortex [27 -22 47] (page 109)

Figure 27 The activity patterns of the left primary motor and left dorsal premotor cortices. The left dorsal premotor activity overlaps the first, fast, and the second, slower learning processes defined in the kinematic (Njerk) data. The left primary motor cortex participates principally in the second phase of motor sequence learning (page 110)

Figure 28 The left primary motor cortex, left dorsal premotor cortex, and left supplementary motor area activity during sequence learning. The left supplementary motor area's participation corresponds to the second, slower phase of sequence learning. Interestingly, given the variability across subjects, the left supplementary motor area was only significantly different from baseline in time bin 3 (page 110)

Figure 29 The left primary motor and dorsal premotor cortices, in relation to the dorsal visual stream (left superior parietal lobule). The left dorsal stream's activity

corresponds to the early, fast learning process in the kinematic (Njerk) data (page 111)

Figure 30 Different regions within the visual system, as sequence learning progresses. Note that the dorsal visual stream (left superior parietal lobule) and the lateral ventral visual stream (left fusiform gyrus) have similar patterns of activity. There is a dissociation between the medial and lateral ventral visual regions (left fusiform and left lingual gyri); as well as between the left superior parietal lobule and the left area MT / V5 (page 111)

Figure 31 Dissociation between the dorsal visual stream (left superior parietal lobule), and cerebellum (medial posterior vermis). The dorsal stream is significantly activated early, coinciding with the first, fast exponential learning process in the kinematic data. The cerebellar activity is contemporaneous with the second, slower, exponential learning process (page 112)

Figure 32 The left anterior putamen's pattern of BOLD signal activity follows that of the left primary motor cortex, through bin 4. In bin 5, the left anterior putamen activity persists, while the left primary motor cortex activity becomes sub-threshold (page 112)

Figure 33 Percent signal change in the BOLD signal for the left primary motor cortex, the left dorsal lateral premotor cortex, and the medial posterior vermis. The

vermis activation coincides with the second, slower learning process, as well as the increase in left primary motor activity (page 113)

Figure 34 Changes in BOLD signal during sequence learning for the left anterior putamen and the right anterior vermis. Note the divergent trajectories in bins 4 and 5, indicating that these two regions participate in different processes during later sequence learning. The differences between the left anterior putamen and the right anterior vermis in bins 4 and 5 are significant ($p < 0.05$, paired t-test) (page 113)

Figure 35 Left and right primary motor cortex, and dorsal-lateral premotor cortex activity during sequence learning. There is a large lateralization of the primary motor activity to the left that is not found in the premotor regions (page 114)

Figure 36 Frontal and temporal pole (left and right) activity during sequence learning. Note the dissociation between the early, significant activation of the left frontal pole, and the late, significant activation of the left temporal pole (page 114)

Figure 37 Selected default mode network regions (left frontal pole, left dorso-medial, prefrontal cortex, and medial posterior cingulate cortex) during sequence learning. Each of the regions decreases as the task is mastered, to a level significantly different from the baseline (page 115)

Figure 38 Limbic (left and right amygdala; left and right hippocampus) activity during motor sequence learning (page 115)

Figure 39 Seed voxel cross-correlation (Bin 1) for the Left primary motor cortex ($p < 0.001$). A. Positive cross-correlation with the right primary motor cortex. B. Positive correlation with the supplementary motor area. C. Negative cross-correlation with the right prefrontal cortex. D. Positive correlation with the right, anterior vermis (page 116)

Figure 40 Seed voxel cross-correlation (Bin 2) for the Left primary motor cortex ($p < 0.001$) (page 117)

Figure 41 Bin Seed voxel cross-correlation (Bin 3) for the Left primary motor cortex ($p < 0.001$) (page 118)

Figure 42 Bin Seed voxel cross-correlation (Bin 4) for the Left primary motor cortex ($p < 0.001$) (page 119)

Figure 43 Seed voxel cross-correlation (Bin 5) for the Left primary motor cortex ($p < 0.001$) (page 120)

Figure 44 Seed voxel cross-correlation (Bin 1) for the left superior parietal lobule ($p < 0.01$) (page 121)

Figure 45 Seed voxel cross-correlation (Bin 2) for the left superior parietal lobule (p<0.01) (page 122)

Figure 46 Seed voxel cross-correlation (Bin 3) for the left superior parietal lobule (p<0.01) (page 123)

Figure 47 Seed voxel cross-correlation (Bin 4) for the left superior parietal lobule (p<0.01) (page 124)

Figure 48 Seed voxel cross-correlation (Bin 5) for the left superior parietal lobule (p<0.01) (page 125)

Figure 49 A model of graphomotor sequence learning, combining the task processes identified from the task analysis; the timing and participation of the regions of interest; and the kinematic (normalized jerk) learning curve (page 126)

Figure 50A-C A. The writing times for each of the first line-pairs are used to segment the dataset, using a 36 second (18 TR or lag) window. B. The windows are then averaged over all characters produced within a time-bin. The resulting average BOLD signal (averaged across all subjects and all characters within the time bin) shows the response per voxel for each line-pair within each time-bin (page 127)

Figure 51 Average movement time (MT) per line-pair during graphomotor sequence learning. Errorbars are standard errors (page 128)

Figure 52 Average normalized jerk (Njerk) per line-pair during graphomotor sequence learning. Errorbars are standard errors (page 128)

Figure 53 The average line-pair analysis for the right amygdala, over all 5 time bins. This regions serves as a control, as differences between line-pairs during sequence learning is not expected. No pattern of line-pair related changes in BOLD activation are present (page 129)

Figure 54 The average line-pair analysis for the left supplementary motor area, over all 5 time bins. A distinct pattern of line-pair related changes in BOLD activation is present (page 130)

Figure 55 The average line-pair analysis for the left primary motor area, over all 5 time bins. The line-pair related changes in BOLD activation appear to be similar to the left and right supplementary motor area patterns (page 131)

List of Abbreviations

a	anterior;	p	posterior	M1	primary motor cortex
d	dorsal;	v	ventral	MCC	middle cingulate cortex
i	inferior;	s	superior	MT	medial temporal visual area V5
m	medial;	l	lateral	SMA	supplementary motor area
ACC	anterior cingulate cortex			PCC	posterior cingulate cortex
AMG	amygdala			PET	positron emission tomography
CH	cerebellar hemisphere			PFC	prefrontal cortex
DLPFC	dorsolateral prefrontal cortex			PMC	premotor cortex
DN	dentate nucleus			PPC	posterior parietal cortex
fMRI	functional magnetic resonance imaging			preSMA	pre-supplementary motor area
FP	frontal pole			PUT	putamen
FUS	fusiform gyrus			S1	sensorimotor cortex
hCN	head of the caudate nucleus			SPL	superior parietal lobule
HIP	hippocampus			TE	echo time
IPL	inferior parietal lobule			TH	thalamus
INS	insula			TP	temporal pole
LIN	lingual gyrus			TR	repetition time
				VER	vermis

Chapter 1: Introduction

Background and Significance of Sequence Learning

Most volitional human movements are a combination of over-learned, movement segments. Once learned, these sequences can be enacted as one unit, with little or no thought during the performance of the individual movement segments. For example, opening a door requires visual target location (doorknob); transport of hand to the target; grasping the doorknob; turning the doorknob; and pulling (or pushing) the door with the arm, while continuing to grasp the doorknob in a turned position. Yet, when an unimpaired person goes to leave the room, the entire sequence is enacted automatically one unit –the person does not have to think “locate target...reach arm towards doorknob...” etc., but can simply “open door.” This ability to combine previously-learned elements into novel sequences and then automate them is crucial to all human movement and cognition (Lashley, 1951). Yet, despite the importance of sequence learning, little is known about how the brain encodes and enacts sequences.

Karl Lashley was one of the first to examine sequence learning in a methodical manner, stating that the dominant theory (that one element of a sequence becomes linked with the next, in a type of “associative chaining”) was inadequate to explain the mistakes people make while typing sentences (Lashley, 1951). Lashley believed that the brain actively organizes elements into sequences, instead of the passively associating contemporaneous events, but he did not know the manner by

which the brain accomplished this task, and termed the issue the “problem of serial order.”

Understanding this “problem of serial order” is important both for uncovering basic neural mechanisms for encoding and enacting sequences in healthy persons; and also for learning how alterations in the neural processes relate to deficits in sequence learning and performance. For example, persons with loss of nigrostriatal dopamine production in Parkinson’s disease have demonstrated impaired sequence learning (Smith & McDowall, 2005), implicating the networks involving the basal ganglia. Degraded sequence learning may also constitute a part of the pathophysiology of Huntington’s chorea (Brown et al., 2001), stuttering (Webster, 1989), and stroke / traumatic brain injury (Pohl et al., 2001). Increasing our knowledge of the encoding and enacting of novel sequences may shed light on how the brain performs the calculations and computational processes needed for sequence learning, which would be invaluable for understanding both healthy and impaired persons.

The core of this dissertation focuses on the neural mechanisms underlying motor sequence learning and production, focusing on healthy, adult subjects. Doyon and Benali have posited a five stage model of motor skill learning (Doyon & Benali, 2005). In this model, motor skill learning begins with a fast (or early) learning phase, where the subject learns rapidly within an initial learning session. The second phase occurs across several learning sessions, where the gains in performance are slower, as the subject practices the new skill. The next stage is consolidation, which occurs

when there has been an idle period (no practice of the task, and no competing task), for more than six hours. After this consolidation period, an increase in performance is noted. The fourth stage is where the new motor task has become automatic (requiring little or no conscious thought to enact). This stage occurs after consolidation, and after further practice. The fifth and final stage of motor skill learning, according to Doyon and Benali, is that of retention. In this phase, the skill has been mastered to the extent that it can be performed automatically, even after long intervals without practice.

The dissertation focuses exclusively on Doyon and Benali's first stage of learning a motor skill, in which a novel sequence of previously-learned elements of the sequence is encoded to form the new representation of the motor sequence. This research endeavor does not examine the developmental processes involved in creating the neural networks involved in learning / encoding novel motor sequences; nor does it explore the alterations of these networks which occur in the pathophysiology of neurological disorders. By centering the study on "routine" motor sequence learning in healthy adults, using an ecologically valid graphomotor (drawing) task, this study is designed to identify the neural networks involved in sequence encoding and performance, the changes in their participation during the process of early motor sequence learning, and the mechanism by which those individual elements are grouped into a new representation during encoding.

The learning of novel sequences can occur with the subject's awareness (explicit learning), or without the subject knowing consciously that the sequence has been learned (implicit learning). Prior research has indicated that these two types of learning involve largely divergent networks (Doyon et al., 1996b; Eliassen et al., 2001; Honda et al., 1998). In the current study, we inform the subject before the experiment that the task involves sequence learning, so that all of the patterns are related to conscious (explicit) learning of the motor skills involved. Also, several significant studies have sought to identify the neural regions related to encoding the order (ordinal) aspects of sequence learning from the neural networks involved in learning the timing of the sequence learning task (Bengtsson et al., 2004; Sakai et al., 2002; Sakai et al., 2004). While this is an interesting and important area in the study of motor sequence learning, the current study focuses on a different issue: can we dissociate the neural networks responsible for creating internal representations of novel sequences (action selection parameter definition, and sequence encoding), from those regions related to the refinement and optimization of the motor plans for the novel sequences?

In the examination of motor sequence learning, an significant issue is to separate the neural processes involved with encoding (learning) the novel sequence from the areas of the brain related to the motor production of the expression of the sequence. The current study addresses this issue through several means. The first is the use of a novel, graphomotor task: learning to draw Chinese-like characters. There are several advantages to this approach, including gaining rich kinematic

measures of learning (in addition to the timing of the movements); having the ability to use the timing of each subject's drawing responses in the formulation of the predicted hemodynamic response function (HRF) in the fMRI analysis; and the use of a distal limb (hand), drawing task minimizes inertial and interaction torques; creating little head movement during neuroimaging. But beyond these benefits, this task isolates sequence learning from the production of the sequence by embedding overlearned segments (drawing short, straight lines), into novel sequence (the Chinese characters). Subjects are only learning the novel sequences, not the elements of the sequence (the lines), the effector, or the method by which the sequence is to be produced (drawing). The second way that sequence learning is isolated from performance, is by the use of a modified baseline (beyond simple, visual fixation on the screen). This baseline includes visual fixation; visual processing of complex, visual feedback; and hand movements. In this manner, the activations from neural regions involved in lower-order visual and motor processing, and complex visual processing, are removed from the analysis. This baseline assists in further isolating the neural processes involved in motor sequence learning from those involved in perception or movement production.

As the current research builds upon previous research on motor sequence learning, the following sections describe seminal and recent articles on the neurophysiology, neuroimaging and modeling of sequence learning, identify current gaps in our knowledge, and provide the rationale for this dissertation study.

Chapter 2: Prior Research on Motor Sequence Learning

Neural structures related to visually-guided limb movements

In order to perform the movements of the hand that are needed in learning to draw the Chinese word characters, the person has to visually guide their hand (with visual feedback from the screen) as the motions are performed. An important series of studies by Georgopoulos, et al., using single-cell recording in primates, found activation in selected regions of the posterior parietal cortex (PPC) that were closely related to both movement and visual processing (Georgopoulos, 1996; Georgopoulos, 1998). Subsequent research focusing on wrist and finger control found that, while individual neurons might have overlapping tuning for more than one finger, the neuron populations were tuned in a hand-centered reference frame, and that their activation predicted the subject's finger movements well (Georgopoulos et al., 1999). These studies formed the basis of further research into how visual processing and motor control are coordinated, in order for the person to make the movements required in performing a motor sequence.

Extensive research by Caminiti and colleagues with primates on visually-guided hand motions has suggested that a specific fronto-parietal network is employed to perform visuomotor transformations (Battaglia-Mayer et al., 2006; Mascaro et al., 2003; Battaglia-Mayer et al., 2003a; Battaglia-Mayer et al., 2001; Marconi et al., 2001; Caminiti et al., 1999; Caminiti et al., 1998; Ferraina et al., 1997; Caminiti et al., 1996; Lacquaniti et al., 1995; Caminiti & Johnson, 1992; Burnod et al., 1992). Figure 1 depicts the elements of this fronto-parietal network (Burnod et

al., 1999). This network is roughly divided into anterior, intermediate, and posterior frontal motor; and anterior, intermediate, and posterior parietal regions. Two important facets of this model are that the neuron populations from the posterior parietal cortex (PPC) to the frontal cortices are differentially tuned, forming a visual to somatic gradient along the parietal to frontal axis (see Figure 1B); and that the individual neural regions in this network have different, but overlapping tuning, resulting in domains with a unified function. These domains serve to combine, modify, and transmit the distributed sensorimotor signals related to visuomotor coordination. This fronto-parietal network serves to interpret visual information about the position of the hand and the target in space, and then to compute the appropriate changes in joint angles needed to move the limb and end effector (in our case, the pen drawing the Chinese characters) to the next appropriate position (Burnod et al., 1999).

Neural structures related to motor sequence learning

Previous research using primate models has indicated that neural structures in cortical (COR), thalamus (TH) basal ganglia (BG), and cerebellum (CB) are related to motor sequence learning. These studies indicate that there are multiple, looping connections between the COR, TH and BG, that are involved in the control of distal limb movements (see Figure 2); and the selection and reinforcement of appropriate limb movement plans (Alexander et al., 1986; Fujii & Graybiel, 2003; Fujii & Graybiel, 2005; Graybiel et al., 1994; Graybiel, 2001; Graybiel, 2004; Strick et al., 1993; Strick et al., 1995).

There are also multiple, looping connections between the COR, TH and the CB, which have been shown to be related to the control of visually-guided limb movements (see Figure 3), and the refinement of movement parameters as the movement is repeated (Middleton & Strick, 1997a; Middleton & Strick, 1997b; Middleton & Strick, 1998; Middleton & Strick, 2000a; Middleton & Strick, 2001). These structures contain neuron populations which respond to different aspects of encoding a novel sequence. The neurons' response patterns can be measured using single neuron or multiple-cell recordings (neurophysiology).

Neurophysiology of motor sequence learning

Within the cortico-striatal regions, specific structures have been shown to demonstrate selective activation during the learning of motor sequences: pre-Supplementary Motor Area (pre-SMA); anterior PUT and the head of the Caudate Nucleus (hCN) (Hikosaka et al., 1998; Hikosaka et al., 1999; Nakamura et al., 1998). These structures have been shown to increase activity selectively for specific positions within a sequence and for specific sequence orders (see Figure 4) (Tanji et al., 1995; Tanji, 2001). A second network, including the middle to posterior PUT and pre-Motor cortex (PMC) has been related to the production of learned sequences of movements (Hikosaka et al., 1998; Hikosaka et al., 1999; Nakamura et al., 1998). Inactivation studies in BG show that deactivating the anterior PUT and head of the CN impacted learning of new sequences, while deactivating the middle-posterior

PUT resulted in degraded ability to produce previously-learned sequences (Miyachi et al., 1997; Miyachi et al., 2002).

Within the cortico-cerebellar regions, specific structures have also shown selective activation during the learning and production of motor sequences (Middleton & Strick, 1997a; Middleton & Strick, 1997b; Middleton & Strick, 1998). One network, involving the Dentate Nucleus (DN), lateral cerebellar cortex (CC), the thalamus (TH), and the ventral Pre-Motor (PMC) and primary Motor (M1) cortices, appears to be related to the initiation of movement plans and control of visually-guided limb movements. This network is also implicated in early sequence learning, in the Hikosaka, et al. model. A second cerebellar network, involving medial CC, and the anterior vermis (aVER), is related to the motor output of movement plans to the spinal cord, and is related to optimizing movement plan parameters. This network relates to the motor cerebellar network in Hikosaka's model, in which sequences of movements are learned in motor coordinates.

Recent work in monkey using retrograde neuronal transport of the rabies virus to trace direct neuronal connectivity, has shown that dentate output from the cerebellum connects to the input portion of the basal ganglia (striatum) (Hoshi et al., 2005). This connection indicates that the BG and CB interact significantly, and any model of motor sequence learning will need to include such interaction.

Structural neuroimaging and motor sequence learning in humans

Recent research using diffusion tensor imaging (DTI) in humans has indicated that there are parallel neural structures within the human brain related to motor sequence learning and production. In DTI, the differences in diffusion between water (which diffuses uniformly in all directions), and white matter tracts in the brain (which diffuses differentially along the direction of the axonal fiber bundle) are measured, and used to detect axonal pathways in the brain. A seed voxel is placed, and an algorithm then searches all neighboring voxels, to find those that show a contiguous directionality, with sufficient signal strength. Studies using DTI neuronal fiber tracing indicate two functionally-distinct cortico-striatal loops (see Figure 5) (Lehericy & Gerardin, 2002; Lehericy et al., 2004a; Lehericy et al., 2004b; Lehericy et al., 2005a). The first, consisting of the pre-frontal cortex (PFC), frontal pole, pre-supplementary area (pre-SMA), anterior putamen (PUT) and the head of the caudate nucleus (CD), has been termed the “associative compartment,” and has been shown to be related to motor sequence learning (Lehericy et al., 2004a). The second cortico-striatal network has been called the “sensorimotor compartment,” and consists of M1, primary sensorimotor cortex (S1), SMA proper, and posterior Putamen. This network has been related to the production of motor sequence movements (Lehericy et al., 2004a).

Functional neuroimaging of motor sequence learning

Positron Emission Tomography

A series of research studies that employed a graphomotor task while subjects were PET (Positron Emission Tomography) scanned has demonstrated several key elements of using neuroimaging to study motor sequence learning (Seitz et al., 1994; Seitz et al., 1997). The behavioral task was to copy letters or nonsense ideograms. In these studies, early learning was compared to late learning, and different performance conditions were used that emphasized speed or accurate drawing of the target. “Early learning” was when the subjects were first exposed to the task; “late” learning was after the drawing task had been automated (able to be completed quickly, accurately and with little conscious attention -measures of sequence learning). Subjects performed these tasks during PET scanning, so that the researchers could collect neuroimaging and kinematic data simultaneously. Data on the changes in pen position were collected using a digitizing tablet, and was analyzed along with the neuroimaging data. The main kinematic measures used were movement duration (the time to complete the drawing), and velocity (the changes in speed within each drawing motion). From these studies, the kinematic data indicated that there were differences in performance between early and late learning, and for novel vs. overlearned characters (see Figure 6). Subjects performed more slowly for initial and novel characters, and increased their speed as the training progressed.

The PET data from the study demonstrated that different cortical and sub-cortical regions were activated for different stages of learning (early vs. late), and for

different performance conditions (exact vs. fast). Specifically, the contralateral (to the subject's drawing hand) PMC, PFC and primary motor (M1) cortices were active in early learning; as well as the ipsilateral cerebellar vermis (VER) and DN in both early and late learning. The Seitz, et al. studies also found changes in bilateral posterior parietal cortex (PPC) activation as a function of the learning parameters (exact vs. fast).

Importantly, these studies demonstrated that the motor sequence learning process could be captured using kinematic analysis of graphomotor movements, and that measures of neuronal activity could be related to the kinematic measures of motor sequence learning. However, these early PET studies contained several significant limitations, including a lack of performance feedback to the subject (measures of how quickly and accurately the characters were drawn); little temporal information on the changes in neural participation during the sequence learning process (early vs. late only); and no means of separating out the neural regions involved in producing the movements from the regions involved in learning the sequence.

A more recent PET study used a timed, synchronous finger tapping task (the subject matches a target rhythm), and three, same-day training periods (Penhume, et al., 2005). In this study, bilateral CC, SMA, pre-SMA, superior temporal gyrus (STG), and medial cerebellar lobule (CBL) were active during early learning (see Figure 7). In later training sessions, the activation shifted to the ipsilateral PUT,

superior parietal lobule (SPL), inferior parietal lobule (IPL), and orbital frontal cortex (OFC); as well as contralateral M1 and PMC. This study suggested that cerebellar participation in early motor sequence learning is limited to error detection and reduction during initial learning. However, this study, by separating the learning periods throughout the day, may have added recency effects to the later scan sessions, compromising the comparisons between “early” and “late” sequence learning. This study also has the same limitations as the Seitz, et al. studies, in that there is no performance feedback; there is limited temporal resolution; and minimal separation of sequence learning and production.

Functional Magnetic Resonance Imaging

Studies using functional magnetic resonance imaging (fMRI) have also contributed to our knowledge of motor sequence learning. A study by Lehericy, et al. (2005) used sequential finger movements practiced for fifteen minutes a day, scanning the subjects on days 1, 14, and 28. This study found bilateral activations of the dorsal PUT, anterior, dorsal globus pallidus (GP), and sub-thalamic nucleus (STN) on day 1 (early learning). The data indicated that there were changes in neural activation related to learning within the first 50 minutes on the first day that the subjects were scanned. These changes included reduced bilateral activation of anterior, dorsal PUT, and increased activation of the posterior, ventral PUT. These patterns, along with related changes in the dorsal and ventral TH, respectively, were stable for the next two weeks –indicating that the majority of motor sequence learning occurred within a relatively short period of time. This is an important contribution to

the study of sequence learning, as this study gives a general timeframe for early sequence learning. However, this study was limited in scope to cortical – BG networks, and did not evaluate the role of the CB, the interactions between the CB and BG, or the timing of these networks in early motor sequence learning.

Another set of studies using fMRI BOLD (blood oxygen level dependent) analysis of cerebellar activation during motor sequence learning demonstrated activation of lateral cerebellar hemispheres (CH) during early motor sequence learning, and a shift of activation to the ventral DN during late motor sequence learning (see Figure 8) (Doyon et al., 2002; Doyon et al., 2003; Doyon & Benali, 2005). While these studies demonstrated differential cerebellar participation in early vs. late sequence learning, additional work needs to be done to examine the changes in participation of the BG and CB networks (and their interactions), as motor sequence learning occurs.

An fMRI study that employed a novel task (having the subjects track a pattern with a hand pressure device) in studying motor skill learning also sheds some light on motor sequence learning (Floyer-Lea & Matthews, 2004). In this study, subjects learned to visually track a pattern of increasing and decreasing pressure on an MRI-compatible pressure pad. The researchers divided the learning period into (initial exposure) learning and late (after stable performance), and found two distinct networks involved in motor learning. The early learning network included the fronto-parietal network (including bilateral PFC, S1, and PPC). Late learning correlated

with a decrease in the fronto-parietal network, and an increase in sub-cortical regions (TH, PUT, DN). While this study wasn't focused on sequence learning, the task was sequential in nature, and the involvement of the fronto-parietal, cortico-striatal and cortico-cerebellar networks in learning the sequence is directly related to motor sequence learning. Additional temporal resolution (number of time-bins) is needed to further clarify the roles and interactions of these networks in the sequence learning process.

A final selected study that explores the learning process of motor sequences is by Muller, et al., and uses an explicit version of the serial reaction time task (SRTT) (Muller et al., 2002). With the SRTT, the subject presses buttons in a regular order (or randomly) as a control for sequence production, and then learns a novel sequence of button pushes, in a block design. Muller and colleagues found that, in brief learning periods, significant activation occurred in bilateral PMC, SMA, and the superior and inferior parietal lobules (SPL and IPL). When the task was altered to allow for the comparison of early (initial exposure) and late (after practice) learning bins, the early learning bin had greater activity in the bilateral SPL, right, dorsolateral PFC, left CN and PMC. Late learning had greater activation in left temporal-occipital and superior frontal cortices, as well as bilateral parahippocampal areas (see Figure 9). These results again confirm the interacting roles of the fronto-parietal, the cortico-striatal, and the cortico-cerebellar networks in motor sequence learning, but do not allow us the opportunity to examine the temporal changes that occur as the sequences are encoded and performed.

Taken together, the animal and human models suggest the involvement of several cortical – sub-cortical networks in motor sequence learning involving hand movements: frontal-parietal network; dorsal and ventral visual streams; lateral and medial pre-motor networks; cortico-striatal and cortico-cerebellar networks (see Table 1 for a summary of selected neuroimaging studies). Each of these networks participates in motor sequence learning, but little is known about how they relate to each other during motor sequence learning, or how their participation changes during the process of motor sequence learning. A more detailed examination of these cortical and sub-cortical networks could increase our understanding of the neural processes involved in motor sequence learning.

Theories of motor sequence learning

Neurophysiological Theory

While both cortico-striatal and cortico-cerebellar networks are actively involved in motor sequence learning, exactly how (and when) the two sets of networks contribute to motor sequence learning is largely unknown. Research on motor sequence learning using single-cell recording in monkey has resulted in a theory of cortico-striatal and cortico-cerebellar network interaction during motor sequence learning (see Figure 10) (Hikosaka et al., 1998; Hikosaka et al., 1999; Hikosaka et al., 2002a; Nakamura et al., 1998). In this model, the motor sequence is learned by two systems simultaneously: a “spatial system” (comprised of the PUTa / CNh and dorsal DN); and a “motor system” (the middle / posterior PUT and the

anterior lobe). In this model, the spatial system is slow, computationally intense, requires high-attention, and is stored in short-term memory; the motor system is fast, automatic (low attentional needs), and is stored in long-term memory. The SMA and pre-motor (PM) regions serve to connect the spatial and motor systems, with the pre-SMA acting to resolve conflicts between the two networks. The Hikosaka, et al. model posits that the two systems operate independently of one another in learning the motor sequence.

The Hikosaka, et al. model is the most advanced theory on sequence learning to date. This model needs to be extended in several ways: include the examination of cortical-striatal, cortical-cerebellar networks, and their interactions; increase the temporal resolution of the examination of the sequence learning process (from “early” and “late”); specifically isolate the neural networks involved in sequence encoding separately from sequence production; and provide a method for the kinematic measures of phases of motor sequence learning to be incorporated in the analysis of the neuroimaging data.

Computational Theories

In addition to examining the regions of the brain that work cooperatively to encode and enact novel motor sequences, there is another level of analysis in the study of sequence learning. The research question is: how are the individual movement plans (that have already been learned) combined into the representation for the new sequence? This is one of the essential questions of how the brain encodes

sequences into an internal representation that can be accessed automatically.

Grossberg, et al., have simulated the encoding, storage and retrieval/production of handwriting movement sequences (Grossberg & Paine, 2000; Paine et al., 2004). In the Grossberg, et al. model (see Figure 13), each element of the sequence is encoded serially (segment 1; segment 1 + segment 2; segment 1 + segment 2 + segment 3; ...). The individual segments are those movement plans that have “won” the competition for being the closest to the intended movement for that part of the sequence (competitive cueing). The transitions between the segments are what are added when a sequence is encoded. Each segment movement in the sequence is started by a peak velocity detection method, where the peak velocity of the current movement triggers the signal for the next movement segment to be prepared and released. Error feedback is posited to be related to the cerebellum in this model. The Grossberg, et al. simulations using this model able to produce movement velocity profiles, speed and size scaling, and decreased writing time with learning that correlated well (0.89 +/- 0.10) with human writing data. The Grossberg, et al. model focuses on the cerebellum, and needs to be expanded to include other regions of the brain that have been shown to participate in sequence learning.

A second model of motor sequence learning involves a multi-level (2 or 3) processing system (see Figure 14), in which a motor processor organizes a set of overlearned and automated motor plans into a “chunk,” and a second processor executes the chunk (Rhodes et al., 2004; Verwey, 2001; Verwey, 2003a; Verwey, 2003b; Verwey & Eikelboom, 2003; Verwey & Wright, 2004; Verwey & Clegg,

2005). Verwey, et al.'s model separates out the process of encoding of the sequence from the process of enacting it. In this model, all of the motor plans are selected for the new sequence in a group, at the same time, by the first processor, and encoded. A second processor then enacts the encoded sequence in the proper order, to produce the motor output.

Both of the major computational theories (Grossberg, et al. and Verwey, et al.) have difficulty relating the mechanisms of their theory to specific regions of the brain that could plausibly produce the necessary computations, given the neurophysiology and neuroanatomical connections of those regions. It is currently an unanswered question as to whether the elements of a sequence are encoded at the same time (Verwey, et al.), or serially (Grossberg, et al.). Providing data that relates the kinematic measures of learning to concurrent neuroimaging data could help to clarify which of these two competing computational models is the most biologically plausible; or could suggest alternative models.

Summary of gaps in our current understanding of motor sequence learning

A survey of the relevant animal and human research on motor sequence learning indicate that our knowledge of the neural processes involved in sequence learning could be enhanced by research emphasizing: 1. specific examination of early motor sequence learning (first 15 - 20 minutes); 2. the use of a methodology that allows for the collection of detailed behavioral data (kinematics) that can be used to predict the changes in neuronal activity during the process of motor sequence

learning; 3. a research design that results in data that facilitate the validation, modification, or rejection of current computational and biological models of motor sequence learning; and 4. the separation and disambiguation of the neural networks related to the performance of the motor sequences from those related to learning the sequences. In addition, a study that examines both cortical and sub-cortical regions (including the cortico-striatal and cortico-cerebellar networks, and their interactions), as well as the functional connectivity of the regions / networks during different phases (time bins) of early motor sequence learning, would be beneficial. Finally, a methodology for examining the neural responses to the individual elements of the sequence as they are encoded over time (to explore the serial vs. group encoding of novel sequence is needed.

Description of the two current research studies

The current investigation addresses these issues by combining behavioral and neuroimaging approaches to examine motor sequence learning in healthy adults, and consists of two studies. The primary study extends the Hikosaka, et al. model of motor sequence learning in humans (Hikosaka et al., 1998; Hikosaka et al., 1999; Hikosaka et al., 2002a; Nakamura et al., 2001), using a mixed model (event / block) fMRI study with synchronized collection of behavioral (kinematic) data while naïve subjects learn Chinese characters. This task is well-suited to the examination of motor sequence learning, as subjects will have previously overlearned the elements of the characters (drawing short, straight lines in English), but will the sequences of lines in the Chinese characters will be completely novel to the subjects. It is important to

note that since the subjects are naïve to written Chinese, the line sequences are not linguistic (the lines have no meaning for the subjects), but constitute a graphomotor (drawing) sequence learning task. In this study, the times of the subject's drawing of the characters are used to create a predicted BOLD response in the analysis of the fMRI data. Other important aspects of the study include: adding whole-brain (cortical and sub-cortical) analysis; including a more detailed exploration of the temporal dynamics of sequence learning; isolation of sequence encoding from sequence performance; and an analysis of functional connectivity (a measure of the level of integration in the neural circuit).

An additional study examined the specific ways in which novel sequences are encoded. This study tested whether there is neuroimaging data to support the theory that a novel sequence is encoded one transition at a time --Grossberg, et al.'s model of sequential encoding (Bullock & Grossberg, 1988; Bullock et al., 1998; Grossberg, 1978; Grossberg & Gutowski, 1987; Grossberg & Paine, 2000), or whether one neural process defines the sequence as a group, and another enacts the sequence -- Verwey, et al.'s multi-processor theory (Rhodes et al., 2004; Verwey, 2001; Verwey, 2003a; Verwey, 2003b; Verwey & Eikelboom, 2003; Verwey & Wright, 2004; Verwey & Clegg, 2005). According to Verwey, et al.'s formulation, the novel sequence should be encoded as a group.

Using the same functional and kinematic data set, the second study examines the average fMRI BOLD responses (across subjects and repetitions) for each of the

three kinematic sub-units (the line-pairs) involved in learning the new sequence (the Chinese character). The timing information from the kinematic data is used to divide the fMRI data to find the average BOLD response for each line-pair. An analysis of the differences in BOLD activation per line-pair in brain regions related to motor sequence learning will provide evidence of the degree to which those regions are active equally for each sub-unit (Verwey et al.'s theory), or in decreasing order (Grossberg, et al.'s model) by the end of the learning period.

Chapter 3: The Neural Substrates of Graphomotor Sequence Learning

Introduction

The brain's ability to automate almost any task –whether cognitive, linguistic, or motoric, is fundamental to all human thought, communication and activity (Lashley, 1951). Sets of complex, multiple-stage movements become so well packaged that little or no thought is needed to initiate or complete them (consider opening a door, typing, or dancing). Once encoded through the learning process, phonemes are readily combined into spoken words that are effortlessly combined into meaningful sentences. While learning a new sequence can be time and attentionally-intensive, after a sequence (of words, thoughts, or actions) has been automated (or “chunked”), it becomes a part of the person's routine behavioral repertoire.

The processes within the brain that are involved in performing this invaluable function have received little attention until recent years. In animal studies, selected portions of the cortico-striatal network (pre-SMA, anterior PUT, CNh) have shown selective activity during motor sequence learning (Hikosaka et al., 1998; Hikosaka et al., 1999; Nakamura et al., 1998). Moreover, this network seems to increase its activity for specific positions within a sequence and during the planning of specific sequence orders (see Figure 4) (Tanji et al., 1995; Tanji, 2001). A second network, (middle to posterior PUT, PMC) has been related to the production of learned sequences of movements (Hikosaka et al., 1998; Hikosaka et al., 1999; Nakamura et al., 1998). Selective inactivation of regions within this network show that

deactivating the anterior PUTa and CNh impacted learning of new sequences, whereas deactivating the middle-posterior PUT resulted in degraded ability to produce previously-learned sequences (Miyachi et al., 1997; Miyachi et al., 2002).

Research involving animal models has also examined cortico-cerebellar networks. These looping circuits have also shown selective activation during the learning and production of motor sequences (Middleton & Strick, 1997a; Middleton & Strick, 1997b; Middleton & Strick, 1998). One network (DN, lateral CC, TH, ventral PM, M1) appears to be related to the initiation of movement plans and control of visually-guided limb movements. This network is also implicated in early sequence learning (in spatial coordinates), in the Hikosaka, et al. model. A second cerebellar network (medial CC, aVER), is related to the motor output of movement plans to the spinal cord, and is related to optimizing movement plan parameters. This network relates to the motor cerebellar network in Hikosaka's model, in which sequences of movements are learned in motor coordinates.

In addition to cortico-striatal and cortico-cerebellar networks, there is recent evidence of interaction between these two systems. Using retrograde neuronal transport of the rabies virus in monkey to trace direct neuronal connectivity, Strick and colleagues have shown that dentate output from the cerebellum connects to the input portion of the basal ganglia (striatum) (Hoshi et al., 2005). This connection indicates that the BG and CB interact significantly, and any model of motor sequence learning will need to include such interaction.

Studies in humans using diffusion tensor imaging (DTI) neuronal fiber tracing indicate two functionally-distinct cortico-striatal loops (see Figure 5) (Lehericy & Gerardin, 2002; Lehericy et al., 2004a; Lehericy et al., 2004b; Lehericy et al., 2005a). The first, (PFC, frontal pole, pre-SMA, anterior PUT, CDh), has been termed the “associative compartment,” and has been shown to be related to motor sequence learning (Lehericy et al., 2004a). The second cortico-striatal network has been called the “sensorimotor compartment,” and consists of M1, primary sensorimotor cortex (S1), SMA proper, and posterior PUT. This network has been related to the production of motor sequences (Lehericy et al., 2004a).

Functional neuroimaging studies (positron emission tomography –PET; fMRI) in humans have shown patterns of cortico-striatal and cortico-cerebellar activation as a motor sequence is learned. In the cortico-striatal network, an fMRI study by Lehericy, et al. (2005) used sequential button / key presses, with neuroimaging on three days, each two weeks apart. This study found bilateral activations of the dorsal PUT, anterior, dorsal globus pallidus (GP), and sub-thalamic nucleus (STN) on day 1 (early learning). Within the first 50 minutes on this first day the neural participation had shifted, with reduced bilateral activation of anterior PUT, and increased activation of the posterior, ventral PUT. These changes, along with related changes in the dorsal and ventral thalamus, respectively, were stable for the next two weeks, indicating that the sequence was encoded within the first 50 minutes or less. These

findings are supportive of the animal studies, and indicate that separate functional networks may be involved in the learning and production of motor sequences.

Cortico-cerebellar activation patterns in humans also change as the novel sequence is learned. A study using finger tapping demonstrated activation of lateral cerebellar hemispheres (CH) during early motor sequence learning, and a shift of activation to the ventral DN during late motor sequence learning (Doyon et al., 2002; Doyon et al., 2003; Doyon & Benali, 2005). A PET study using a finger tapping task and three, same-day training periods (Penhume, et al., 2005) found that bilateral CC, SMA, pre-SMA, superior temporal gyrus (STG), and medial cerebellar lobule were activated during early learning (see Figure 7). In later training sessions, activation shifted to the ipsilateral PUT, superior parietal lobule (SPL), inferior parietal lobule (IPL), and orbital frontal cortex (OFC); as well as contralateral M1 and PM. These studies suggest that cerebellar participation in motor sequence learning may involve error detection and reduction during early motor sequence learning, and the refinement and optimization of the movement plans during later sequence learning.

Research questions

This dissertation examines how a set of individual movements are assembled into a movement sequence, focusing on the neural regions involved, and the timing of their participation. A second, related question is whether the order of encoding of the individual movements can be detected with kinematic and neuroimaging methods. Specifically, we will examine what networks of brain areas are involved (that is, what

are the neural substrates); and how the neural regions relate to each other during the time course of motor sequence learning (e.g. task-related functional connectivity). A second, but related set of questions focus on the manner in which the elements of the novel sequence are encoded: are the segments of a sequence encoded as a group, or one at a time (serially)? How does the participation of the brain networks related to the order of encoding, and how does this participation changes over time? Importantly, kinematic measures of learning will be used to partition the neuroimaging data into several stages of motor sequence learning.

Task analysis of ideographic graphomotor sequence learning task

Task Description

The behavioral task consisted of subjects learning to draw novel graphomotor sequences (in fact, Chinese characters), as neuroimaging data was collected with functional magnetic resonance imaging (fMRI). Each character consisted of six movements (three line-pair sets), which were presented and drawn one line-pair at a time. After each character was completed, knowledge of results (KR) was given to the subject, presenting their speed and spatial accuracy on that character (error feedback learning). The characters were randomly selected and randomly presented, to avoid positional effects. Each of the four characters was repeated nine times, for 36 total iterations (the first 30 during the fMRI scanning period). Kinematic data was collected while the subjects learned to draw the characters on an MRI-compatible digitizing tablet. Importantly, it was assumed that the motor programs for the sequence segments (drawing short, straight strokes) were highly automated, while the

sequence (the character) was new to the subject, isolating the sequence learning process. Kinematic measures of learning focused on movement smoothness (normalized jerk –Njerk), a unitless measure that controls for variations in speed and size of drawing across and within subjects. The fMRI data was collected on a 3 Tesla, GE scanner at the National Institutes of Health, Bethesda, Maryland, USA, with the kinematic data synchronized to the fMRI scanning.

Task Analysis

As the regions of the brain involved in the sequence learning process are largely dependent upon the requirements of the behavioral task, an in-depth analysis of the graphomotor task was needed. Figure 11 depicts the elements of the learning task, starting with the presentation of the target template for Character 1 (of 4); Iteration 1 (of 9); line-pair 1 (see Figure 11A). Once the line-pair is presented, the subject locates targets (T1, T2) in the Example space on the screen. The targets are the endpoints of the first and second strokes of LP1, respectively, and they are located visually. The subject must also locate his / her current hand position (starting point for first LP) (Figure 11B). Current hand position is located visually in the Writing Space on the screen, and by proprioceptive feedback of hand position on the digitizing tablet. Visual and proprioceptive feedback must be integrated, in order to determine current hand position.

Using the current hand position and the target locations, difference vectors (DVs) are computed for Line 1 and Line 2 (Figure 11C). The first DV is the spatial

computation of the difference from the starting hand position to T1, for Line 1; and the second DV computes the difference from T1 to T2 for Line 2. These DVs are the kinematic programs for the movements, in spatial terms. The kinematic motor program for the line-pair is then scaled for speed (Figure 11D). The kinematic motor program is transformed into a muscle force motor program (dynamics) (Figure 11E). This transformation is an inverse kinematic and dynamic process for computing joint angles and torques. The dynamic motor program DVs for LP1 is then enacted (Figure 11F); this produces a vector of joint angles ($\theta_{1:n}$), and a vector of pen positions ($X_{1:n}$).

A visual comparison of the lines drawn by the subject in the Writing Space, and the Target Template shown on the example screen, gives an error measure per line-pair (Figure 11G). This error measure informs the error feedback learning process for each of the line-pairs. If the set of 3 line-pairs (1 character) is not completed, then the next line-pair (LP_n) is presented (Figure 11I). When all three line-pairs are completed (1 character), then the knowledge of results (KR –speed and spatial accuracy) are presented to the subject (Figure 11H). The KR is involved in the conscious learning of the entire character. After the first character is completed, the next iteration of the character (or next character) is presented, by line-pairs (Figure 11J), until 9 iterations of the 4 characters are completed.

Neural Resources Needed to Perform the Behavioral Task

From this examination of the ideographic graphomotor sequence learning task, we can summarize the task's requirements, and predict of the neural regions that should be involved in the motor sequence learning process. Basic visual processing and visual attention will be involved; as will the motor control of the wrist and fingers. Also, the visual processing of complex objects will be required by the behavioral task. Yet, because these elements were included in the baseline period (visual fixation for basic visual processing; feedback screen for complex scene processing; and the hand movement for lower-level motor control of wrist and fingers), we expect the contributions of the neural regions responsible for these processes to be attenuated to some degree. The study was designed in this manner, in order to emphasize the neural regions related to motor sequence learning, instead of those related to basic visual and motor processing.

More specifically related to graphomotor sequence learning, we predict that the dorsal visual stream (SPL) will be involved in visual location of the lines targets (T_1 and T_2) in the example space, as well as the pen / hand position in the writing space (Andersen, 1997; Seitz et al., 1994; Seitz et al., 1997). left MT / V5 should also be involved in visual location and tracking (Hamzei et al., 2002; Oreja-Guevara et al., 2004). Proprioceptive feedback of the current hand / pen position in the writing space should involve the left sensorimotor cortex (S1) and IPL (Gardner et al., 2006; Naito & Ehrsson, 2006). The integration of the visual and sensorimotor modes of feedback of the hand / pen position is predicted to involve IPL, lateralized to the left

(Andersen, 1997; Gardner et al., 2006). Visuomotor mapping of the DVs (kinematic movement planning) should involve the frontal-parietal network for reaching (Burnod et al., 1999; Caminiti & Johnson, 1992; Caminiti et al., 1996; Caminiti et al., 1998; Caminiti et al., 1999; Georgopoulos, 1996; Georgopoulos, 1998; Georgopoulos et al., 1999; Georgopoulos, 2000).

The DVs are scaled for speed of the movements. This is important, because the subjects were instructed to produce the sequence “as quickly and accurately as possible.” The sensorimotor compartment of the basal ganglia (left pPUT) should be involved in this scaling process. The transformation from kinematic to dynamic motor plans (inverse kinematics and dynamics) should involve the left SPL, left dPMC and left M1 (Wise et al., 1996; Wise et al., 1997); and the execution of the motor plans should involve left M1 (Carey et al., 2006).

The comparison between the target template (the line-pair example) and the actual drawing of the line-pair made by the subject in the writing space, results in an error signal that is used in error feedback learning of the line-pairs. The anterior vermis is predicted to participate in error feedback learning. (Hikosaka et al., 1998; Hikosaka et al., 2002a; Hikosaka et al., 2002b; Lehericy et al., 2004b; Lehericy et al., 2005a; Lehericy et al., 2005b).

In addition to the error feedback learning of the line-pairs, the paradigm includes knowledge of results (KR) after the completion of each character. The KR is

used to modify the process leading to sequence encoding, which will involve the associative basal ganglia (anterior putamen and head of caudate nucleus), and target cortical areas like the pre-SMA (Hikosaka et al., 1998; Hikosaka et al., 1999; Hikosaka et al., 2002a; Nakamura et al., 1998). Both error feedback learning of the individual line-pairs, and KR based learning of the entire character continue over the successive iterations of the characters during the task. Figure 12 gives a general depiction of the relative involvement of each of the task elements during early, middle and late sequence learning. Note that all of the neural regions related to sequence learning participate throughout (primary motor / sensorimotor cortices, for example); however we predict that some networks will be emphasized during certain phases of sequence learning.

Methods

A mixed (event-block) fMRI design was used, in which the subjects repeatedly drew four ideographic characters (3 sets of line-pairs each), while they were scanned in a GE 3 Tesla MRI scanner at the National Institutes of Health, Bethesda, Maryland, USA (see Figure 15A). The characters were randomly drawn from a pool of ten characters, and randomly presented, using custom Matlab (Mathworks, Inc.) software (see Figure 16 for the timing of the behavioral task). Kinematic data was acquired using a non-ferromagnetic, digitizing tablet (TouchScreen, MagConcepts Inc., Sunnyvale, CA), sampling $\{x\ y\}$ coordinates at 66 Hz (see Figure 15B). In addition to the kinematic measure of learning, time-stamps were recorded for each line-pair response that the subject produced. The predicted

hemodynamic response function (HRF) used in the analysis of the fMRI data was generated (AFNI's waver function, see AFNI website: <http://afni.nimh.nih.gov/afni/doc>) using these time-stamps (see Figure 17). This predicted HRF (WRITE) should identify the changes in neural BOLD activity related to the production of the writing movements (including visual processing, somatosensory feedback and kinematic-to-dynamic transformations).

In order to separate the neural resources related to the sequence learning process from those supporting the motor performance processes, a baseline subtraction paradigm was used. During the baseline condition, subjects viewed a simple visual fixation (a plus sign); viewed a more complex pattern (the feedback screen of their performance on the prior character); and made a simple hand movement with the pen (one inch left, then back to center). By including these elements in the baseline, we sought to remove basic visual processing (fixation screen), complex visual pattern processing (feedback screen), and basic motor control of distal limb (hand / pen movement). This complex baseline allowed us to disambiguate the neural regions related to graphomotor sequence learning from those involved in basic and complex visual processing, and lower-level motor control. The relative proportion of each section of the baseline task is presented in Figure 19A; the proportion of the baseline as related to the entire experimental task is depicted in Figure 19B.

To examine the changes in participation of the neural regions related to graphomotor sequence learning over time (temporal dynamics), the total learning period (approximately 13:30 minutes) was divided into 5 equally-spaced periods (bins). With a repetition time (TR) of 2 seconds, each bin was 100 volumes (the length of 5 characters), or approximately 2 minutes and 44 seconds long. The times are approximate, due to a randomized jitter that was introduced between line-pairs (1 second jitter, on a 0.5 second grid from 0 to 2); and a 4 second jitter between characters (also on a 0.5 second grid, from 3 to 5 seconds). This jittering increased the statistical power of the deconvolution process (3dDeconvolve, AFNI), in sampling the hemodynamic response function of the fMRI data (Dale & Buckner, 1997).

Examination of the functional connectivity between regions of interest within the networks involved in sequence learning and production, a seed-voxel cross-correlation analysis was performed for the primary motor cortex (M1) during each of the five learning time bins (see AFNI website: <http://afni.nimh.nih.gov/sscc/gangc/SimCorrAna.html>). Maps of significant relationships ($p < 0.001$) were computed.

Subjects

Nineteen right-handed healthy subjects were successfully scanned, with Mini-Mental Status Exam (MMSE) scores greater than 27 (mean 29.58, std 0.79). Of the nineteen, twelve subjects demonstrated significant sequence learning on the kinematic measure employed (normalized jerk), and were included in the study (4F, 8M;

average age = 34.08 years; std = 6.69 years) . All subjects were pre-screened for absence of neurological disorders, neurological disorders, chronic substance abuse and chronic mental illness, as well as for MRI safety. All subjects gave informed consent, according to National Institutes of Health Protocol 92-DC0-0178, and University of Maryland IRB requirements; and were screened for MRI safety according to the National Institutes of Health Nuclear Magnetic Resonance Center Policy. Subjects were paid \$100.00 for the scan session.

Procedures

Each subject was given the Mini Mental Status Exam (MMSE), to screen for basic orientation and cognitive functioning, and completed a pre-scan training on drawing stars to acclimate the subjects to drawing holding the pen tip down continuously. After a one minute practice session of drawing random, straight lines on the tablet, the same stars task was performed in the scanner for two and one-half minutes. This was to familiarize the subjects with the mapping of the visuomotor task in an unfamiliar position (lying supine, with the writing tablet by the subject's hip). Due to the length of the single continuous scan during the sequence learning task, a vacuum pillow was used to help stabilize the subject's head. Subjects had their right arm supported by a custom designed, Plexiglas© support, to constrain motion (see Figure 15B), and the writing tablet and holder were positioned for greatest subject comfort and ease of writing.

A mirror on the head coil allowed the subject to see a screen, upon which instructions and the experimental tasks were presented (see Figure 15A). The subject was instructed to focus on three important things during the entire experiment: keeping their head still, keeping the stylus tip on the tablet, and copying the templates as quickly and accurately as possible. The start of the behavioral task was synchronized with the first TTL pulse from the GE MRI scanner, using a data acquisition card (National Instruments, NI-DAQ 6062e PCMCIA board), and the Matlab data acquisition toolbox (Mathworks, Inc.). This allowed for the time-stamping of each instruction presented, each response made by the subject, each feedback screen, and the fixation times, all relative to the first MRI TTL pulse, synchronizing the kinematic and fMRI datasets.

The experiment provided both real-time visual feedback of the pen's position on the digitizing tablet (with a line trace) during each line-pair, and knowledge of results (KR) after each ideographic character was completed (see Figure 15C for an example of a character). In the KR paradigm, subjects were shown an example of how to draw the line-pair; and then copied the example on a separate writing area on the screen while the exemplar remained on the screen. Ideographic characters were randomly chosen from the pool of ten characters, and were presented in three, two-pair segments (transition 1, line segment 1; transition 2, line segment 2; etc.), in order, and with direction cues given in the Example window. The sample of characters was constrained to include only characters with three straight lines and three straight transitions. Real-time, visual feedback of the stylus' position on the

digitizing tablet (with a line trace) was provided to the subject. Learning occurred through repeated iterations of each character's line-pairs, with a performance feedback screen (giving speed and accuracy) presented to the subject after each character's completion. Figure 16 depicts the timing of the graphomotor sequence learning task

The echo-planar imaging (EPI) scan parameters for the functional images were: repetition time (TR)=2000 ms; echo time (TE)=30.0 ms; field of view (FOV)=24; slice thickness=5.0 mm; number of slices/volume=30; number of volumes=585; flip angle=90 degrees; with a voxel size of 3.75 x 3.75 x 5 mm. A high-resolution (1 mm), FSPGR anatomical scan was performed for each subject, and co-registered with the functional images in AFNI.

Data Analysis

Kinematic

To determine if learning had occurred during the repetitions of the characters, kinematic data (normalized jerk –Njerk, a measure of movement smoothness) was examined with a repeated measures ANOVA, with Bonferroni correction (SAS Institute, Inc., Cary, NC). The Njerk score for each iteration was compared to every other iteration, to determine if there were significant differences that would indicate a learning period. Before Njerk was computed, the kinematic data was low-pass filtered (Butterworth filter; Matlab dual-direction, filtfilt function; filter order = 4; cut off frequency = 5 Hz; Nyquist frequency = 33; sampling period = 0.0152s; sampling

rate = 66 Hz). N_{jerk} was computed using the following equation (Contreras-Vidal et al., 1998; Kitazawa et al., 1993; Teulings et al., 1997):

$$N_{jerk} = \sqrt{0.5 \int dt \text{ jerk}^2(t) \times \text{duration}^5 / \text{length}^2}$$

Where duration is the time to complete the stroke, length is the stroke distance, and jerk is the third time derivative of the pen position at a given time point, t .

Neuroimaging

The neuroimaging data was pre-processed in AFNI (National Institute of Mental Health, National Institutes of Health, Bethesda, Maryland, USA; see website: <http://afni.nimh.nih.gov>), with motion correction, binary masking of the brain, and 8 mm Gaussian blurring. Because the fMRI data needed to be acquired in one scan (to avoid order effects), and the total scan time (with stars task and sequence learning task) was almost 20 minutes. Long fMRI scans present additional challenges for data analysis, as the effects of scanner baseline drift have to be addressed. Due to the length of the scan, the baseline (instrumental) drift was non-linear, and could not be effectively modeled using standard, AFNI methods (polort polynomial fitting, see 3dDeconvolve documentation: http://afni.nimh.nih.gov/pub/dist/doc/program_help/3dDeconvolve.html). To remove spurious global BOLD signal drift effects, each subject's fMRI dataset was normalized by the grand mean (mean over all volumes and voxels) and average ventricle signal (any BOLD signal present will be non-physiological). The average value for eight, 2 mm spherical ventricular

locations (anterior and posterior ventricle locations, bilateral, at two different z levels) was collected for each subject (Fox et al., 2006). This average (dividing on a per-volume basis) was used to remove the proportional instrumental drift over time. In addition, the same per volume ventricle values were included in the baseline model of the deconvolution (3dDeconvolve, AFNI), along with removal of each subject's mean (polort 0, 3dDeconvolve, AFNI) in order to remove additive instrumental effects. This method proved effective in reducing drift effects, as indicated by visual inspection of spurious activation per subject.

The predicted hemodynamic response function (HRF) was created by inputting the timestamps of each subject's drawing times (for each line-pair) into AFNI's waver function, and convolving the duration of each line-pair movement with a gamma function (an ideal hemodynamic response function –see Figure 17). The equation for the gamma response function is $h_G(t;b,c) = (t/(bc))^b \times \exp(b-t/c)$; where $b = 8.6$ and $c = 0.547$ (Cohen parameters), and the function peaks when $t=bc$, at the value of 1 (see AFNI documentation: <http://afni.nimh.nih.gov/pub/dist/doc/manual/waver.pdf>).

Before the deconvolution of the fMRI data with the predicted HRFs, the predicted HRFs were multiplied by binary square wave functions corresponding to the 5 time bin segments, in order to produce a predicted HRF for each of the time bins (see Figure 18). Deconvolution of the predicted HRF from the fMRI data involves calculating the estimated impulse response function per voxel by minimizing the sum

of squares error between the fit of the predicted HRF to the data, and the data (see AFNI documentation: <http://afni.nimh.nih.gov/pub/dist/doc/manual/Deconvolve.pdf>). Once deconvolved (AFNI: 3dDeconvolve) the resulting beta coefficients per voxel for each subject were entered into a mixed-effects ANOVA (Bin x Subject) model (using AFNI 3dANOVA2, see website: http://afni.nimh.nih.gov/pub/dist/doc/program_help/3dANOVA2.html). The mean for each time bin was computed (t-test maps), and was smoothed with a 3 mm Gaussian filter for presentation purposes. For visualization purposes, the group ANOVA results are projected over a selected subject's high resolution anatomical scan.

Functional connectivity was measured using voxel-based cross-correlation (see AFNI website: <http://afni.nimh.nih.gov/sscc/gangc/SimCorrAna.html>). Each subject's EPI dataset was transformed into common (Talairach) space (AFNI `adwarp` function); then the brain was masked with a group average, binary mask (AFNI `3dautomask`); the time-series for the region of interest (M1) was extracted (AFNI `3dmaskave`); transposed to column format; and analyzed for correlations using `3dDeconvolve`. The use of the `3dDeconvolve` function allows for the use of the same mean removal and ventricle baseline correction as in the sequence learning analysis. The same pre-processing was also used (grand mean and ventricle normalization) as in the sequence learning study. The beta values for each subject were converted to z scores, for comparison across subjects (AFNI `3dcalc`). A one sample t-test across all subjects tested the null hypothesis that there were no differences across subjects, for

each voxel. Voxels with a $p < 0.001$ were reported in the form of a t-map image of the brain, overlaid on the same subject's high resolution anatomical scan.

Results

Kinematics

Figure 20 shows the average normalized jerk (Njerk) values for all subjects, for the 30 character iterations that occurred during the fMRI scanning. The repeated measures ANOVA (with Bonferroni correction for multiple comparisons) of the average Njerk values produced only two sets of iterations that were significantly ($p < 0.05$) different from each other. The first character iteration was significantly different than iterations 20 – 26; and the second character iteration was significantly different than iterations 20; 23-25 (see Figure 20). All other pairings of the iterations were not significantly different. This significant difference between the first baseline character and the 20th – 26th character iterations indicates that the subjects learned the graphomotor trajectories within this time period. This is important, in that it substantiates that sequence learning had occurred, and that the learning occurred during the functional neuroimaging scans. Njerk values for character iterations 26 – 30 rise above the lowest level found between iterations 20 – 26, but the differences are not significant, and may reflect to attentional shifts from the task.

The decrease in the normalized jerk values indicates that the subjects improved their performance as they learned the novel sequences, and suggest a learning period between the time they started (iteration 1) and when they had

acquired the task (iterations 20-26). This learning period was used to divide the fMRI data into five equal time bins (see Figure 21), in order to examine the neural activations related to these time periods during motor sequence learning. A double exponential curve ($\text{Fit} = 29010 * \exp(-0.016748*x) + 22734 * \exp(-0.75962 * x)$; x =character iterations) best explained the normalized jerk data, and suggests that there are two processes involved in motor sequence learning: an early, fast process (bins 1-2); and a second, slower process (bins 3-5). Thus, the neural activity reflected in the BOLD signal change will be related to both the two learning processes (early fast; and later, slow), and to the changes in the kinematic measure during the five time bins over the course of sequence learning. In contrast to prior studies, “early” sequence learning refers to the subjects’ initial changes in performance and neural activity during learning related to the early, fast kinematic process (bins 1-2); “middle” learning refers to bins 3-5 (the second, slower learning process); and “late” sequence learning refers to bin 5, when the subjects’ performance plateaus.

The first time bin (bin 1) corresponded to the earliest phase of motor sequence learning, with the steepest decrease in normalized jerk (see Figure 21, Bin 1). In this time period (approximately 2 minutes and 45 seconds), the subject was taking the most time per character, and was making the least smooth movements (see Figure 21). The second time bin was a time of transition between the early, fast learning process in bin (the first exponential of normalized jerk fit); and the second, slower exponential-like process that occurs in bins 3 - 5. The timeframe of the second bin was from approximately 2 minutes, 45 seconds into the task, to around 5 minutes, 30

seconds (timing varied per subject due to randomized jitter to maximize deconvolution of effects). Subjects performed drawing motions more smoothly (normalized jerk), but their performance was still variable (see Figure 21).

By the third time period of the graphomotor sequence learning task, the subjects had been repeatedly writing the ideographic characters for approximately five and one-half minutes. Their performance was slowly improving as seen in the gradually decreasing NJerk scores (see Figure 21, Bin 3). Bin 4 was again a transition time in the process of motor sequence learning (see Figure 21, Bin 4). In this time period (approximately 8 minutes, 15 seconds to 11 minutes from the start of the task), average normalized jerk score were reduced more from the beginning of the time bin to the end, than in bin 3. The subjects' motor performance continued to improve and reached a plateau by the end of the fourth time bin.

In the fifth time bin, the subjects reached their maximal performance on the graphonomic sequence learning task. Their normalized jerk indices were significantly different from when they started ($p < 0.05$, repeated measures ANOVA, with Bonferroni correction for multiple comparisons). Their level of performance was relatively stable across the time bin (see Figure 21, Bin 5), as there was a reduction in the variability across subjects (see Figure 21; compare standard error bars for bins 2-4 and bin 5). Note that the subjects' performance decreased after bin 5. While this difference was not statistically significant from bin 5, it may represent a

change in attention, since the subjects had mastered the task, and had been repeating the same four Chinese word characters for almost fifteen minutes.

Neuroimaging Results by Time Bin

In the first bin, the bilateral frontal pole (see Figure 22A) and dorsal visual stream (superior parietal lobule, lateralized to the left –Figure 22D) were significantly active beyond baseline (all significance values reported at $p < 0.01$, unless noted otherwise). The inferior parietal lobule was also active bilaterally, lateralized to the left (Figure 22C). The left lateralized ventral visual stream (fusiform gyrus, see Figure 22B) was also active during the first time bin.

In the second time bin, there were several noteworthy shifts in activation patterns. The initial bilateral frontal pole activation became left lateralized, and focused in a smaller spatial area. The activations in the left-lateralized dorsal (see Figure 23D) and ventral visual (Figure 23A) streams increased in spatial extent, and became more bilateral. In the same manner, the extent of inferior parietal lobule activation increased in bin 2, and became less lateralized (Figure 23C). Significant activation in bilateral lateral pre-motor cortex also began in bin 2 (Figure 23B).

In the third time bin of motor sequence learning, there was a marked change in participating networks. The left superior parietal lobule decreased participation and lateralized to the right (Figure 24A); while the sub-cortical basal ganglia (bilateral anterior putamen and head of caudate nucleus) and cerebellar (right

posterior vermis) networks became significantly active for the first time (Figure 24B-C).

Cerebellar activation, especially right dentate nucleus and anterior vermis, were increased in bin 4 (see Figure 25A). During this period of increased performance, the subgenual anterior cingulate cortex was active (Figure 25B), as was the left primary sensory cortex near the hand area (Figure 25F). Also during bin 4, the striatum decreased in activation on the left side, shifting to right lateralization (Figure 25C). The right motor strip was significantly active (Figure 25E). during bin 4 as well. Interestingly, in bin 4 there were initial indications of midline deactivation (see Figure 25D).

The activation in the right dentate nucleus and vermis increased from bin 4 to bin 5, and the anterior cingulate cortex activation persisted (see Figure 26C); while the posterior parietal, motor, lateral premotor, and primary somatosensory cortical regions were all sub-threshold. The anterior basal ganglia activity was exclusively right lateralized at this threshold in bin 5 (Figure 26B). The midline deactivations noted in bin 4 increased in bin 5 (Figure 26D).

Neuroimaging Results of Selected Neural Systems

Neocortical

In contrast to the limbic, sub-cortical and proisocortical regions, the neocortical areas were predominantly activated at the beginning and middle of the

sequence learning process. The dorsal premotor cortices were significantly active in the first three bins, while the left primary motor cortex was active in the middle three time bins (see Figure 27). Interestingly, the left SMA was only active in bin 3 (see Figure 28); while the bilateral pre-SMA were not significantly different from baseline. Change in the left M1 were seen in the later bins (see Figure 29).

The ventral stream had differing responses in the medial (lingual gyrus) and more lateral (fusiform gyrus) regions (see Figure 30). The lingual gyrus was deactivated early, but not late; while the fusiform gyrus was activated early (bins 1-2), but was deactivated from bins 3 – 5. In contrast, the dorsal visual stream was very active in the early bins, and decreased rapidly to sub-threshold by the later bins, with the left side leading the right regions. Figure 31 depicts the dissociation between the early fast process (i.e., SPL), and the second, slower process (i.e., aVER). Some association areas (left inferior parietal lobule; left inferior gyrus; left frontal pole / pre-frontal cortex) followed the same pattern of activation as the dorsal visual stream and the lateral premotor cortices –in that they were significantly active early, and then less active later. Three of the four areas with the most significant activation ($p < 0.001$) in early sequence learning were in association regions (left and right frontal pole; inferior parietal lobule), while the fourth was in the dorsal visual stream (SPL).

Subcortical

The participation of the subcortical regions was clearly during the second, slower phase of motor sequence learning (bins 3-5). Cerebellar, basal ganglia, and

thalamic regions were significantly deactivated during early motor sequence learning. Basal ganglia (left hCN, aPUT) were super-threshold for the first time in bin 3, and persisted through bin 5 (see Figure 32 for an example). The ventral lateral thalamic region (vl TH) followed a similar pattern.

The cerebellum also participated in the middle to late portions of sequence learning, during the second, slower learning process (Figure 33). The right aVER became significantly activated in bin 4, after the basal ganglia had already engaged in bin 3, and followed a different time-course of activation than the basal ganglia. The basal ganglia peaked in activation in bin 4, then receded in bin 5, when the subject's performance reached a plateau. In contrast, right aVER engaged after the basal ganglia, but continued to increase in activation level in bin 5, after the basal ganglia had begun to disengage (see Figure 34).

Hemispheric Differences

As expected, there were hemispheric differences observed during the task. Figure 35 shows the difference between the left and right primary / sensorimotor cortices during motor sequence learning. Note that the difference is not solely due to the left hemisphere's role in moving the wrist / fingers, because that process has been included in the baseline condition. The remaining left M1/S1 activity should be related to sequence learning or production.

Default Mode Network (DMN)

Midline regions related to the default mode network (DMN) have been found to be deactivated relative to attentionally-intensive activity (Greicius & Menon, 2004; Greicius et al., 2004). So it is surprising that during early graphomotor sequence learning (bins 1-2), one of the most active regions is the bilateral frontal pole. After bin 2, the left frontal pole becomes sub-threshold, and by bin 4-5, it is significantly deactivated. In contrast, the left temporal pole is significantly deactivated early (bins 1-2), and is significantly activated during late sequence learning (bin 5 –see Figure 36). The midline, default mode network regions became significantly deactivated only in bins 4-5 (see Figure 37).

Limbic system

In general, the limbic and paralimbic regions followed a pattern of significant deactivation early in motor sequence learning (bins 1 and 2), and moved in a relatively linear manner to significant activation in bins 4 and 5 (see Figure 38). The negative and positive peak values were usually bin 1 (negative peak) and bin 5 (positive peak). When significant transitions occurred, they were exclusively between bins 1 and 2, or 2 and 3, and were always in a positive direction.

Functional connectivity during motor sequence learning

Introduction

Functional connectivity, as measured by cross-correlation, is a measure of the cohesiveness of activation patterns between neural regions. In a preliminary analysis

of functional connectivity, we have focused on two regions of interest: the left primary motor cortex; and the left superior parietal lobule. M1 is a focus, because the production of the pen motions in the character sequence learning task is ultimately a motor task, so we have examined the changes in connectivity between the contralateral primary motor cortex (left M1) and other regions of the brain involved with sequence learning, during the five time bins. In the kinematic analysis of sequence learning, two distinct processes (early, fast; and later, slow) were found. For the preliminary functional connectivity analysis, the left superior parietal lobule was examined during motor sequence learning, because it participated in the early, fast portion of sequence learning; while the primary motor cortex participated differentially in the second, slower phase.

Left Primary Motor Cortex

In early learning (bin1: early, fast phase of sequence learning), left M1 was positively connected bilaterally (to right M1); to the left SMA, and to the right aVER (see Figure 39). left M1 was also negatively coupled with the right FP in bin 1. By the second time bin, M1 was positively connected to bilateral aPUT, to left pre-SMA; while the functional connection with right aVER persisted (Figure 40). In the third bin (second, slower sequence learning process), left M1 was positively connected to left anterior and middle PUT, bilateral TH, pre-SMA and aVER (Figure 41). Negative cross-correlations existed between left M1 and B dPMC, as well as the left v insula. In the fourth time bin, M1 was positively functionally connected to: right DN, right aVER, SMA / pre-SMA; and bilateral TH (Figure 42). There was also a

negative functional connection between left M1 and right FP in bin 4. And, in the final bin, M1 was positively connected to: left middle PUT, SMA / pre-SMA (decreased from bin 4), bilateral TH, right DN and right aVER (Figure 43).

Left Superior Parietal Lobule

During bin 1, the left SPL was positively connected with the left IPL, and the ventral stream (fusiform gyri) bilaterally (see Figure 44). There was a significant ($p < 0.01$) negative relationship between left SPL and: m subgenual ACC; left aPUT; left hCN; middle PUT; posterior PUT; left SMA; and left M1 during the early, fast portion of motor sequence learning. The majority of these connections changed in bin 2, leaving significant positive cross-correlations only between left SPL and the right cerebellar hemisphere; left fusiform gyrus; and the left IPL (see Figure 45). In bin 3, the positive functional connection between left SPL and left IPL became bilateral (left and right IPL); and the connection with left fusiform persisted (see Figure 46). A negative relationship with the right DN and left M1 began in bin 3. Bin 4 showed numerous changes in the functional connectivity of the left SPL (see Figure 47). Negative connections included: bilateral frontal pole; m subgenual ACC; left hCN; and left M1. the positive cross-correlations with left SPL in bin 4 were: m aVER; left vLPFC; and the left middle temporal gyrus. In the final learning bin (bin 5), left SPL was positively functionally connected to: right DN; B aVER; left middle temporal; B MT/V5; and right SPL (see Figure 48). Negative couplings included: right FP; left globus pallidus; right dmPFC; left m PMC; left dIPFC; and left M1.

Discussion

This dissertation has sought to expand current understanding of how the brain learns and programs motor sequences, specifically, sequences of stroke movements by the wrist and fingers. Further insight into sequence learning will increase our knowledge of how regions of the brain work together mechanistically, in order to represent and transform information; and may eventually help us to understand aspects of neurological disorders such as Parkinson's disease, stuttering, or aphasia.

Prior animal and human research on sequence learning has led us to focus on a set of neural regions related to: control of visuomotor reaching tasks (frontal-parietal network); visually locating and identifying objects in space (dorsal and ventral visual streams; visual areas MT / V5); encoding and organizing movement plans (cortico-striatal networks; pre-motor regions); error detection and movement refinement (cortico-cerebellar networks). An analysis of the task being employed in the study (learning ideographic characters) led to predictions that: the dorsal visual stream would be involved in location of hand and target (line) positions in space, visual feedback, and motion tracking; motor plan formulation would also involve premotor regions; execution of the motor plans would include primary motor cortex; somatosensory feedback as the hand moved would involve primary somatosensory cortex; encoding movement sequences would involve the cortico-striatal networks; and refinement / optimization of the movement plans would involve the cortico-cerebellar networks.

The current study adds to this knowledge base by adding a novel, graphomotor task; separation of the sequence learning process from basic motor and visual processing; concurrent analysis of cortical and sub-cortical regions, and their interactions; detailed kinematic analysis of performance; and an analysis of the temporal dynamics of the neural regions participating in graphomotor sequence learning.

Sequence Learning

How graphomotor sequences are learned

The primary question of the current research study was to find out how motor sequences are learned, or “chunked;” what brain regions are involved in the process; and to gain a basic understanding of the timing of the brain regions’ participation in sequence learning. From the results of the study we can posit the elements of a model to explain how graphomotor sequences are learned (see Figure 49).

The results (kinematic and neuroimaging) indicate that sequence learning of graphomotor trajectories involved overlapping processes. Initially, the movements for the sequences were mapped spatially (visuomotor mapping) (Battaglia-Mayer et al., 2003a; Battaglia-Mayer et al., 2001; Battaglia-Mayer et al., 2003b; Battaglia-Mayer et al., 2006). This involved the dorsal and ventral visual streams being coactive with premotor regions; as well as visual motion tracking of the pen movement in area MT / V5 (Burnod et al., 1999; Caminiti & Johnson, 1992; Caminiti et al., 1996; Caminiti et al., 1998; Caminiti et al., 1999). These regions appeared to

participate in identifying the appropriate set of motor plans of the lines for the novel sequences (consonant with Seitz, et al., 1994, 1997). During this early, fast learning phase, the subcortical regions were surprisingly deactivated; and the bilateral frontal poles were activated –perhaps managing the rules for the task (Wise et al., 1996).

In the next process in graphomotor sequence learning, the motor plans “winners” became gradually more accurate, as did the modified motor parameters. This was probably accomplished through interactions with the error detection system (CB, dPMC). The discrepancies between the ideal line-pairs and the actual line-pairs drawn were used to modify the sets of motor plans, criteria for best motor plan parameters for best motor plan, and parameters for transitions between lines. In this manner, the sequence was progressively encoded in a more accurate representation, probably in the dPMC and associative basal ganglia. As the sensorimotor and visual feedback refined the selection criteria to a stable level, the visual areas were not needed, and were no longer activated with respect to the basic “visuomotor network” –similar to Muller, et al.’s findings (Muller et al., 2002) . The emphasis shifted from mapping to refining the internal representation of the novel sequences (best motor plans, motor plan parameters, and transition encoding); and to optimizing the movements for speed and efficiency. This optimization persisted after the sequence had been encoded (optimal performance), and involved the anterior vermis in the cerebellum, which fits Hikosaka, et al.’s findings and model (Hikosaka et al., 1998; Hikosaka et al., 1999; Hikosaka et al., 2002a; Hikosaka et al., 2002b; Nakamura et al., 1998; Nakamura et al., 1999).

Default Mode Network

Prior research would predict that the default mode network regions would be deactivated during early motor sequence learning (Greicius et al., 2003; Greicius & Menon, 2004; Greicius et al., 2004). The surprising timing of the deactivation of the default mode network (DMN) regions (only after the graphomotor sequences have been encoded) and the *activation* of the medial prefrontal cortex during early learning may indicate the need to re-evaluate the current theories on the DMN's relationship to task performance. From the current results, it appears that the DMN deactivations commonly found when effortful tasks are performed were not present until the tasks had been nearly completed. This finding would be consonant with the understanding of the DMN as participating in internally-generated neural processes, but would indicate that effortful tasks require the suspension of the DMN activity, and that DMN deactivation only occurs when the task is less effortful (Greicius et al., 2003; Greicius & Menon, 2004).

Relationship of kinematic and neuroimaging results to the task analysis and predictions

Visuomotor mapping

The roles of visual processing systems in early graphomotor sequence learning were confirmed. The dorsal stream activation early (SPL) is reflective of target and hand location in space; visual motion (tracking of the pen motion) was related to MT /V5 activity. Object encoding –efforts to classify the novel examples

as objects –involved the ventral visual stream (fusiform and lingual gyri), and visual and somatosensory feedback integration was indicated by IPL activation during early sequence learning.

The parietal-frontal network for reaching was involved in the sequence learning task, with the exception of the dorsolateral prefrontal cortex (only significantly different from baseline in the third time-bin). This difference may be related to the graphomotor task, in which the exemplar was present continually, so less visual working memory was required (Burnod et al., 1992; Burnod et al., 1999; Caminiti & Johnson, 1992; Caminiti et al., 1996; Caminiti et al., 1998; Caminiti et al., 1999). Supplementary motor area and pre-supplementary motor areas were also expected to participate in motor sequence learning and production, from the Hikosaka, et al. model (Hikosaka et al., 1998; Hikosaka et al., 1999; Hikosaka et al., 2002a; Hikosaka et al., 2002b). This difference from prior findings may be related to the task not being self-generated, but externally-guided (Elsinger et al., 2006). The dorsal PMC, M1, and PPC were involved in graphomotor sequence learning beyond the basic production of hand / pen movements (Seitz et al., 1994; Seitz et al., 1997).

Sequence Learning

The results of the current study indicate that the premotor regions play a critical role in sequence learning. Interestingly, the lateral premotor (dorsal PMC) areas that were involved, and not the medial (SMA and pre-SMA) as previously reported by Hikosaka, et al. (Hikosaka et al., 1998; Hikosaka et al., 1999; Hikosaka et

al., 2002a; Nakamura et al., 1998; Nakamura et al., 1999). In Hikosaka, et al.'s task (sequential button push), the exemplar was not present throughout the time that the subject performed the sequence. Because of this, Hikosaka, et al.'s task involved both self-initiated movements and working memory, while the current task was externally-initiated and didn't require extensive working memory (exemplar was always present) (Elsinger et al., 2006). This may account for the participation of the dorsal PMC instead of the SMA / pre-SMA. The importance of the dorsal PMC is also reflected in its activation throughout both the visuomotor mapping and encoding / reinforcing phases of sequence learning. The activity of the dorsal PMC bridged the first, fast and the second, slow phase of sequence learning, reflecting involvement in both the early (cortical visual-motor kinematic mapping) and later (subcortical motor dynamic encoding) processes (Wise et al., 1997).

In the first, fast portion of sequence learning, we expected associative compartment (aPUT, hCN) basal ganglia activation, but the associative BG did not participate until middle of sequence learning process. This finding may be because the exemplar was given; so little exploration of the workspace was needed (a BG function). In Hikosaka, et al.'s research, the task involved trial and error learning, which would necessitate BG activation early; the current task used error feedback learning, which may not have necessitated early BG activation. Another possibility for the timing of the BG participation is that the visuomotor mapping processes have not been separated from early sequence learning before the current study. By having

an ‘early’ and ‘late’ binning of the neuroimaging data, previous studies may have inadvertently combined these processes.

Hikosaka, et al.’s Model

Hikosaka, et al.’s model of anterior compartment activation (hCN, aPUT) before sensorimotor compartment (mPUT, aVER) activation was supported by current data. The timing is somewhat altered (associative compartment was primarily active in the middle section of the learning process; sensorimotor was primarily active in the late section, when the performance was optimal). As a part of Hikosaka, et al.’s model, we expected cerebellar activation (lateral cerebellar cortex) early in sequence learning (performing error feedback) as well as late (performing movement refinement by adjustment of motion parameters). The results of the current study only found cerebellar participation in the latter portions of motor sequence learning. The form of error feedback found predicted at the beginning of sequence learning may be related to basic movement initiation and correction, which was removed by using a hand movement in the baseline. The finding of cerebellar error feedback participation only during later learning indicates that error detection during early sequence learning may involve the visual and dorsal premotor systems; and that later sequence learning error detection involves anterior vermis error detection.

Additional Findings

It was interesting to note that there was a shift from bilateral, frontal pole activation during early sequence learning, to left temporal pole activation as the

characters were encoded. This shift during the process of sequence learning may reflect conscious effort to master the task (FP activation early); and later, less effortful performance of the sequences (TP activation late). The timing of this shift corresponds to the changes in the default mode network –when sequence encoding is nearing completion (bin 4), the DMN becomes deactivated, and that deactivation increases as the performance is optimized in bin 5. The frontal pole to temporal pole shift may reflect both the change in level of automaticity of sequence learning and performance, and that neural resources have been freed up from sequence learning task for other, internal processes (reflected in increased DMN deactivation) (Greicius et al., 2003; Greicius & Menon, 2004).

Functional Connectivity

Preliminary functional connectivity analysis produced useful, complementary data to the standard contrast methods, indicating that neural regions participated in motor sequence learning networks prior to activations that were significantly different from baseline. An important example was the cross-correlation between the left primary motor cortex and the left anterior putamen beginning in bin 2, when the left anterior putamen only became activated significantly beyond baseline in bin 3.

Chapter 4: Encoding of Graphomotor Sequences

Introduction

In a healthy human adult, most of the routine activities of the day –walking, talking, opening a door, reaching for a glass of water – are tasks that are done with little or no conscious thought or effort. These (and many other) motor sequences have been “chunked” into easily accessible, highly automatic sequence units. Once packaged as a unit, these often complex sequences of motor behaviors can be produced easily and effortlessly.

Because of the ubiquitous nature of this function of the brain (organizing previously-learned sequences into a novel unit), as well as the impairment of this process through a variety of neurological disorders (Parkinson’s disease, for example –see Smith and McDowall, 2005), it is important that we understand how the brain encodes and represents sequences. It is also possible that the study of the mechanisms by which novel sequences are encoded in the brain may give us insight into the neural strategies for representing environmental context, physical sensory information, and the translation of intention into motor activity.

Prior research in this area has resulted in at least two principle, competing theories of how novel sequences are encoded in the brain. The first, exemplified by the Grossberg, et al. model, posits that the first element of the sequence is selected by a competitive process (competitive cueing), in which numerous movement plans are compared against the intended movement (Cohen & Grossberg, 1986). The “winner”

of this competition becomes the first element of the movement sequence. After a second competition, the second element is selected, and is attached to the first (see Figure 13). In this manner, all of the elements of the new sequence are assembled, serially, until the final sequence is encoded. To enact the newly-coded sequence, the first movement is initiated, and a peak-velocity detection network is triggered. This system senses when the movement has reached its peak velocity, and when this is accomplished, begins the preparation of the next movement segment. Grossberg, et al. have modeled this method for sequence encoding successfully with the VITE, VITEWRITE, and AVITEWRITE models (Contreras-Vidal & Stelmach, 1995; Grossberg & Paine, 2000; Paine et al., 2004). The Grossberg, et al. model has also served as the theoretical framework for later neurophysiological studies of sequence learning (Hikosaka et al., 1998; Hikosaka et al., 1999; Hikosaka et al., 2002a; Nakamura et al., 1998; Nakamura et al., 1999). A limitation of the Grossberg, et al. model is that it focuses principally on cerebellar interactions with motor and parietal cortices, when animal (Alexander et al., 1986; Fujii & Graybiel, 2003; Fujii & Graybiel, 2005; Middleton & Strick, 1994; Middleton & Strick, 1997c; Middleton & Strick, 1997a; Middleton & Strick, 1997b; Middleton & Strick, 2000b; Middleton & Strick, 2000a; Middleton & Strick, 2001; Middleton & Strick, 2002; Strick et al., 1993; Strick et al., 1995; Tanji et al., 1995; Tanji, 2001) and human research (Doyon et al., 1996a; Doyon et al., 2002; Doyon et al., 2003; Doyon & Benali, 2005; Lehericy & Gerardin, 2002; Lehericy et al., 2004a; Lehericy et al., 2004b; Lehericy et al., 2005a; Lehericy et al., 2005b; Sakai et al., 1998; Sakai et al., 2000; Sakai et al., 2002; Sakai et al., 2003; Sakai et al., 2004; Seitz et al., 1994; Seitz et al., 1997) on motor

sequence learning have indicated that broad networks of cortico-striatal, cortico-cerebellar, and cortico-cortical networks are involved in encoding and producing new sequences.

A second theoretical framework for the encoding of novel sequences has been contributed by Verwey, et al. (Verwey, 2001). In this model, there are at least two processing systems involved in motor sequence learning. The first processor selects the appropriate movement programs from the available pool of learned movements, and organizes them into a sequence as closely related to the intended sequence as possible. The second neural processor then enacts the newly-defined sequence, in the proper order (see Figure 14). The implication of the Verwey, et al. model is that the new sequence is “chunked” at one time, instead of serially, in the Grossberg, et al. theory (Cohen & Grossberg, 1986).

Research questions

Building on the prior study on the neural substrates of graphomotor sequence learning, we will examine candidate brain areas that potentially could show activations related to the methods of encoding employed by neural networks during sequence learning. To examine the neural networks and mechanisms involved in establishing the internal representations of novel motor sequences, we have developed a novel behavioral task – learning to draw novel ideographic characters, from well-learned handwriting strokes. This task is ideal for examining motor sequence learning during neuroimaging (functional magnetic resonance imaging –

fMRI) of the subject's brain. The utility of this graphomotor task in studying sequence learning lies in the fact that the strokes (drawing short, straight lines) are highly overlearned for adult writers; while the sequential aspect of the task (the order of the strokes that comprise each character) is completely novel to the subject. This graphomotor (drawing) task is also ideal for use in the MRI scanner, as handwriting strokes produce little movement that would create artifacts in the imaging.

Another advantage of this task was the ability to collect relatively rich, kinematic data (the changes in pen position on the digitizing tablet). This kinematic data yielded information on the speed, accuracy, and smoothness of character production, in addition to timing information (when the movement occurred). Changes in the subjects' performance in producing the characters were captured by kinematic measurement during the fMRI scanning (see Figure 20). The functional neuroimaging dataset was then divided into bins using the changes in subject performance (Figure 21). The timing information from the kinematic data collection was also important for the event-related fMRI analysis to determine whether sequences are encoded sequentially or in a group; and to determine which cortical and sub-cortical networks are involved in sequence encoding.

In the graphomotor task, subjects learned ideographic characters. Each character consisted of six movements –three line pairs, which the subjects saw on a screen, and drew (with real-time feedback). Thus the task required subjects to learn a sequence of three line-pairs (that is, two-stroke movements). By examining the

relative BOLD response of candidate neural regions participating in motor sequence encoding to each line-pair (LP), the two competing theories (serial vs. group encoding) can be tested. By averaging across each of the bins, we examined the differences in BOLD signal activity in all line-pair ones (LP1) vs. line-pair twos (LP2) vs. line-pair threes (LP3). If Grossberg, et al.'s model (Cohen & Grossberg, 1986) is correct, then the average neuronal effort for LP1 should be greater than for LP2, which should be greater than for LP3 ($LP1 > LP2 > LP3$) by the end of the sequence learning process. This decreasing pattern would indicate that LP1 has been encoded multiple times (LP1; LP1+LP2; LP1+LP2+LP3), which would reflect serial encoding. If the Verwey, et al., model is correct, then the neuronal effort reflected in the BOLD response should be the same for all three line-pairs ($LP1 = LP2 = LP3$). This equal pattern would potentially reflect the simultaneous encoding by one processor, with subsequent enactment by a separate processor.

Predictions

It is expected that candidate brain areas will show ordered encoding effects in the kinematic and neuroimaging measures. If the sequences were encoded serially, then the kinematic and neuroimaging measures of the candidate regions should reflect a higher level of performance (in the kinematic measures) for line-pair 1 (it is encoded repeatedly as the other line-pairs are attached). This repetition of line-pair 1 should also produce a larger fMRI BOLD response in candidate regions for line-pair 1 than for line-pairs 2 and 3. If the sequences are encoded simultaneously, then there should be no difference between the kinematic and fMRI BOLD response in

candidate areas for line-pairs 1, 2 and 3. It is also expected that if the sequences are encoded serially, the encoding should begin relatively early in the sequence learning process; however, if the sequence is encoded as a group, it may be encoded later in sequence learning.

Methods

Subjects

Nineteen right-handed healthy subjects were successfully scanned, with Mini-Mental Status Exam (MMSE) scores greater than 27 (mean 29.58, std 0.79). Of the nineteen, twelve subjects demonstrated significant sequence learning on the kinematic measures employed (normalized jerk, see below), and were included in the study (4F, 8M; average age = 34.08 years; std = 6.69 years) . All subjects were pre-screened for absence of seizure, neurological disorders, chronic substance abuse and chronic mental illness, as well as for MRI safety. All subjects gave informed consent, according to National Institutes of Health Protocol 92-DC0-0178, and University of Maryland IRB requirements; and were screened for MRI safety according to the National Institutes of Health Nuclear Magnetic Resonance Center Policy. Subjects were paid \$100.00 for the scan session.

Behavioral task.

In this paradigm, naïve subjects learned to draw ideographic word characters (Figure 15C) while being scanned in a 3 Tesla G.E. MRI scanner (see Figure 15A). The subjects saw an example of a pair of lines from the character, and then would

draw them on a digitizing tablet, (with real-time, visual feedback on a separate space on the screen –see Figure 15B). Each character (four characters randomly chosen from a pool of ten) that the subject learned had three pairs of lines, and was repeated 9 times each (the first 30 iterations were during the fMRI scan session). The ten characters were constrained to all have only three straight lines and three straight transitions (for a total of six lines, or three line-pair sets). Subjects drew each of the three line-pairs (1 character), and were then given visual knowledge of results (KR), showing their speed and accuracy on that character. They also received real-time visual feedback of the pen movements during the copying of each line-pair. Subjects drew their characters on a non-ferromagnetic, digitizing tablet.

Data collection.

All fMRI data was collected on a 3 Tesla, GE scanner at the National Institutes of Health, Bethesda, Maryland, USA with a standard head coil. Kinematic data was collected with a TouchScreen non-ferromagnetic, digitizing tablet (MagConcepts, Inc), sampling $\{x\ y\}$ at 66 Hz. Each subject completed a pre-scan training on drawing stars (26 stars, drawn outside the scanner), and the same task was performed in the scanner (six stars, for two and one-half minutes), in order to familiarize the subjects with the mapping of the visuomotor task in an unfamiliar position. A vacuum pillow was used to help stabilize the subject's head, and the subjects had their right arm supported by a custom designed, Plexiglas© support, to constrain motion (see Figure 15B).

A mirror on the head coil allowed the subject to see a screen, upon which instructions and the experimental tasks were presented (see Figure 15A). The start of the behavioral task was synchronized with the first TTL pulse from the GE MRI scanner, using a data acquisition card (NI-DAQ 6062e PCMCIA board, National Instruments, Austin, TX), and the Matlab data acquisition toolbox (Mathworks, Inc., Natick, MA). This allowed for the time-stamping of each instruction presented, each response made by the subject, each feedback screen, and the fixation times, all relative to the first MRI TTL pulse.

The echo-planar imaging (EPI) scan parameters for the functional images were: repetition time (TR)=2000 ms; echo time (TE)=30.0 ms; field of view (FOV)=24; slice thickness=5.0 mm; number of slices/volume=30; number of volumes=585; flip angle=90 degrees; with a voxel size of 3.75 x 3.75 x 5 mm. A high-resolution (1 mm), FSPGR anatomical scan was performed for each subject, and co-registered with the functional images in AFNI.

Data analysis.

The neuroimaging data was pre-processed in AFNI (National Institute of Mental Health, National Institutes of Health, Bethesda, Maryland, USA; see website: <http://afni.nimh.nih.gov>), with motion correction, binary masking of the brain, and 8 mm Gaussian blurring. Because the fMRI data needed to be acquired in one scan (to avoid order effects), and the total scan time (with stars task and sequence learning task) was almost 20 minutes, effects of scanner baseline drift had to be addressed.

Due to the length of the scan, the baseline (instrumental) drift was non-linear, and could not be effectively modeled using standard, AFNI methods (polort polynomial fitting). To remove spurious white matter “activation” and overall scan drift effects, each subject’s fMRI dataset was normalized by the grand mean (mean over all volumes and voxels). The average ventricle value for eight, 2 mm spherical locations (anterior and posterior ventricle locations, bilateral, at two different z levels) was collected for each subject. (Fox et al., 2006) This average (dividing on a per-volume basis) was used to remove the proportional instrumental drift over time.

To examine the order of line-pair encoding, each subject’s EPI dataset was transformed into common (Talairach) space; and was binned into the 5 time bins defined in the sequence learning kinematic (Njerk) analysis. For each time bin, the average response across all iterations (5) of the characters was computed, using the time-stamps of each first line-pair (Figure 50). A custom program (Rasmus Birn, National Institute of Mental Health, National Institutes of Health, Bethesda, MD, USA) was used to find each first line-pair time point, and to segment the dataset to include the next 18 repetition times (TRs) as lags from that time point. The BOLD responses of the five character iterations were averaged per lag, giving an average BOLD response per voxel, per line-pair, per subject, for each of the five time bins. A one sample t-test was used to examine the BOLD response for the three line-pairs, per voxel, for each time bin. Candidate neural regions (left primary motor cortex, left and right supplementary motor cortex, left ventral lateral thalamus), defined in the sequence learning analysis as being involved in graphomotor sequence learning were

examined. These regions were compared to a control (right amygdala), to examine changes in BOLD activation patterns that might reflect the organization of the line-pairs into a novel sequence, per the Grossberg, et al. or the Verwey, et al., theories.

Statistical Analyses

Kinematic

A two-way, repeated measures ANOVA, with correction for multiple comparisons was undertaken for each of the two kinematic measures: movement time (MT) and normalized jerk (Njerk), per time bin (line-pair x bin). The analyses used average MT and Njerk per time-bin as the repeated measure, with line-pair as a covariate.

Neuroimaging

In a proof of concept analysis, descriptive measures of the BOLD signal (percent signal change) per line-pair were used to determine if differences between the candidate regions and the control region could be detected. Caution: the results should be viewed as exploratory, due to the unknown effects of temporal jittering of the second and third line-pairs, which precluded meaningful statistical analyses.

Results

Kinematic

Movement time (MT) for line-pairs 1 and 2 were relatively similar during sequence learning (see Figure 51) LP3 was produced more quickly from the first

iteration, and shows a much sharper learning curve than LPs 1 and 2. A repeated measures ANOVA of MT showed significant line-pair ($p < 0.0001$), bin ($p < 0.005$), and line-pair by time-bin interaction effects ($p = 0.0001$). In a similar manner, LP3 was produced more smoothly, and demonstrated a different learning trend than LP1 and LP2 (Figure 52). A repeated measures ANOVA for Njerk indicated that there was a significant effect for line-pairs ($p < 0.0001$), and the interaction between bins and line-pairs ($p < 0.005$), but not for bins ($p > 0.05$).

Neuroimaging

The BOLD activations for each line for the right amygdala (used as a control), showed no line-pair related differences in the BOLD signal (see Figure 53). In contrast to the control, the left supplementary motor areas (SMA) showed BOLD activity that was related to the line-pairs (see Figure 54). In left SMA there appeared to be an ascending pattern ($LP1 < LP2 < LP3$) in bin 1, during the early, fast phase of motor sequence learning. During bins 2 and 3 (the beginning of the second, slower phase of sequence learning), the pattern shifted, and the BOLD response for LP2 was larger than for both LP1 and LP3. In the later time-bins (4-5), the BOLD activation pattern again shifted, with LP1 and LP2 being approximately equal; and both being larger than the response for LP3.

The clearest response to the three line-pairs was found in the left primary motor cortex (Figure 55). In bin 1, left M1 displayed an ascending pattern of BOLD activation relative to LP order ($LP1 < LP2 < LP3$). In bin 2, the pattern was similar to

the left SMA (in bins 2-3): the LP2 BOLD response was larger than the response for LP1 or LP3. However, the left M1 pattern diverges in bin 3, where the BOLD activations for the three line-pairs were equal. In bin 4, there was a descending order (LP1>LP2>LP3); and in bin 5, the BOLD activation pattern shifted to LP1=LP2; both LP1/LP2> LP3. This pattern was similar to the bin 5 pattern seen in the left SMA.

Discussion

The current study examined the kinematics of individual line-pair stroke production during the learning of novel graphomotor sequences, to find if differences due to the order of encoding were evident. There are two main, competing hypotheses on the manner in which the brain encodes sequences of actions: either serially, per Grossberg, et al. (Cohen & Grossberg, 1986), or as a group, consonant with the Verwey, et al. model (Verwey & Dronkert, 1996; Verwey, 2001; Verwey, 2003a; Verwey & Eikelboom, 2003). Because the sequence learning task (learning to draw ideographic characters) involved three, distinct sets of line-pairs, the average kinematic measure of performance (normalized jerk) could be captured for multiple time-frames (bins) during the sequence learning process. It was predicted that Grossberg, et al.'s theory of serial encoding (Cohen & Grossberg, 1986) would result in a decreasing pattern of line-pair differences in the kinematic measures of sequence learning. This difference would be due to the repeated encoding of line-pair 1, as line-pairs 2 and 3 were added to line-pair 1. However, if the group encoding model was correct (Verwey & Dronkert, 1996; Verwey, 2001; Verwey, 2003a; Verwey &

Eikelboom, 2003), there should be little or no difference between line-pairs in the kinematic results for the line-pairs.

Order of Encoding of Graphomotor Sequences

The kinematic data indicate that the third line-pair was produced in a different manner than line-pairs 1 and 2. Significant effects were found for line-pairs in repeated measures ANOVAs for movement time and normalized jerk. LP3 was produced more quickly and more smoothly throughout sequence learning than LPs 1 and 2, and had a decrease across bins (in both MT and Njerk) while LP1 and LP2 did not. LP3 had access to the error feedback from all three line-pairs, as well as the knowledge of results, while LPs 1 and 2 had less error feedback. This discrepancy may relate to the differences in kinematic performance (movement time and normalized jerk). If so, then the preliminary data do not support either the Grossberg, et al. sequential encoding model (Cohen & Grossberg, 1986), or the Verwey, et al., multi-processor group encoding theory (Verwey, 2001; Verwey, 2003a; Verwey, 2003b; Verwey & Eikelboom, 2003), but may indicate that the order of learning is dependent on the availability and quality of error feedback and knowledge of results information.

Chapter 5: Conclusions

Summary of findings

The current study consisted of two analyses: the first analysis was a systematic examination of the neural regions participating in motor sequence learning, including the temporal dynamics of each brain network's involvement, and the functional connectivity between selected regions during the learning process. The second analysis involved a kinematic examination of the order in which the elements of the novel sequence are encoded. A novel graphomotor task (drawing ideographic characters) was introduced, which proved to be effective for the combined collection of kinematic and neuroimaging data during sequence learning. A review of previous animal and human research on sequence learning, and analysis of the ideographic character task led to specific predictions of cortico-striatal, cortico-cerebellar, and cortico-cortical networks involved in sequence learning.

In the examination of the sequence learning process, the statistical analysis of a selected kinematic measure of learning (normalized jerk) resulted in the definition of a significant learning period that occurred during fMRI scanning. The kinematic data also allowed for the sectioning of the neuroimaging data into time bins that related to sections of a double exponential learning curve, which best characterized the kinematic data. The double exponential fit also indicated that an early, fast learning process merged with a slower process. The changes in BOLD activity in fMRI data over the time course of sequence learning within specific neural networks has led to a model of how the brain encodes graphomotor sequences.

A model of graphomotor sequence learning

Graphomotor sequence learning involved the interplay of numerous cortical and subcortical neural regions, as the novel sequences are learned. In early learning, visuomotor mapping involved dorsal visual stream and the dorsal premotor areas (per (Burnod et al., 1999; Caminiti & Johnson, 1992; Caminiti et al., 1996; Caminiti et al., 1998; Caminiti et al., 1999; Lacquaniti et al., 1995). The dominant role of the posterior parietal cortex in this graphomotor sequence task is consonant with the Seitz, et al. studies involving graphomotor learning (Seitz et al., 1994; Seitz et al., 1997).

Selected cortical activation and subcortical (associative basal ganglia and cerebellum) deactivation occurred during early, fast sequence learning. This pattern shifted to specific areas of subcortical activation and cortical (dorsal visual stream) inactivation in the later, slower process of sequence learning, which is reminiscent of the results from the Floyer-Lea, et al. study (Floyer-Lea & Matthews, 2004). The early deactivation of subcortical may represent a resetting function within the sequence encoding networks, as the highest level of errors (measured by Njerk) were produced in the early, fast phase.

In the second, slower learning phase, the visual regions become less active, and the encoding networks become activated –which is comparable to the findings of the Muller, et al. study (Muller et al., 2002). This indicates the shift from a predominantly visual emphasis in the first learning phase, to a motor encoding

emphasis during the second, slower phase of sequence learning. Within the second learning phase, there was also a difference between the basal ganglia and cerebellar patterns of activity. This suggests two distinct processes, perhaps related to encoding the novel characters, using knowledge of results (anterior putamen, head of the caudate nucleus); and the refinement of the motor plans for the individual line-pairs (anterior vermis). While the early cerebellar activity seen in the Hikosaka, et al. research was not evident, the activation patterns of the associative basal ganglia (aPUT, hCN) and the sensorimotor cerebellum (aVER) were comparable to Hikosaka, et al.'s model. (Hikosaka et al., 1999; Hikosaka et al., 2002a; Hikosaka et al., 2002b; Nakamura et al., 1998; Nakamura et al., 1999). The lack of early cerebellar activity in the current study may be related to the explicit error feedback given for every line-pair, which may have not necessitated the involvement of the sensorimotor cerebellum in early sequence learning.

Default mode network

The medial neural regions relate to the default mode network appeared to only become deactivated after the novel sequences had been encoded, and the task was becoming routine (bins 4-5), and –in the case of the prefrontal cortex, there was *activation* in early learning (bins 1-2). While this finding is consistent with the role of the default mode network as participating in internally-generated processes (Greicius et al., 2003; Greicius & Menon, 2004), it may indicate the suspension of such processes during attentionally-intensive tasks.

Functional connectivity and motor sequence learning

The functional connectivity analysis provides an important, alternate method of examining the fMRI data, complementary to the standard contrast methods. This analysis demonstrated, for example that some neural regions (such as the anterior putamen) participate in sequence learning prior to reaching significant levels of activity when compared to baseline.

Neural encoding of elements of motor sequences

Kinematic data indicated that the third line-pair was produced in a different manner than line-pairs 1 and 2. The third line-pair was faster and smoother, and demonstrated a learning curve; while line-pairs one and two did not. Because line-pair 3 had access to the error feedback learning of line-pairs 1 and 2, as well as the knowledge of results for the entire character, it is possible that the order of sequence encoding was related to the availability and quality of error feedback and knowledge of results. While this finding does not directly support either the Grossberg, et al., or the Verwey, et al. models of sequence encoding, it does demonstrate that effects related to the order of encoding can be detected by kinematic techniques.

Taken together, a model of graphomotor sequence learning emerges, including patterns of neural activation and functional connectivity that correspond to changes in subject performance, and differences in performance and hemodynamic measures of neural activity related to the order of sequence encoding. This model adds to our current understanding of the neural substrates of graphomotor sequence

learning, and may be important in explaining the alterations to these networks in persons with neurodegenerative disorders.

Limitations

Methodological issues and limitations.

For all current neuroimaging techniques, there are limitations to the temporal and spatial precision of the data that is collected. Because the current study examined learning, one long fMRI scan was needed. This necessitated the use of a longer repetition time (due to fMRI scanner limitations), which reduced the temporal resolution of the dataset. In addition, because of the repetitions needed to overcome instrumental noise (and the relatively small size of the change in the BOLD signal), the length of the time bins used to examine the temporal dynamics of sequence learning was limited to approximately 100 volumes (200 seconds), before the effect was lost.

An issue that arose during data collection was one of physical movement (jittering) of the non-ferromagnetic digitizing tablet during kinematic data collection, which resulted in the loss of data for three subjects. Subsequent testing found that the custom made stand fabricated to hold the tablet and the subject's arm steady during the task had worn, resulting in an x-axis jitter during the data collection. Additional supports restored the tablet holder to its previous state, and data collection resumed.

In addition to the temporal limitations of the fMRI data, the kinematic data temporal resolution was constrained as well. Kinematic data collection was limited to 66 Hz, which was caused not by the tablet itself (able to send {x,y,z} at up to 500 Hz), but rather by the limited refresh rate of computer video card.

Multiple artifacts were produced by having one, long scan. Baseline drift during data collection created 2 types of artifact: spurious white matter “activity” and a progressive, negative drift over the five time-bins, as GE scanners drift downwards over scan time (Friedman & Glover, 2006). The inability to model with conventional methods (linear, quadratic, cubic detrending) necessitated the use of grand mean and ventricle average normalization (as described in the Methods section, Chapter 3)(Fox et al., 2006). It is possible that this combination of established data processing schemes be idiomatic to current study, and may be of little use for other studies using long scan times. A systematic evaluation of this method and other methods of baseline artifact removal for long scans is needed, before these methods can be applied.

In the examination of line-pair encoding order, the fMRI analysis was preliminary and descriptive. Subsequent statistical measures could test differences in the fMRI BOLD response for each of the line-pairs. The use of a deconvolution methodology, (instead of averaging the BOLD signal across all character iterations within the bins), would better control for timing discrepancies and baseline drift.

Theoretical limitations

A significant theoretical issue in the current study is the distinction between Learners vs. Non-Learners. While the subjects who were defined as “Learners” showed both a negative normalized jerk trend and had their final iteration Njerk score lower than the initial iteration, the methodology for defining learners is arbitrary. This method was substantiated by the repeated measures ANOVA showing that Learners had significant differences in Njerk performance over the 30 iterations; while the Non-Learners did not; but a more comprehensive and methodological study of the differences in Learners and Non-Learners (differences in both kinematic performance and neural activation patterns) is needed.

An additional limitation of the current study is that the measure of learning used (normalized jerk) represents only one aspect of learning –the changes in smoothness of hand / pen movements during sequence learning. If another measure was used, the learning curve could vary, which would influence the interpretation of both the kinematic and neuroimaging data. In a similar manner, the nature of the task used (the ideographic character graphomotor sequence learning task) emphasizes certain processes (i.e. visual encoding), and de-emphasize others (early exploration). The type of task used limits the generalizability of the current results.

A final limitation of the study lies in the composition of the baseline. In addition to simple visual processing (visual fixation on a plus sign), complex visual processing (feedback screen) and a simple hand motion were included as baseline

tasks. While these additions were theoretically driven (to remove effects not directly related to motor sequence learning), the choice of these tasks and their inclusion was arbitrary. To reduce the effect of this methodological choice on the reader, plots of the main interaction between regions of interest were included, which can be interpreted in a baseline-free manner (trends only).

Further Research

Additional uses for current research methodology

Parkinson's disease patients have been shown to have deficits in sequence learning (Carbon et al., 2004; Carbon & Eidelberg, 2006; Ghilardi et al., 2006; Siegert et al., 2006). The same kinematic and neuroimaging methodology could be used for a comparison of clinical populations (Parkinson's disease, stroke patients) with healthy controls, to examine the neural regions associated with abnormal motor sequence learning.

It would also be interesting to use the current paradigm with transcranial magnetic stimulation (TMS) or other inactivation method, to isolate the roles of pre-frontal, cerebellar and parietal regions in sequence learning (Arunachalam et al., 2005; Koch et al., 2006; Lee & van Donkelaar, 2006; Schluter et al., 1999). Another possibility that we are pursuing is to modify the sequence learning task, so that instead of learning to draw sequences of lines, sequences of nonsense words (mapping the movement trajectories to a roughly analogous vocal space) would be learned, in order to examine sequence learning in speech (Smith et al., 1996; Ullen &

Bengtsson, 2003; Ullen et al., 2005). In this study, comparisons between motor sequence learning in distal limb (hand) and in vocal / speech modalities could then be made.

Tables

Table 1	Early Activations		Late Activations		Main Point
Studies	Ipsi	Contra	Ipsi	Contra	
Seitz, et al., 1994 (PET, n=8, graphomotor copying).	+DN +Ver	+M1	+DN / +Ver +PM +ICC +ESC	+M1 +SMA	Multiple kinematic representations are stored in the PPC.
Seitz, et al., 1997 (PET, n=8, graphomotor copying).	+DN +Ver +SMG +PC +IPS +sPL	+M1 +PM +FMC +aPL +pPL	>DN / >Ver +aCB <IPS +sPPC	+M1 +PM	Learning new movements involves the cerebellum; overlearned movements, the PM cortex.
Sakai, et al., 1998 (fMRI, n=7, trial & error pointing).	+dIPFC +pre-SMA +IPS +pre-CU	+IPS +pre-CU	<IPS <pre-CU	>dIPFC >pre-SMA <IPS <pre-CU	Learning new sequences require frontal activity; retrieval involves parietal activation.
Müller, et al., 2002 (fMRI, n=7, explicit learning with serial reaction time task (SRTT)).	+sPL +dIPFC	+sPL +CN +PM	+PCH	+TOC +sFC +PHC	Early learning related to PFC – CN interaction; late learning involves increased BG and CB activity as the task is automated.
Floyer-Lea, et al., 2004 (fMRI, n=15, hand pressure tracking)	+PM +S1 +SMA +PFC, +FP +BG, +TH +CC	+PM +S1 +SMA +PFC +BG, +TH +CC	>FP >PFC >PM >S1 >SMA >BG >TH >CB <DN <vPUT <TH	>FP >PFC >PM >S1 >SMA >BG >TH >CB <DN <vPUT <TH	Early learning related to PFC – CN network (PFC, bilateral S1, PPC, DN, CH); in later learning these areas were reduced, and there were increases in DN, TH & PUT.
Penhume, et al., 2005 (PET, n=12, timed, synchronous finger taps).	+CC +SMA +pre-SMA +STG +mCLob- (V/VI/VIIa)	+CC +SMA +pre-SMA +STG +mCLob- (V/VI/VIIa)	+PUT +sPL +iPL +oFC	+M1 +PM	Early activation in cerebellar hemispheres related to error correction; with DN output to M1 encoding learning.
Lehericy, et al., 2005 (fMRI, n=14, finger movements –key press).	+dPUT +adGP +STN	+dPUT +adGP +STN	(session 1) >adPUT <pvPUT	(session 1) >adPUT <pvPUT	Motor representations learned in anterior BG; stored in posterior BG for increase speed.

(+ =Increase; - = Decrease; > = Reduced from prior state; < Increased; Ipsi = Ipsilateral to hand; Contra = Contralateral); d = dorsal; v = ventral; l = lateral; m = medial; a = anterior; p = posterior; o = orbital; s = superior; I = inferior; PM=pre-motor cortex; PFC=prefrontal cortex; M1=primary motor cortex; S1=primary somatosensory cortex; SMA=supplementary motor area; FP=frontal pole; BG=basal ganglia; TH=thalamus; GP=globus pallidus; STN=sub-thalamic nucleus; PUT=putamen; PL=parietal lobule; FC=frontal cortex; STG=superior temporal gyrus; CLob=cerebellar lobule; CC=cerebellar cortex; pre-CU=pre-cuneus; IPS=intra-parietal sulcus; PPC=posterior parietal cortex; DN=dentate nucleus; VER=vermis; FMC=fronto-medial cortex; ESC=extrastriate cortex; pre-SMA=pre-supplementary motor area; PHC=parahippocampal; TOC=temporal-occipital cortex.

Table of Percent Signal Changes for Selected Regions of Interest

Region of Interest	Percent Signal Change					Talairach Location
	Bin 1	Bin 2	Bin 3	Bin 4	Bin 5	
LEFT HEMISPHERE						
Left Amygdala	- <u>0.326</u>	-0.180	+0.036	+0.191	+0.243	[29 7 -13]
Left Hippocampus	- <u>0.367</u>	- <u>0.143</u>	+0.070	+0.181	+ <u>0.185</u>	[30 14 -11]
Left Parahippocampal Gyrus	- <u>0.523</u>	- <u>0.112</u>	+0.121	+ <u>0.280</u>	+ <u>0.251</u>	[22 24 -12]
Left Temporal Pole	- <u>0.412</u>	- <u>0.125</u>	-0.020	+0.130	+ <u>0.406</u>	[42 -5 -23]
Left Dentate Nucleus	- <u>0.326</u>	-0.075	+0.109	+ <u>0.240</u>	+ <u>0.296</u>	[28 49 -26]
Left Medial Head of Caudate	- <u>0.280</u>	- <u>0.107</u>	+ <u>0.070</u>	+ <u>0.196</u>	+ <u>0.173</u>	[7 -15 0]
Left Anterior Putamen	- <u>0.146</u>	+0.004	+ <u>0.128</u>	+ <u>0.184</u>	+ <u>0.175</u>	[28 -5 4]
Left Posterior Putamen	-0.052	+0.044	+ <u>0.096</u>	+0.089	+0.088	[29 10 6]
Left Ventral-Lateral Thalamus	- <u>0.134</u>	+0.010	+ <u>0.083</u>	+ <u>0.128</u>	+0.091	[11 13 10]
Left Anterior Ventral Insula	- <u>0.459</u>	-0.023	+ <u>0.208</u>	+ <u>0.192</u>	+ <u>0.235</u>	[42 -5 -8]
Left Primary Motor Cortex	-0.015	+ <u>0.120</u>	+ <u>0.210</u>	+ <u>0.279</u>	+0.114	[43 13 51]
Left Dorsal Pre-Motor Cortex	+ <u>0.204</u>	+ <u>0.184</u>	+ <u>0.148</u>	+0.183	+0.073	[29 5 52]
Left Supplementary Motor Area	+0.020	+0.052	+ <u>0.107</u>	+0.177	+0.151	[4 5 58]
Left Pre-Supplementary Motor Area	-0.099	-0.030	-0.011	+0.039	-0.051	[5 -9 57]
Left Fusiform Gyrus	+0.176	-0.064	- <u>0.337</u>	- <u>0.343</u>	- <u>0.265</u>	[28 68 -12]
Left Lingual Gyrus	- <u>0.289</u>	- <u>0.195</u>	-0.129	-0.108	-0.107	[13 71 -9]
Left V5 / MT	+ <u>0.252</u>	+ <u>0.211</u>	+ <u>0.224</u>	+0.181	+0.013	[42 62 -2]
Left Superior Parietal Lobule	+ <u>0.576</u>	+ <u>0.300</u>	+0.038	-0.035	-0.102	[18 62 55]
Left Inferior Parietal Lobule	+ <u>0.400</u>	+ <u>0.223</u>	+ <u>0.143</u>	+0.117	-0.055	[34 45 45]
Left Middle Temporal Gyrus	+ <u>0.189</u>	+0.033	-0.036	-0.002	+0.009	[53 60 -10]
Left Frontal Pole	+ <u>0.503</u>	+ <u>0.180</u>	-0.111	- <u>0.339</u>	- <u>0.372</u>	[12 -58 -2]
Left Dorso-Lateral Pre-Frontal Cortex	+0.013	+0.094	+ <u>0.080</u>	-0.018	- <u>0.243</u>	[27 -22 47]
Left Anterior Vermis	- <u>0.583</u>	- <u>0.245</u>	+0.094	+ <u>0.299</u>	+ <u>0.472</u>	[8 36 -16]
Left Primary Somatosensory Cortex	+0.088	+0.136	+ <u>0.207</u>	+ <u>0.281</u>	+0.107	[46 30 49]

Legend: Differences from Baseline (BL):

0.000 = Not significantly different from BL
0.000 = Positively different from BL (p<0.05)
0.000 = Positively different from BL (p<0.01)
0.000 = Positively different from BL (p<0.001)

0.000 = Negatively different from BL (p<0.05)
0.000 = Positively different from BL (p<0.01)
0.000 = Positively different from BL (p<0.001)

MEDIAL

Region of Interest	Percent Signal Change					Talairach Location
	Bin 1	Bin 2	Bin 3	Bin 4	Bin5	
Medial Cerebellum	-0.322	-0.057	+0.167	+0.333	+0.318	[-11 58 -42]
Medial Posterior Vermis	-0.324	-0.070	+0.187	+0.289	+0.301	[5 49 -18]
Medial Subgenual Anterior Cingulate	-0.316	-0.146	+0.110	+0.300	+0.302	[0 -32 2]
Medial Dorsal Cingulate Cortex	+0.010	+0.037	+0.131	+0.079	-0.027	[2 -5 27]
Medial Posterior Cingulate Cortex	-0.154	-0.149	-0.036	-0.112	-0.261	[2 44 32]

RIGHT HEMISPHERE

Region of Interest	Percent Signal Change					Talairach Location
	Bin 1	Bin 2	Bin 3	Bin 4	Bin5	
Right Amygdala	-0.413	-0.205	-0.002	+0.183	+0.239	[-31 6 -13]
Right Hippocampus	-0.222	-0.112	+0.018	+0.103	+0.156	[-29 15 -11]
Right Parahippocampal Gyrus	-0.212	-0.063	-0.023	+0.041	+0.145	[-22 24 -12]
Right Temporal Pole	-0.140	-0.055	-0.021	+0.020	+0.093	[-36 -4 -24]
Right Dentate Nucleus,	-0.413	-0.133	+0.110	+0.318	+0.449	[-25 45 -26]
Right Medial Head of Caudate	-0.240	-0.139	+0.050	+0.176	+0.206	[-5 -8 -2]
Right Anterior Putamen	-0.227	-0.058	+0.093	+0.191	+0.244	[-19 -8 0]
Right Posterior Putamen	-0.030	+0.019	+0.078	+0.073	-0.000	[-29 10 6]
Right Ventral-Lateral Thalamus	-0.183	-0.042	+0.076	+0.100	+0.173	[-13 12 4]
Right Anterior Ventral Insula	-0.313	-0.195	-0.025	+0.135	+0.206	[-33 -15 -6]
Right Primary Motor Cortex	+0.022	+0.063	+0.070	+0.094	+0.015	[-41 12 51]
Right Dorsal Pre-Motor Cortex	+0.244	+0.226	+0.191	+0.132	+0.028	[-28 6 52]
Right Supplementary Motor Area	+0.005	+0.041	+0.080	+0.149	+0.125	[-4 4 58]
Right Pre-Supplementary Motor Area	-0.024	-0.016	-0.002	+0.028	-0.068	[-4 -9 57]
Right Fusiform Gyrus	+0.242	+0.042	-0.170	-0.305	-0.407	[-28 68 -12]
Right Lingual Gyrus	-0.238	-0.220	-0.160	-0.113	-0.084	[-12 71 -6]
Right V5 / MT	+0.191	+0.211	+0.196	+0.118	+0.001	[-38 62 -2]
Right Superior Parietal Lobule	+0.079	+0.215	+0.218	+0.217	+0.123	[-20 60 56]
Right Inferior Parietal Lobule	+0.259	+0.254	+0.212	+0.178	+0.006	[-35 39 46]
Right Frontal Pole	+0.261	+0.047	-0.022	-0.150	-0.370	[-10 -65 7]
Right Dorso-Lateral Pre-Frontal Cortex	-0.027	-0.013	-0.011	-0.033	-0.133	[-29 -22 46]
Right Anterior Vermis	-0.533	-0.234	+0.045	+0.334	+0.549	[-8 35 -16]
Right Primary Somatosensory Cortex	+0.010	+0.107	+0.112	+0.123	+0.025	[-44 24 49]

Legend: Differences from Baseline (BL):

0.000 = Not significantly different from BL

0.000 = Positively different from BL (p<0.05)

0.000 = Positively different from BL (p<0.01)

0.000 = Positively different from BL (p<0.001)

0.000 = Negatively different from BL (p<0.05)

0.000 = Positively different from BL (p<0.01)

0.000 = Positively different from BL (p<0.001)

Figures

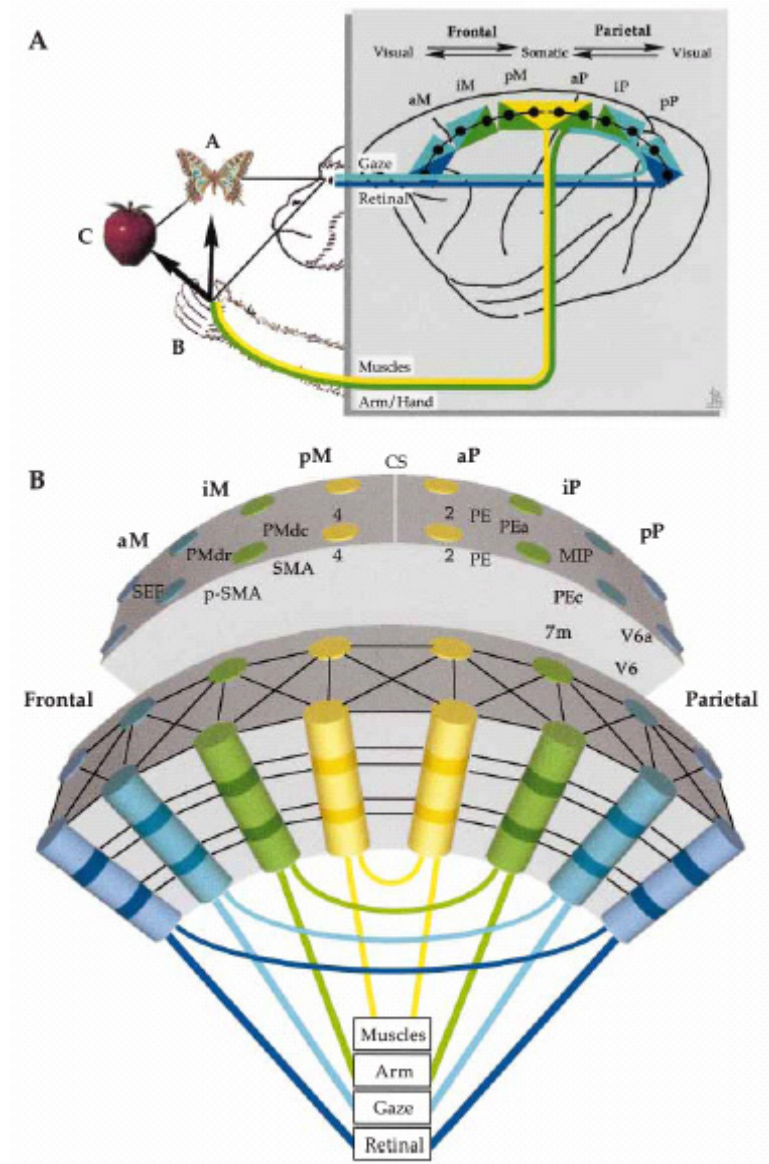


Figure 1 Frontal-parietal network for reaching (per Bernod, et al., 1999). A. Retinal information (dark blue) represents information about the hand and target location as the monkey moves his hand to the target. Gaze information (light blue) contains information about the direction and movement of eye position (gaze). Arm and hand position and direction are represented in the green. Muscle commands and proprioceptive feedback of arm dynamics. B. The distribution of tuned neuron populations forms a visual to somatic gradient along the parietal to frontal axis. The overlapping regions of tuned neurons create functional domains that combine and distribute signals

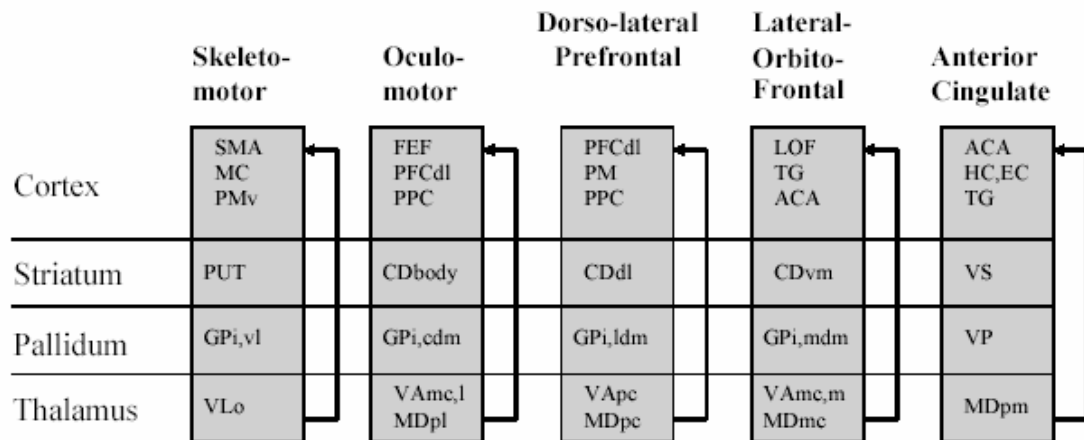


Figure 2 Multiple, cortico-basal ganglia loops (Alexander et al., 1986). Regions related to sequence learning include putamen (PUT); globus pallidus, internal (GPi); and ventral lateral thalamus (Vlo)

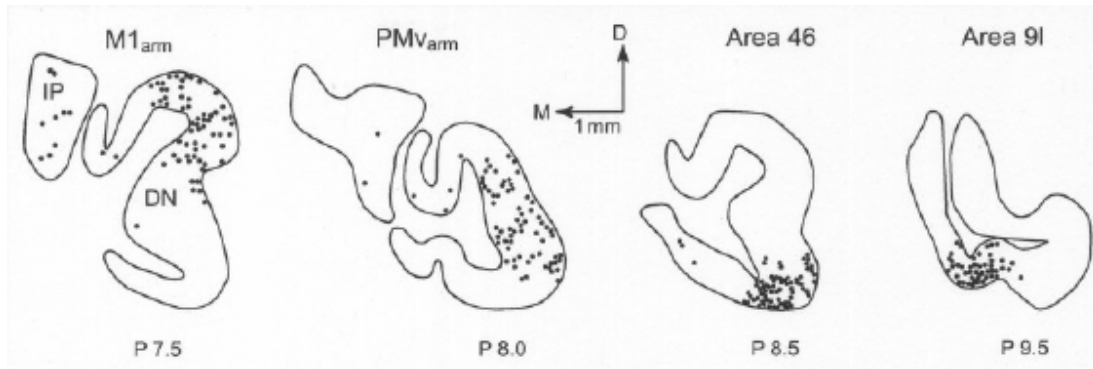


Figure 3 Multiple cerebellar output channels from the dentate project to diverse cortical regions, which connect to the same cerebellar area (Middleton & Strick, 2000a)

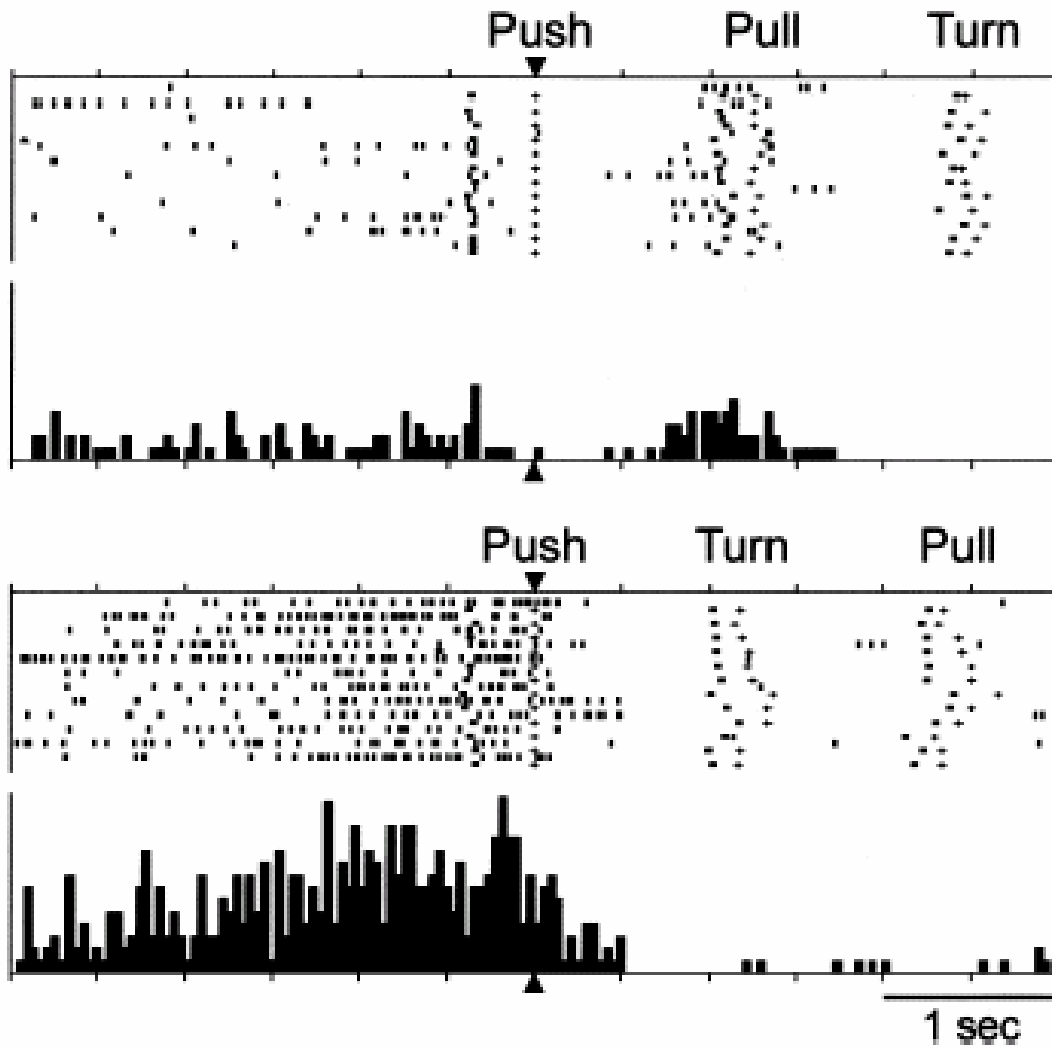


Figure 4 Activity of a pre-supplementary motor neuron in monkey during the waiting period before the performance of an incorrect (top) and correct (bottom) sequence of movements (Tanji, 2001)

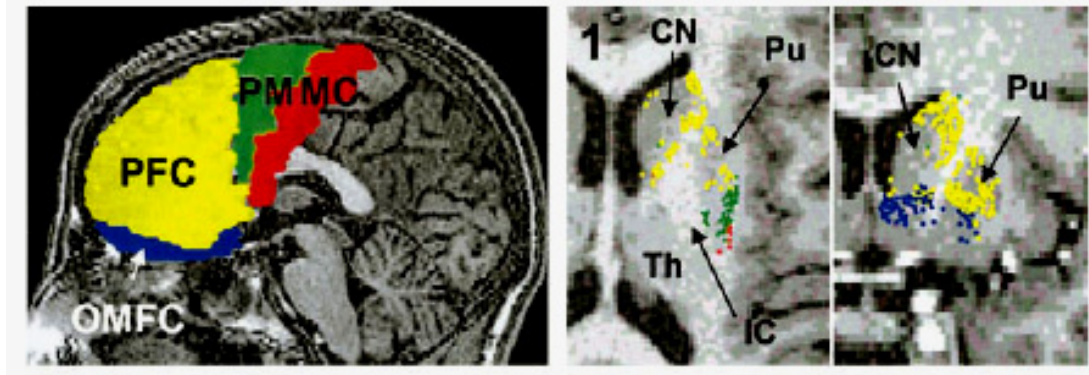


Figure 5 Axonal tract tracing from the cortex to the striatum (modified from Lehericy, et al., 2004)

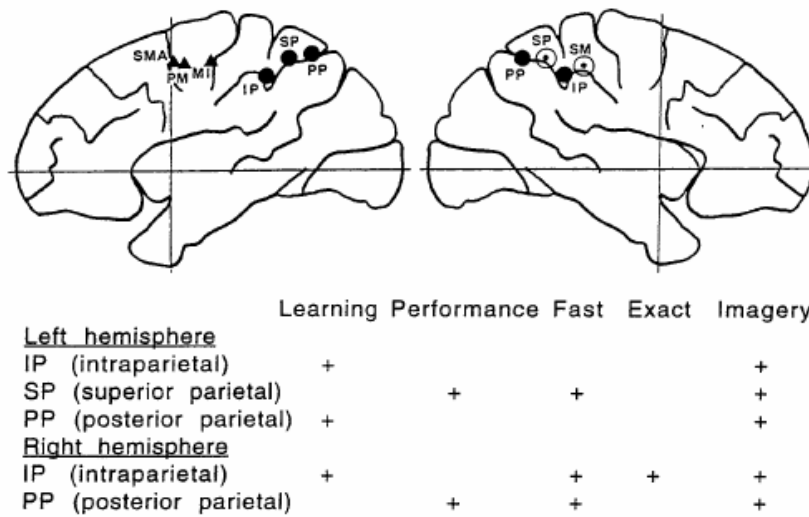


Figure 6 Cortical regions activated during the learning of a graphomotor trajectory sequence under different performance conditions (Seitz, et al., 1997)

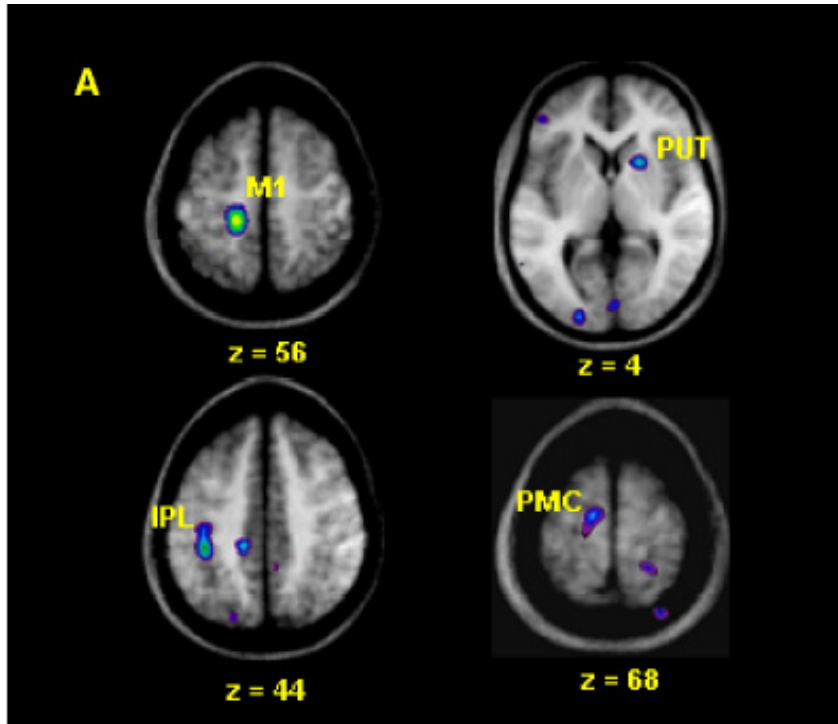


Figure 7 Cortical regions activated during the learning of a finger movement sequence in the third vs. second learning blocks (adapted from Penhume & Doyon, 2005). M1 = primary motor cortex; PUT = putamen; IPL = inferior parietal lobule; PMC = pre-motor cortex.

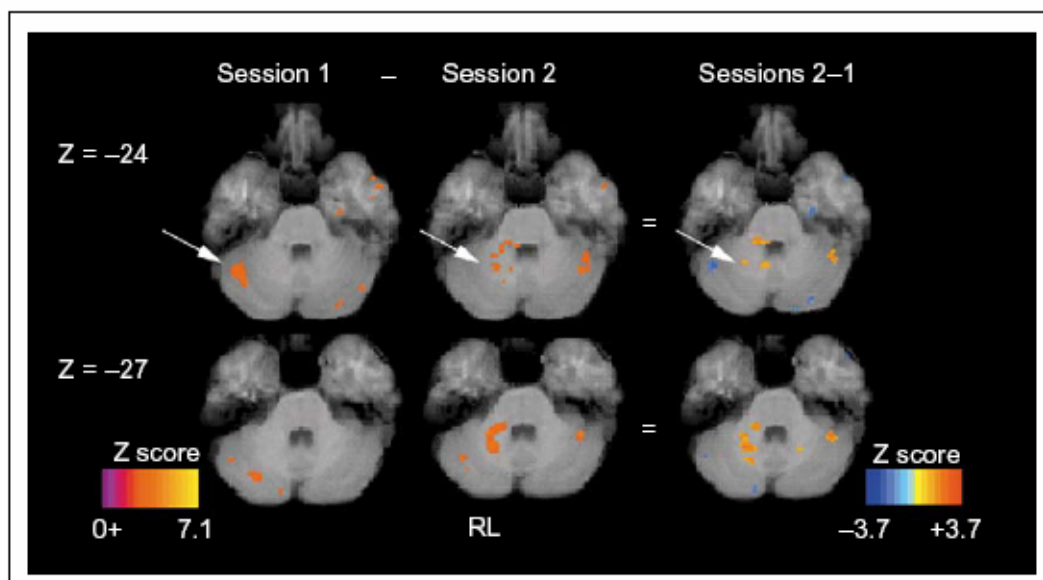


Figure 8 Changes in cerebellar activation during the learning of a sequence of finger movements (Doyon & Benali, 2005)

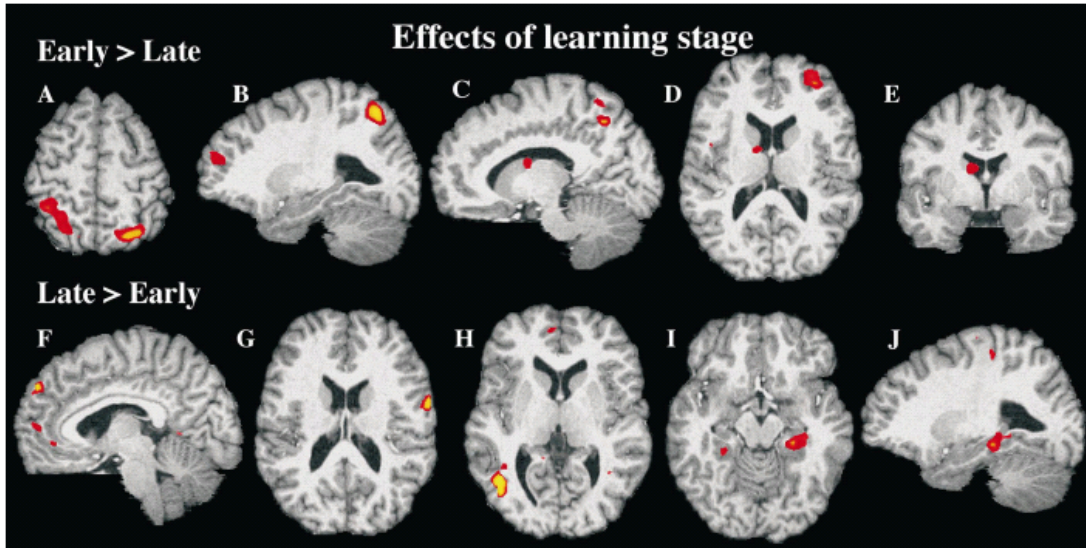


Figure 9 Comparison of activations in early vs. late learning, using a modified (explicit) serial reaction time task (Müller, et al., 2002)

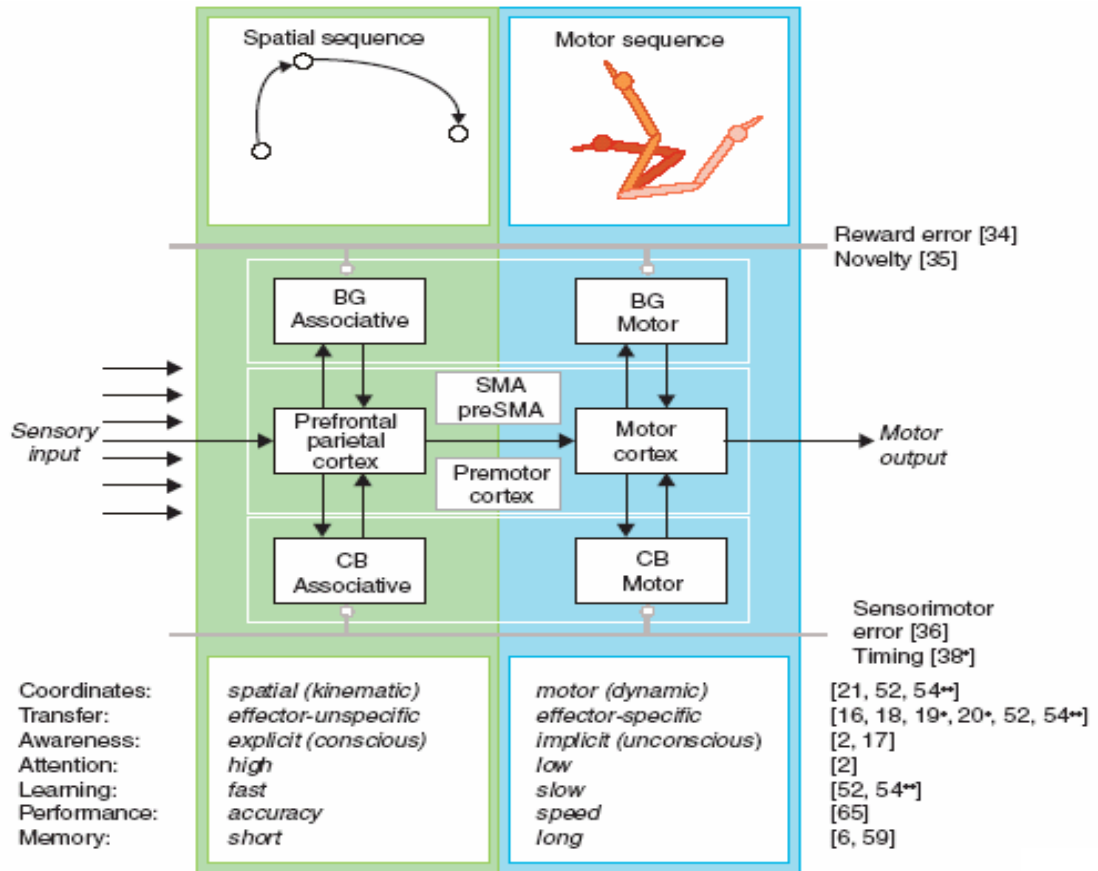


Figure 10 Hikosaka, et al. model of motor sequence learning (Hikosaka, et al., 2002)

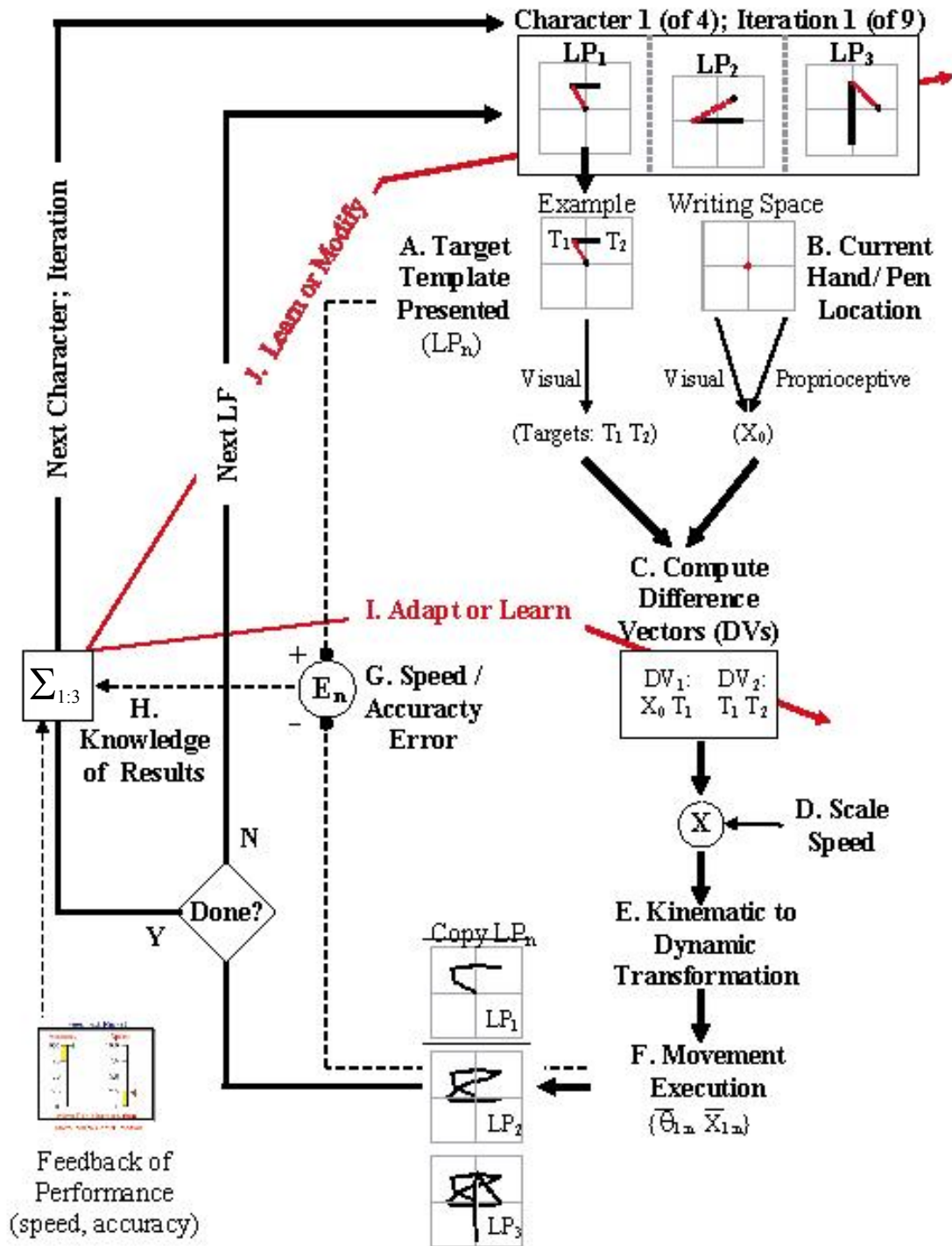


Figure 11 Task analysis of the Chinese character sequence learning task: presentation of the target template for first line-pair (A); visuomotor mapping (B); kinematic planning (C); scaling the speed of the motor plan (D); kinematic to dynamic transformation (E); movement execution (F); computation of speed and accuracy errors (G); knowledge of results (H); modification of DVs in individual line-pairs (I); and modification of DVs for whole character sequence (J).

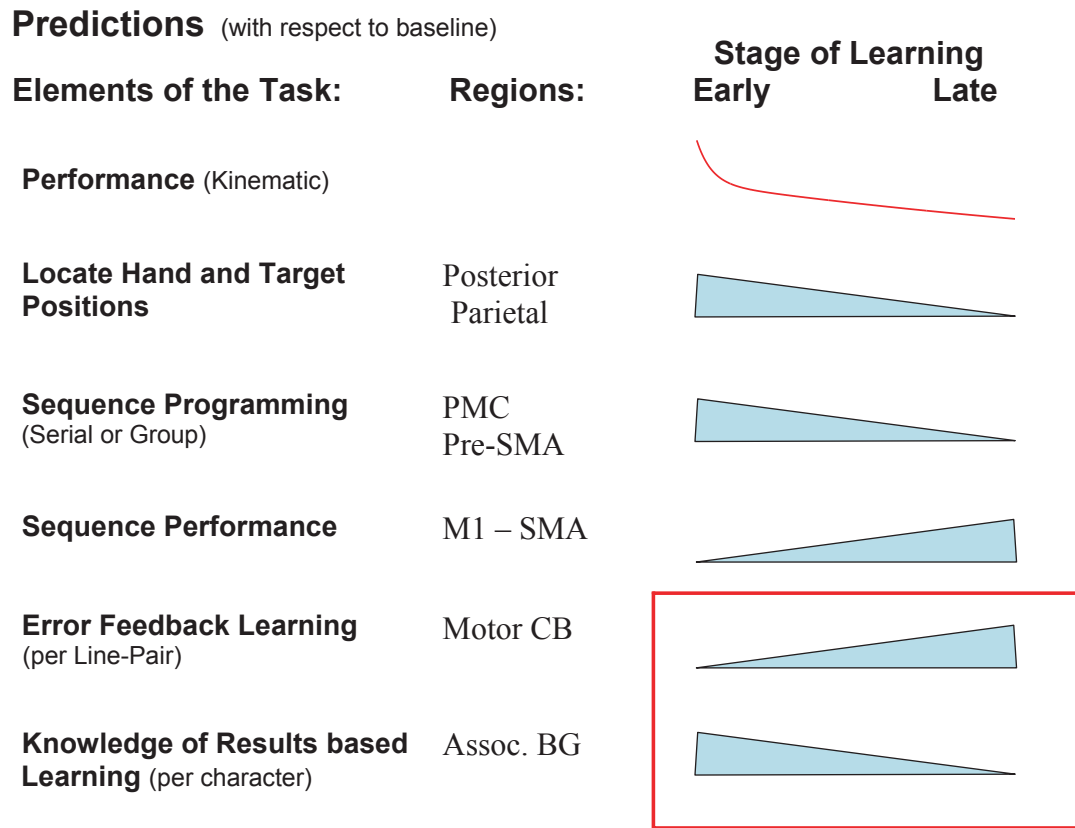


Figure 12 Predicted timing of the elements of the task analysis of the graphomotor sequence learning task. **Note:** all of the elements are involved throughout sequence learning; what is depicted are the relative emphases during the process

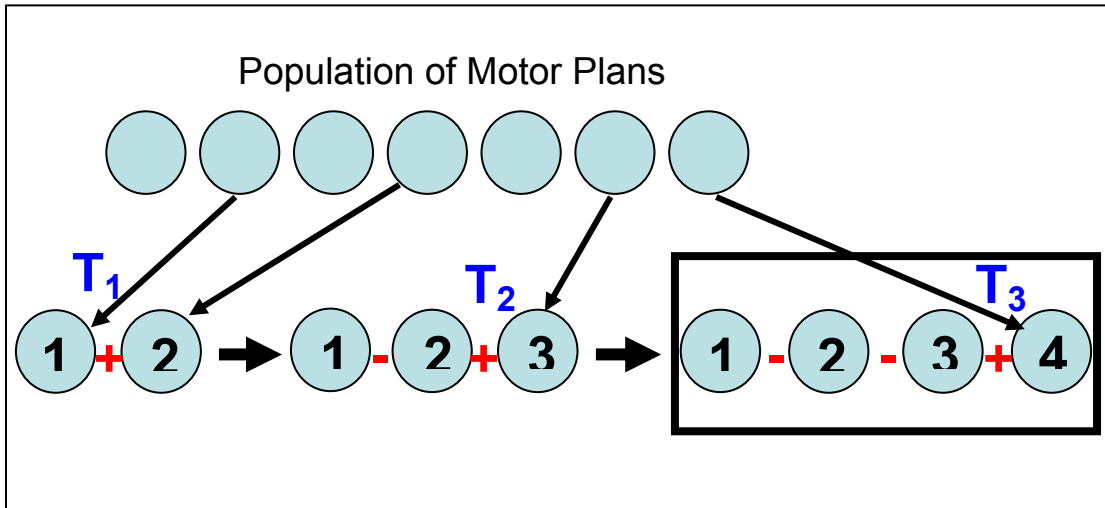


Figure 13 Model of serial encoding of motor sequences, per Grossberg (Cohen & Grossberg, 1986)

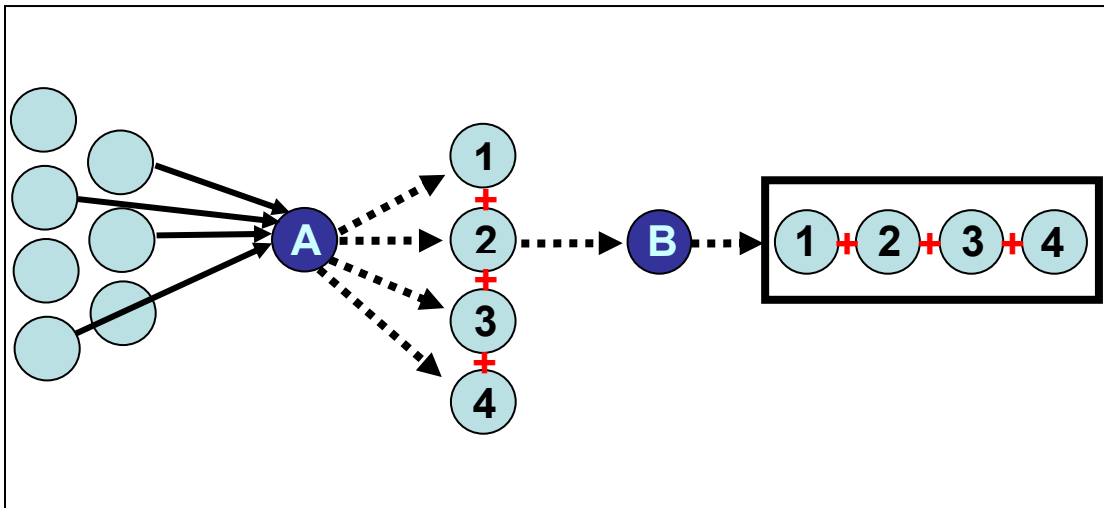


Figure 14 Model of group encoding of motor sequences (per Verwey, et al., 2001, 2003)

A



B



C

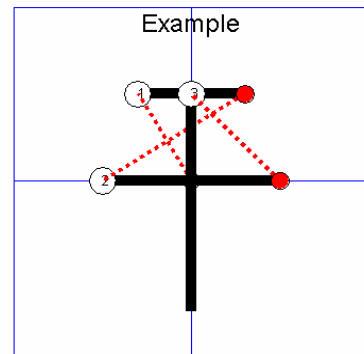


Figure 15A-C Experimental setup. A. Position of the subject in the scanner –subject views screen through mirror on the head coil. B. The non-ferromagnetic, digitizing tablet mounted on the holder and arm support. C. Example of a Chinese word character (starts from the center)

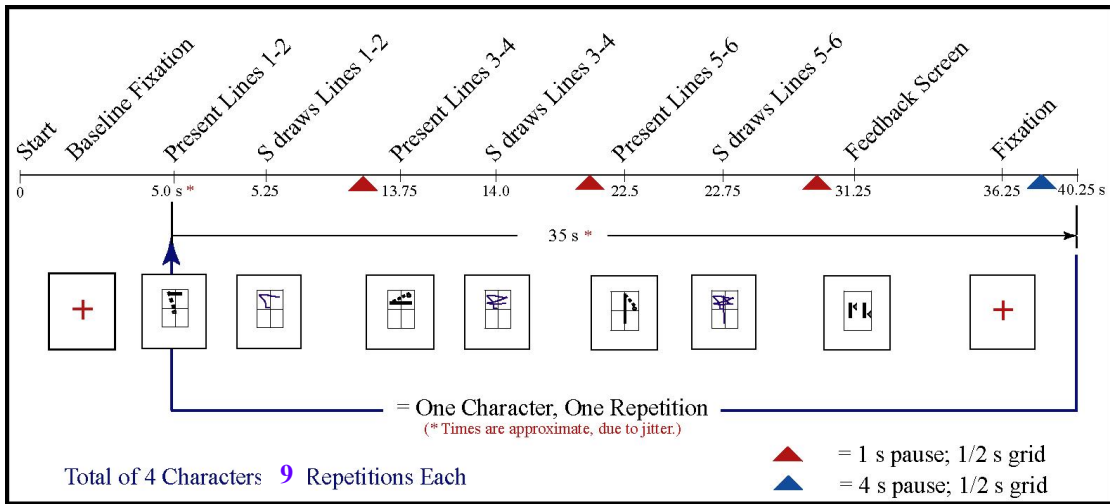


Figure 16 Behavioral time line detail for fMRI study

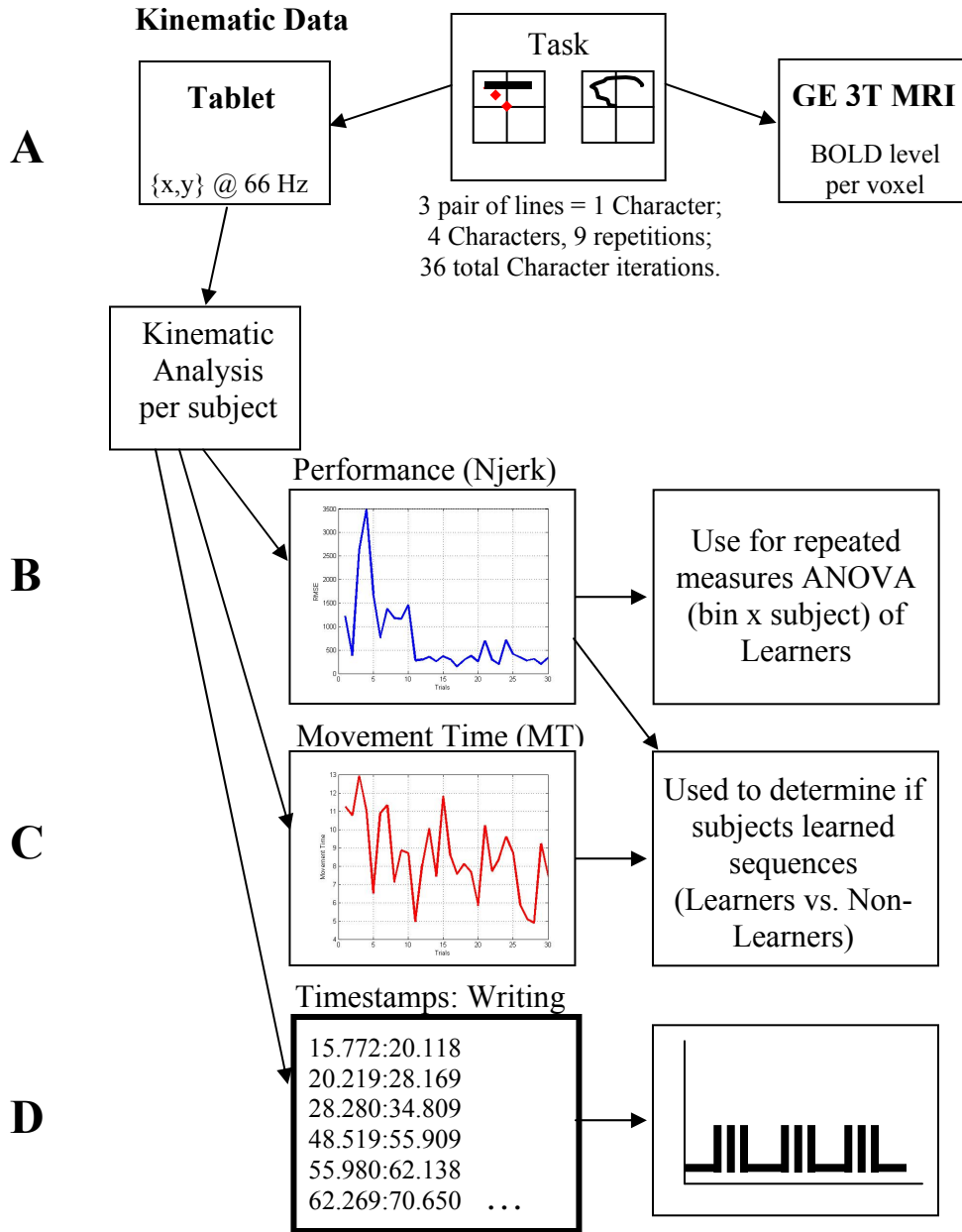


Figure 17A-D The $\{x,y\}$ data from the kinematic data was analyzed per character by computing normalized jerk (Njerk – B), which was used as a measure to determine Learners from Non-Learners with movement time (MT –C). Njerk was also used in a repeated measures ANOVA, to determine if significant learning of the sequences occurred, and if so, to identify a learning period. The timestamps of when the subject wrote each line-pair were transformed into a format for use by AFNI's waver function, to produce a predicted hemodynamic response function (HRF)

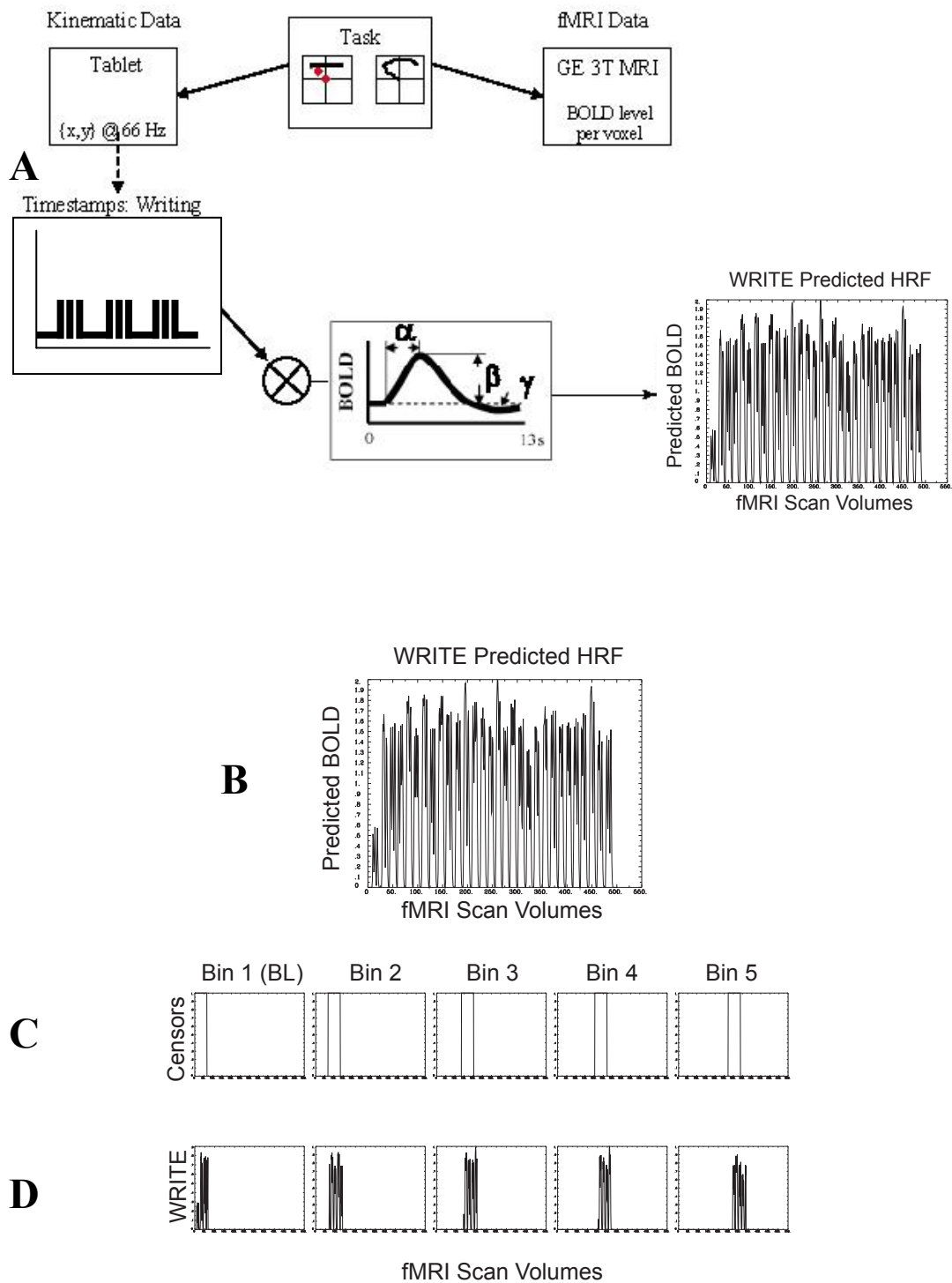


Figure 18A-D A. The predicted hemodynamic response function (HRF) for writing only for one subject, created by convolving the time series of writing times with a gamma function (AFNI: waver function). B. The predicted HRF for writing times were multiplied by censor files for each time bin within the learning period (C) to produce predicted HRFs for each time bin

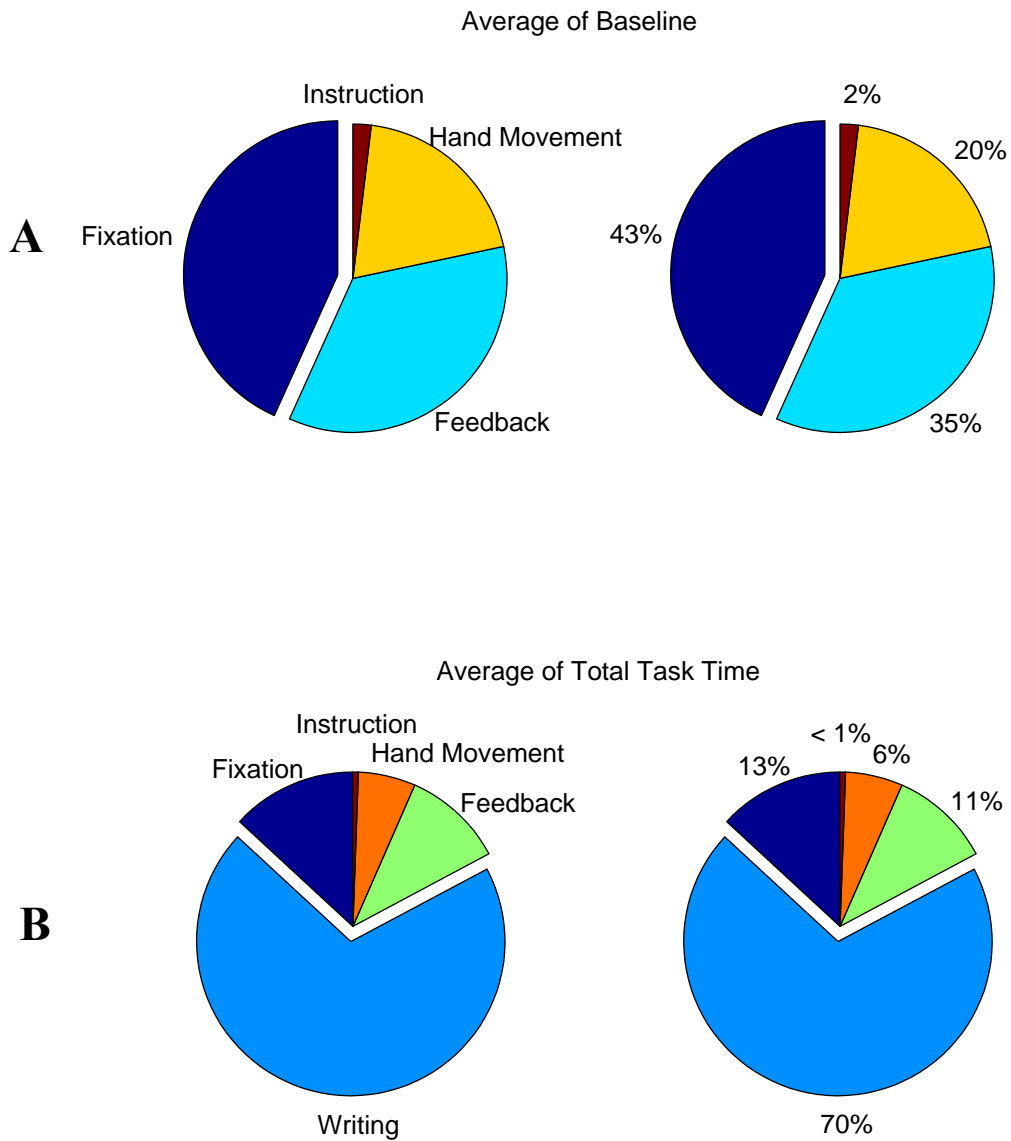


Figure 19A-B A. The relative composition of the baseline included the fixation screen (a plus sign); complex visual stimuli (performance feedback screen); and a simple hand motion (one inch to the left, then back to the center position). B. Baseline activities as they relate to the overall behavioral paradigm

$$\text{Fit} = 29010 * \exp(-0.016749 * x) + 22734 * \exp(-0.75964 * x); x=\text{Iterations}$$

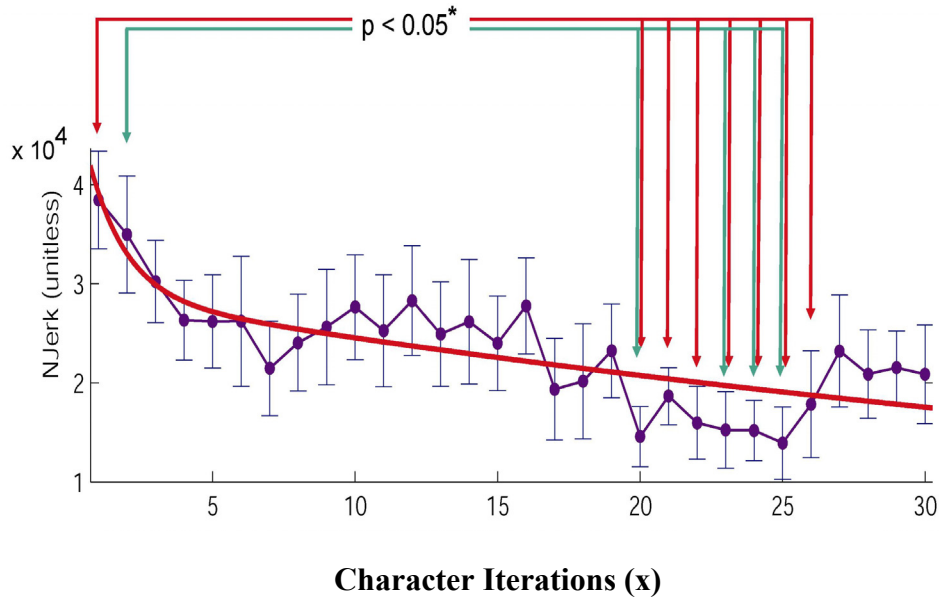


Figure 20 Average normalized Jerk (NJerk), with repeated measures ANOVA (Bonferroni corrected for multiple comparisons). Significant differences between bins 1-2 and bins 20-26 define an average learning period. Errorbars are one standard error; fit is double exponential (adjusted $r^2 = 0.66$)

$$\text{Fit} = 29010 * \exp(-0.016749 * x) + 22734 * \exp(-0.75964 * x); x=\text{Iterations}$$

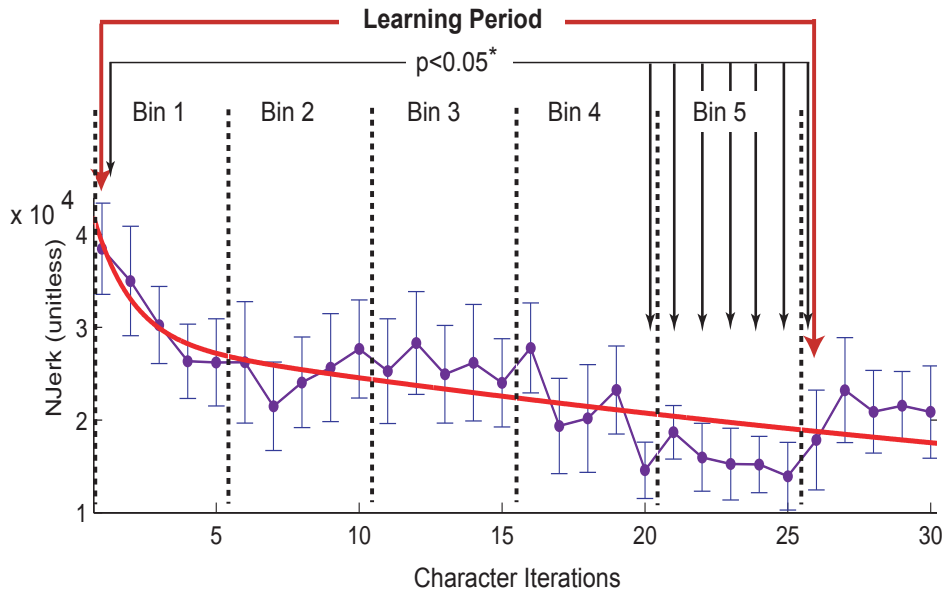


Figure 21 Division of the average learning period into five equal bins

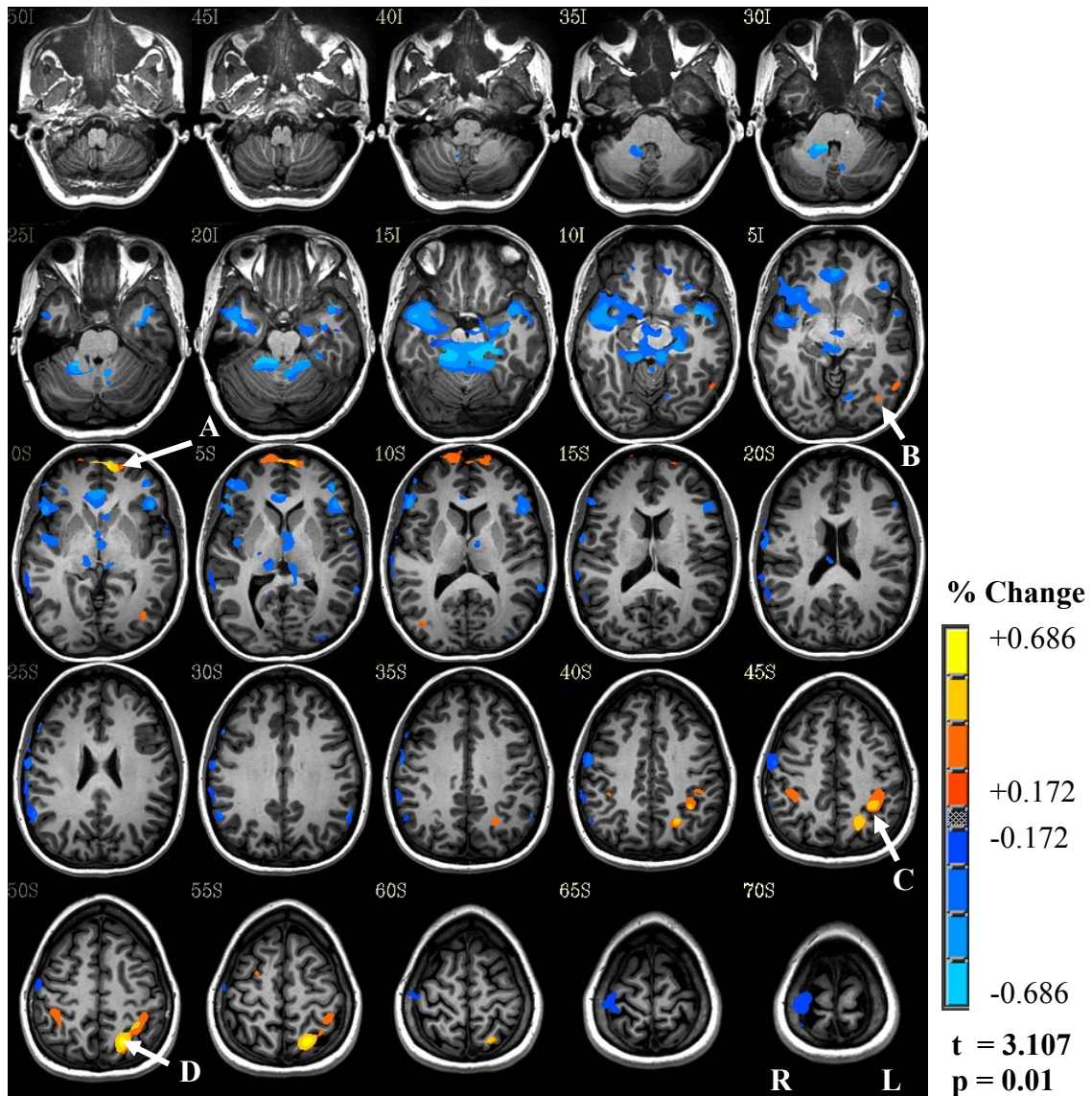


Figure 22 Bin 1 of graphomotor sequence learning. All images are functional MRI group statistics (repeated measures ANOVA, $p < 0.01$; with a $p < 0.05$ minimum cluster size threshold to control for type I error, per Monte Carlo simulation), presented over a high-resolution anatomical MRI of one subject from the group. All images are in radiological convention (left = right); coordinates are Talairach-Tournoux, in RAI order (right to left; anterior to posterior; inferior to superior; in mm), and represent the center of maximal activity for that region. Z level is noted on top left of each slice. Area A is left frontal pole [12 -58 -2]; B is left fusiform gyrus [28 68 -12]; C is left inferior parietal lobule [34 45 45]; D is left superior parietal lobule [18 62 55]

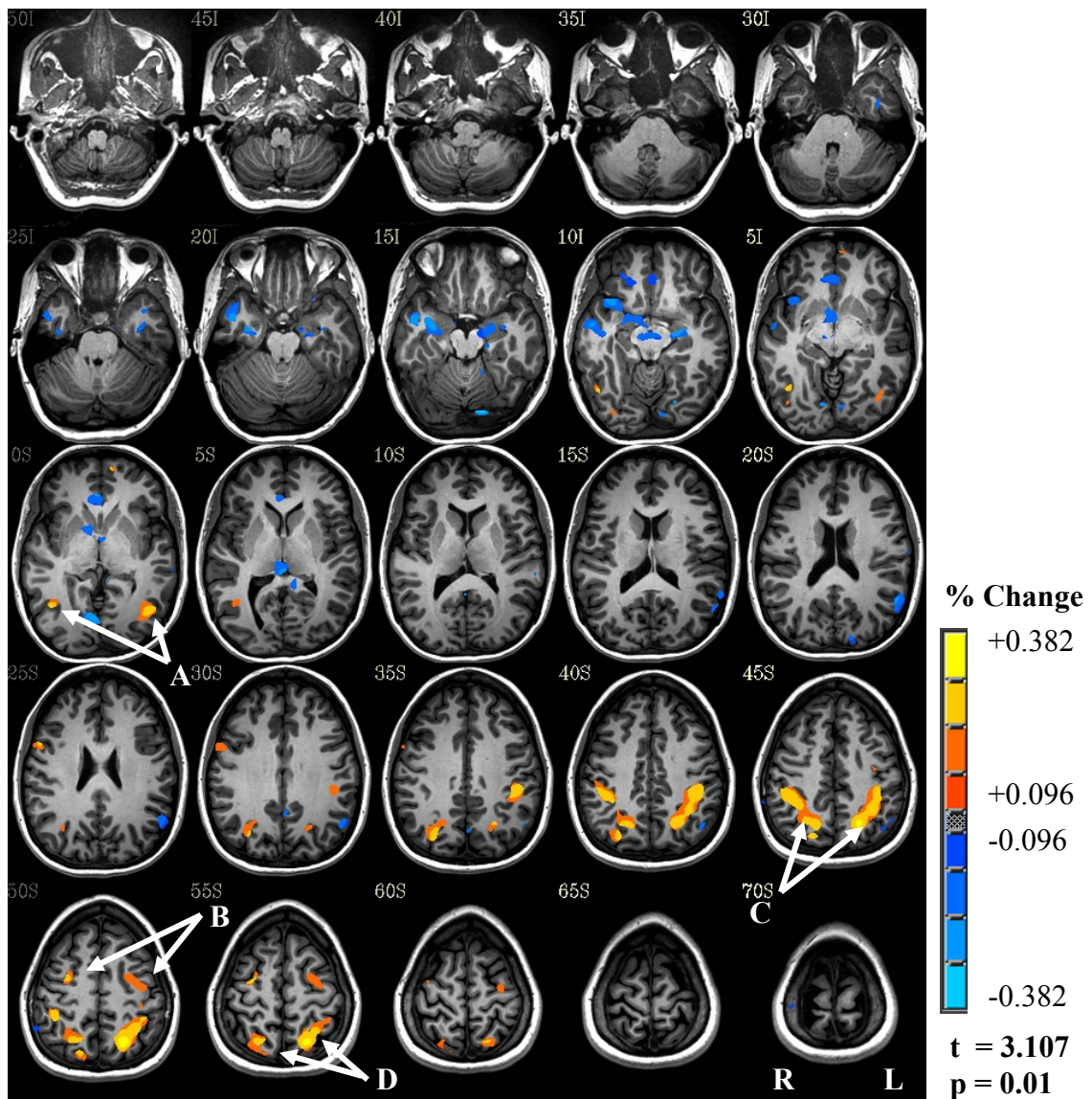


Figure 23 Bin 2 of graphomotor sequence learning. Area A is bilateral MT / V5 [left=42 62 -2; right=-38 62 -2]; B is bilateral, lateral pre-motor cortex [left=29 52;right=-28 6 52]; C is bilateral inferior parietal lobule [left=34 45 45; right=-35 39 46]; D is bilateral superior parietal lobule [left=18 62 55; right=-20 60 56]

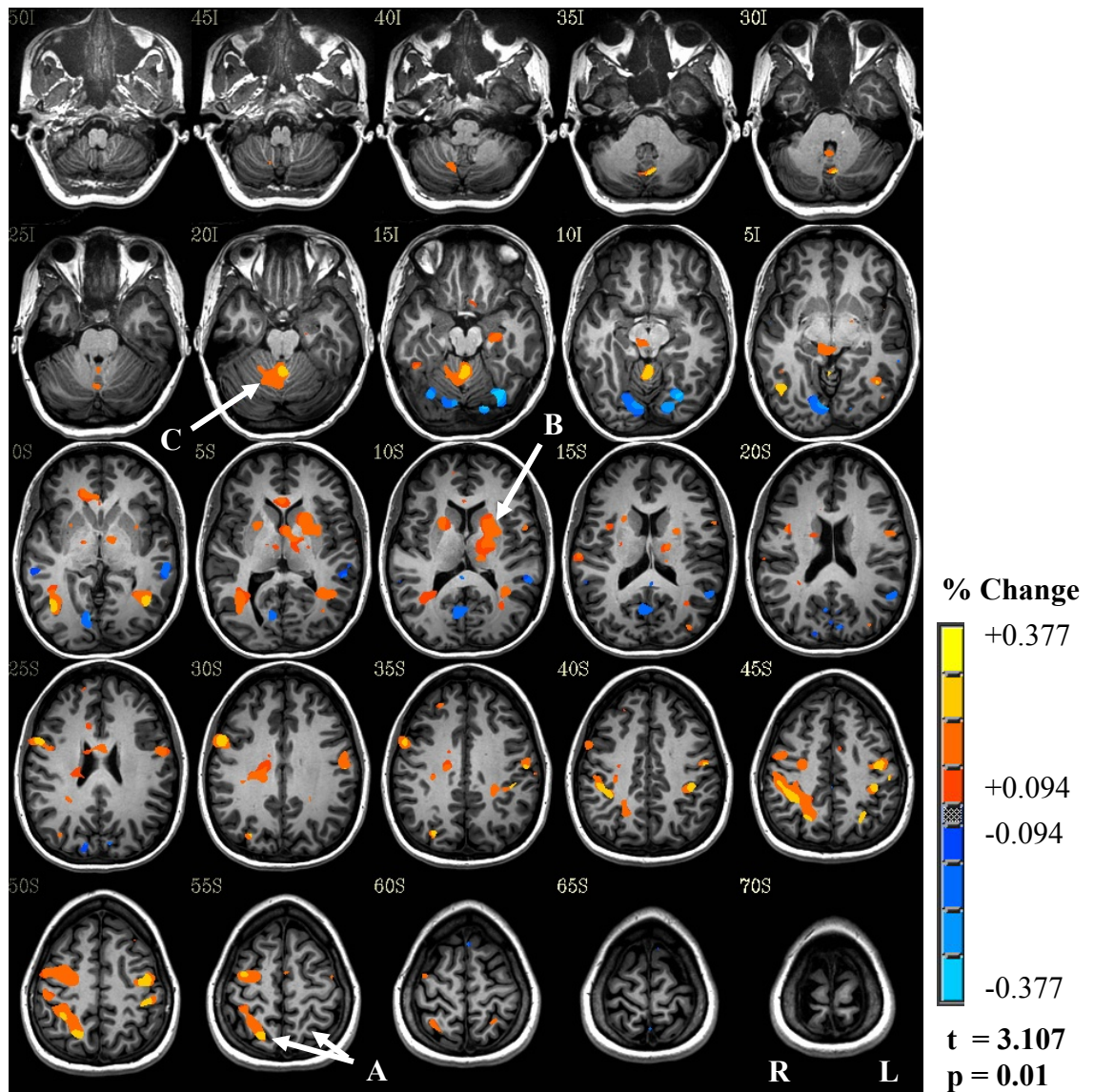


Figure 24 Bin 3 of graphomotor sequence learning. Area A is bilateral superior parietal lobule [left=18 62 55; right=-20 60 56]; B is the left anterior putamen 28 -5 4]; and C is the medial posterior vermis [5 49 -18]

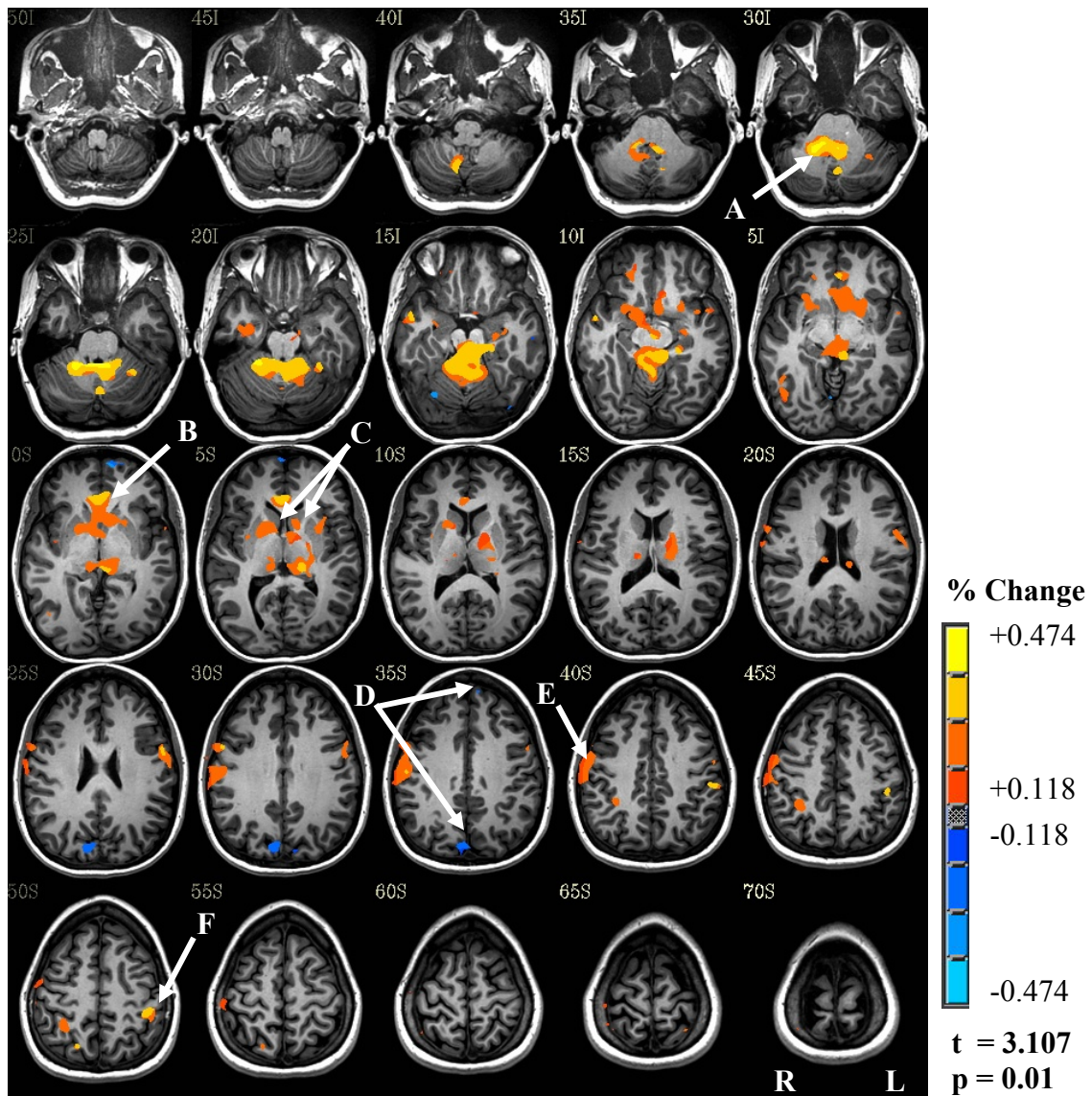


Figure 25 Bin 4 of graphomotor sequence learning. Area A is the right dentate nucleus [-25 45 -26]; B is the subgenual anterior cingulate cortex [0 -32 2]; C is the bilateral anterior putamen [left=28 -5 4; right=-19 -8 0]; area D is the superior medial gyrus [11 -55 32] and right cuneus [-7 82 32]; E is right primary motor cortex [-56 6 37]; and F is the left primary somatosensory cortex [46 30 49]

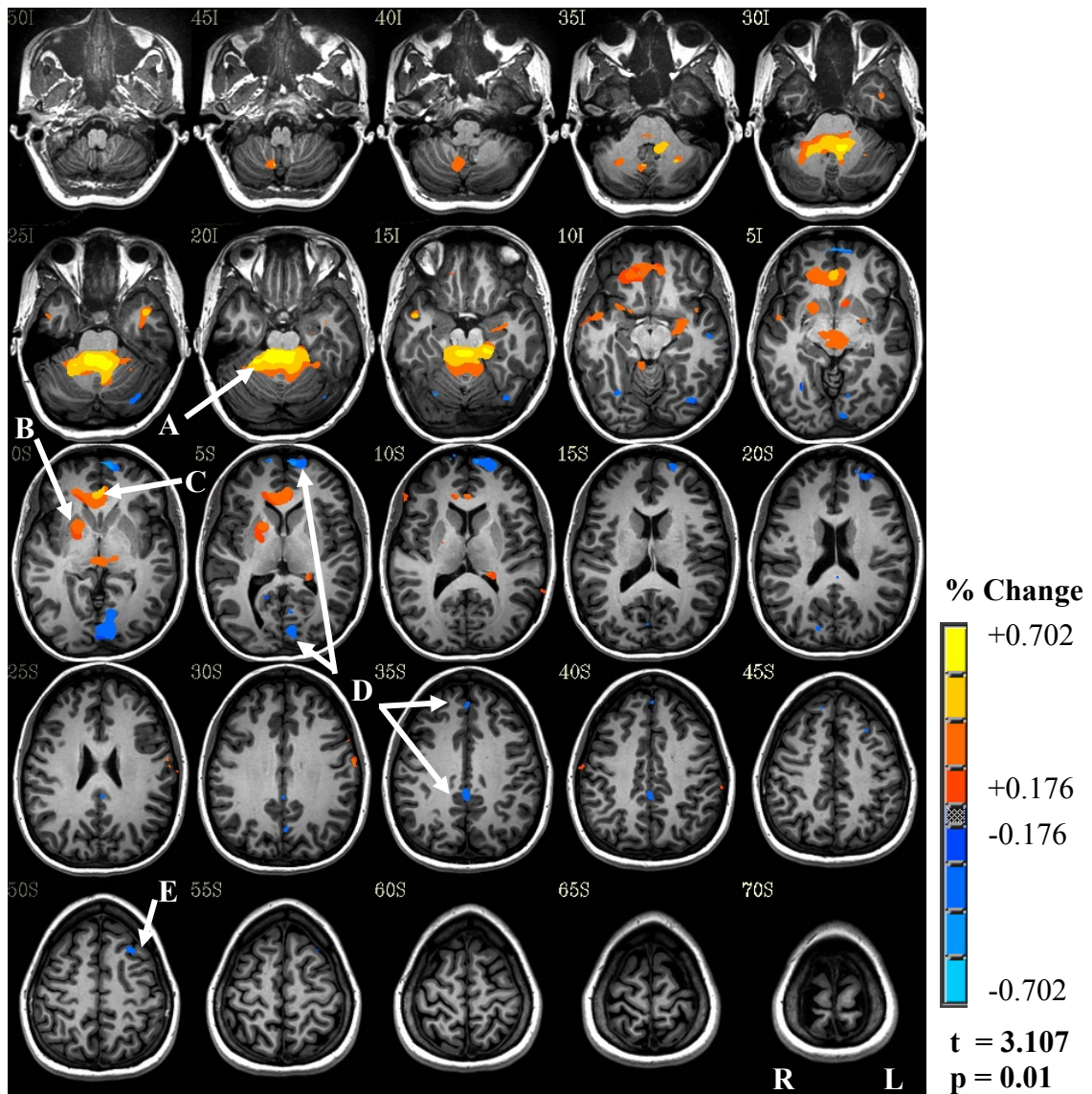


Figure 26 Bin 5 of graphomotor sequence learning. Area A is the right dentate nucleus [-25 45 -26]; B is the right anterior putamen [-19 -8 0]; C is the subgenual anterior cingulate cortex [0 -32 2]; area D is left frontal pole [12 -58 -2]; left precuneus [2 80 37]; left frontal pole [12 -58 -2]; and the midline dorsal cingulate cortex [2 -5 27]. Area E is left dorso-lateral prefrontal cortex [27 -22 47]

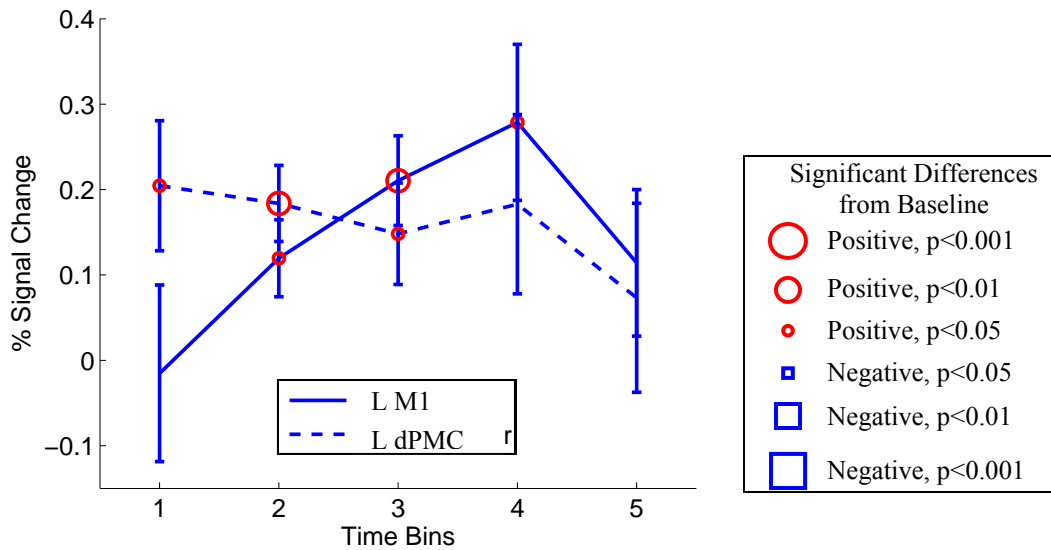


Figure 27 The activity patterns of the left primary motor and left dorsal premotor cortices. The left dorsal premotor activity overlaps the first, fast, and the second, slower learning processes defined in the kinematic (Njerk) data. The left primary motor cortex participates principally in the second phase of motor sequence learning

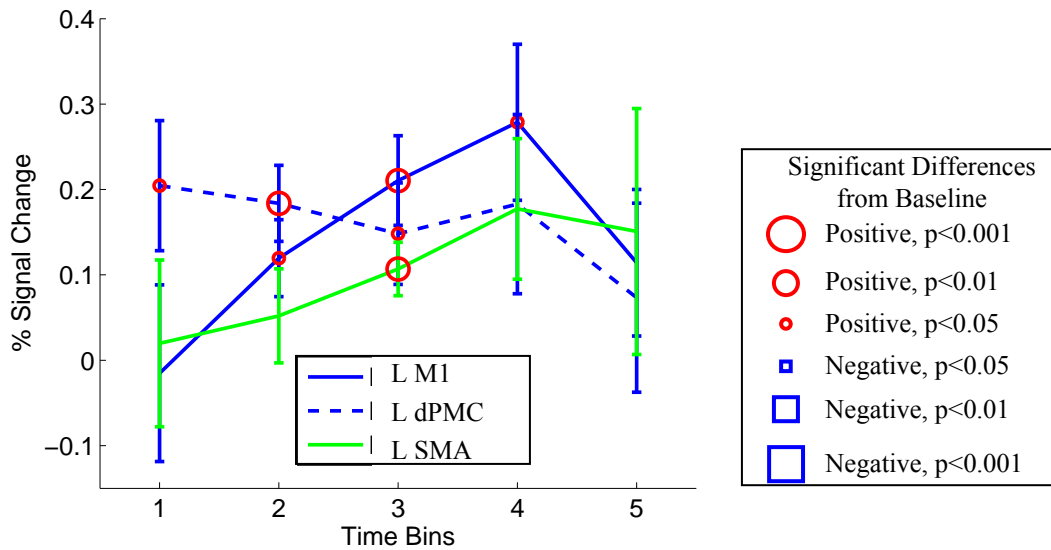


Figure 28 The left primary motor cortex, left dorsal premotor cortex, and left supplementary motor area activity during sequence learning. The left supplementary motor area's participation corresponds to the second, slower phase of sequence learning. Interestingly, given the variability across subjects, the left supplementary motor area was only significantly different from baseline in time bin 3

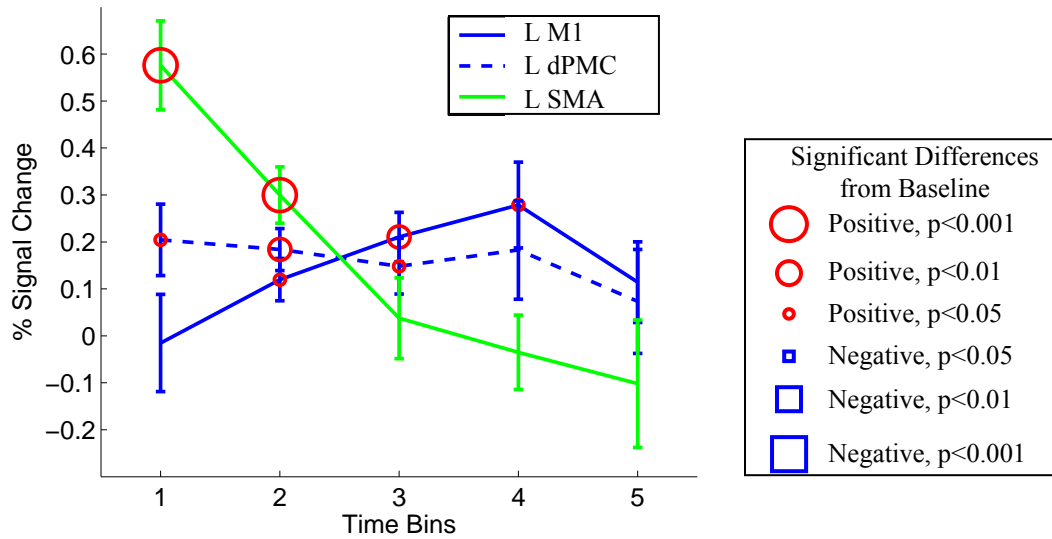


Figure 29 The left primary motor and dorsal premotor cortices, in relation to the dorsal visual stream (left superior parietal lobule). The left dorsal stream’s activity corresponds to the early, fast learning process in the kinematic (Njerk) data

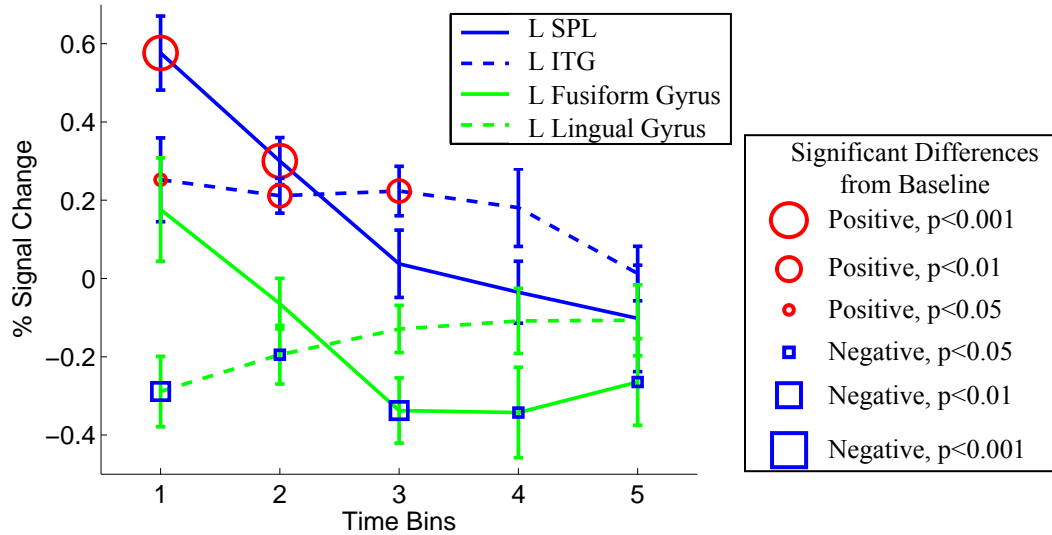


Figure 30 Different regions within the visual system, as sequence learning progresses. Note that the dorsal visual stream (left superior parietal lobule) and the lateral ventral visual stream (left fusiform gyrus) have similar patterns of activity. There is a dissociation between the medial and lateral ventral visual regions (left fusiform and left lingual gyri); as well as between the left superior parietal lobule and the left area MT / V5

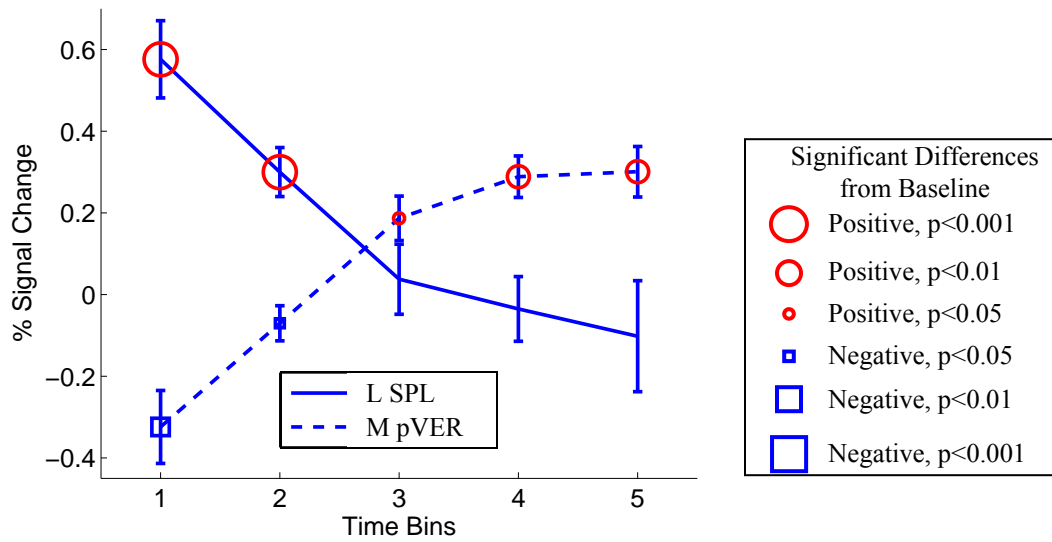


Figure 31 Dissociation between the dorsal visual stream (left superior parietal lobule), and cerebellum (medial posterior vermis). The dorsal stream is significantly activated early, coinciding with the first, fast exponential learning process in the kinematic data. The cerebellar activity is contemporaneous with the second, slower, exponential learning process

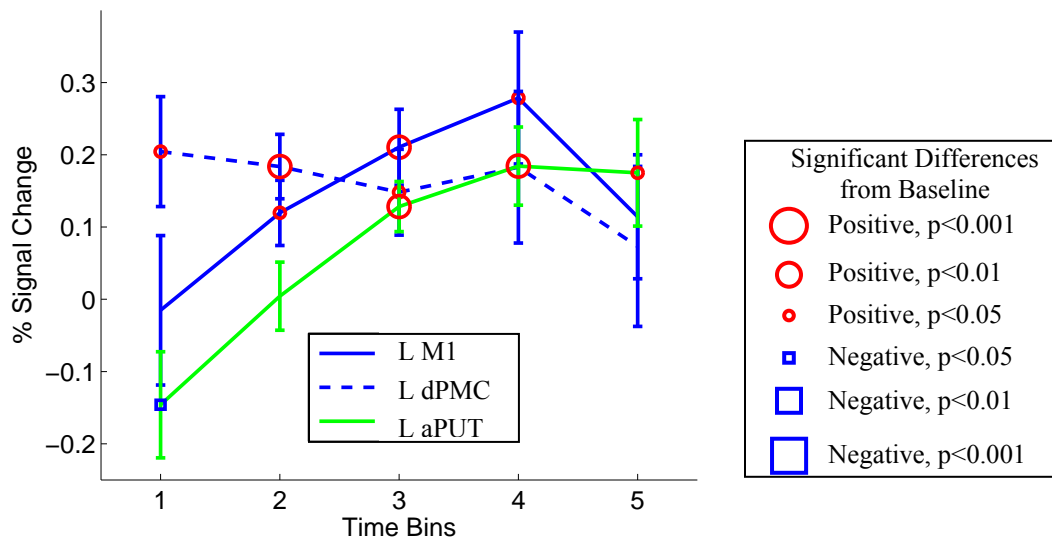


Figure 32 The left anterior putamen’s pattern of BOLD signal activity follows that of the left primary motor cortex, through bin 4. In bin 5, the left anterior putamen activity persists, while the left primary motor cortex activity becomes sub-threshold

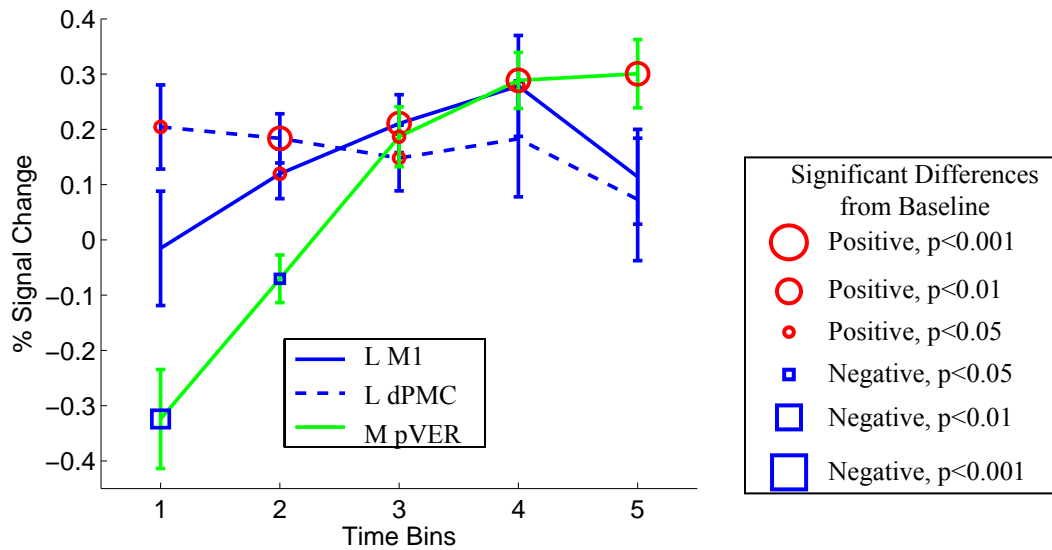


Figure 33 Percent signal change in the BOLD signal for the left primary motor cortex, the left dorsal lateral premotor cortex, and the medial posterior vermis. The vermis activation coincides with the second, slower learning process, as well as the increase in left primary motor activity

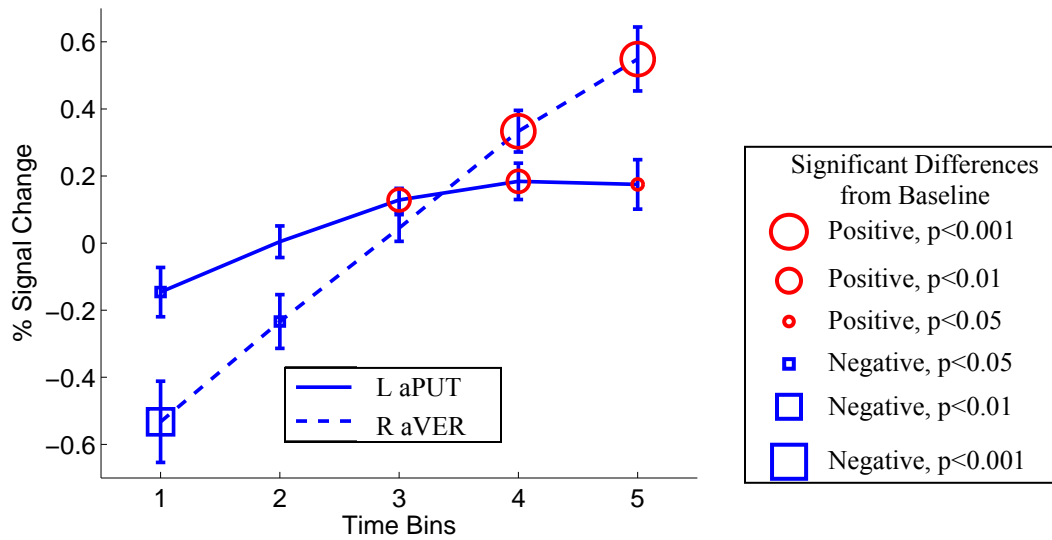


Figure 34 Changes in BOLD signal during sequence learning for the left anterior putamen and the right anterior vermis. Note the divergent trajectories in bins 4 and 5, indicating that these two regions participate in different processes during later sequence learning. The differences between the left anterior putamen and the right anterior vermis in bins 4 and 5 are significant ($p < 0.05$, paired t-test)

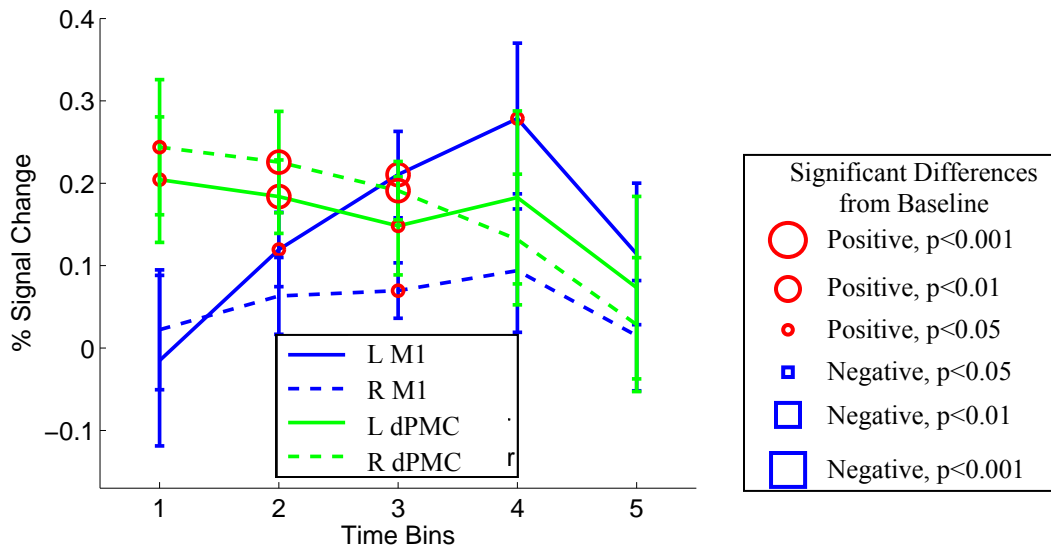


Figure 35 Left and right primary motor cortex, and dorsal premotor cortex activity during sequence learning. There is a large lateralization of the primary motor activity to the left that is not found in the premotor regions

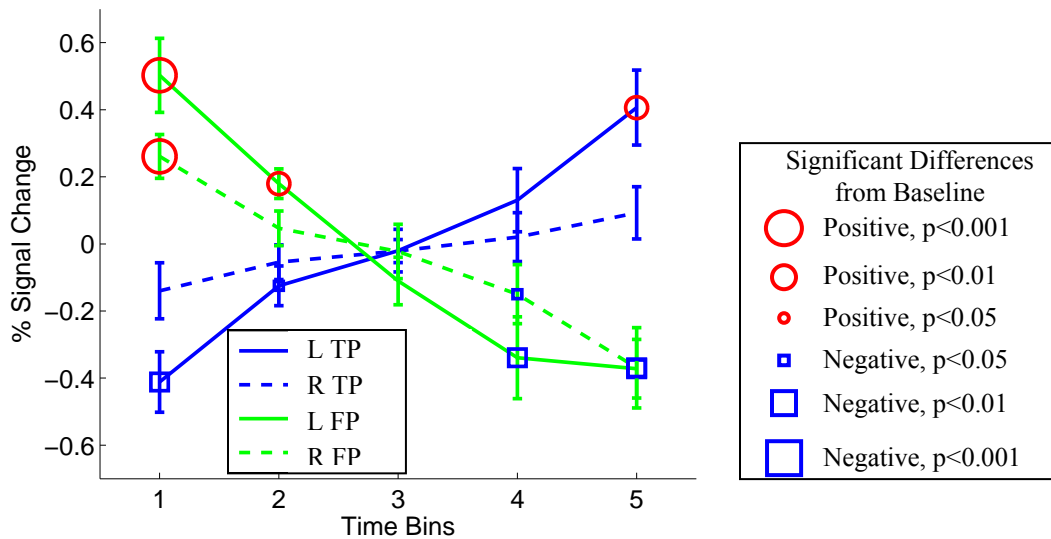


Figure 36 Frontal and temporal pole (left and right) activity during sequence learning. Note the dissociation between the early, significant activation of the left frontal pole, and the late, significant activation of the left temporal pole

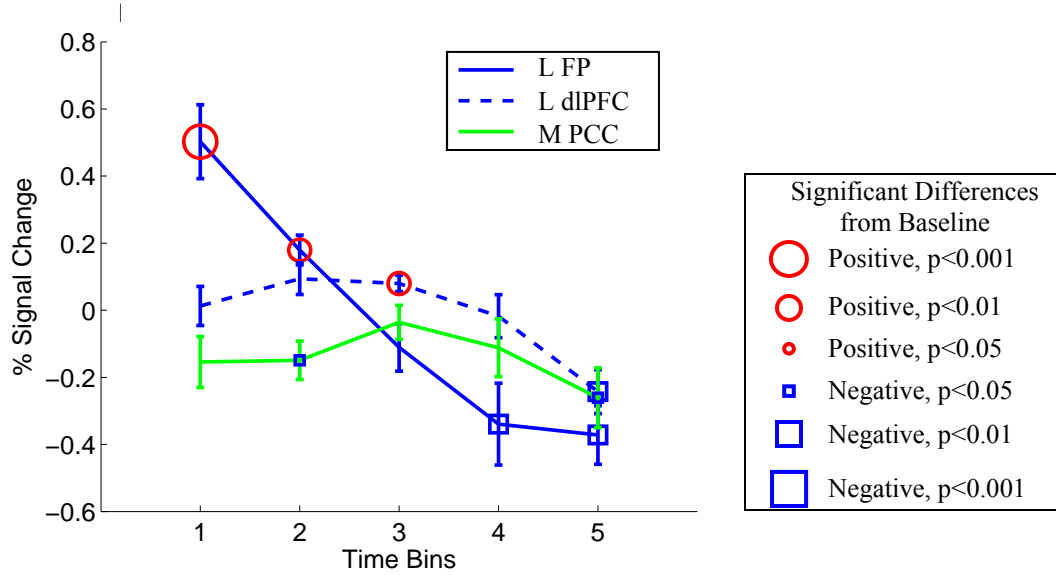


Figure 37 Selected default mode network regions (left frontal pole, left dorso-medial, prefrontal cortex, and medial posterior cingulate cortex) during sequence learning. Each of the regions decreases as the task is mastered, to a level significantly different from the baseline

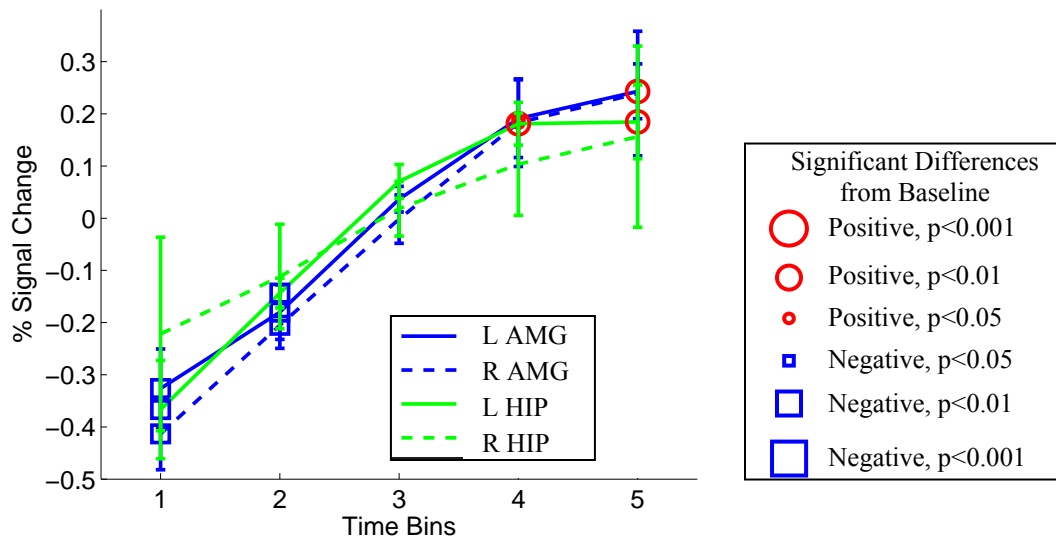


Figure 38 Limbic (left and right amygdala; left and right hippocampus) activity during motor sequence learning

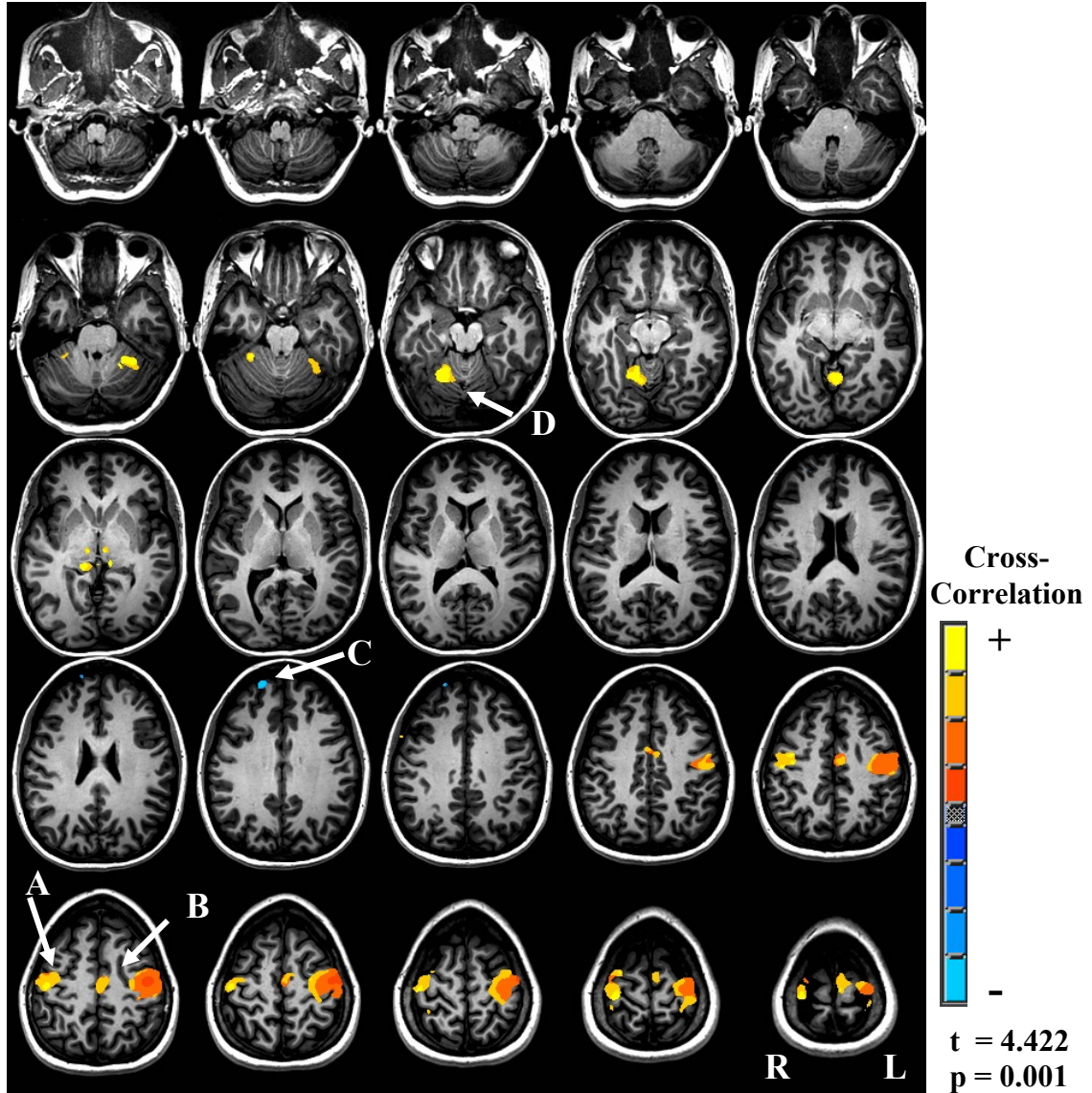


Figure 39 Seed voxel cross-correlation (Bin 1) for the Left primary motor cortex ($p < 0.001$). A. Positive cross-correlation with the right primary motor cortex. B. Positive correlation with the supplementary motor area. C. Negative cross-correlation with the right prefrontal cortex. D. Positive correlation with the right, anterior vermis

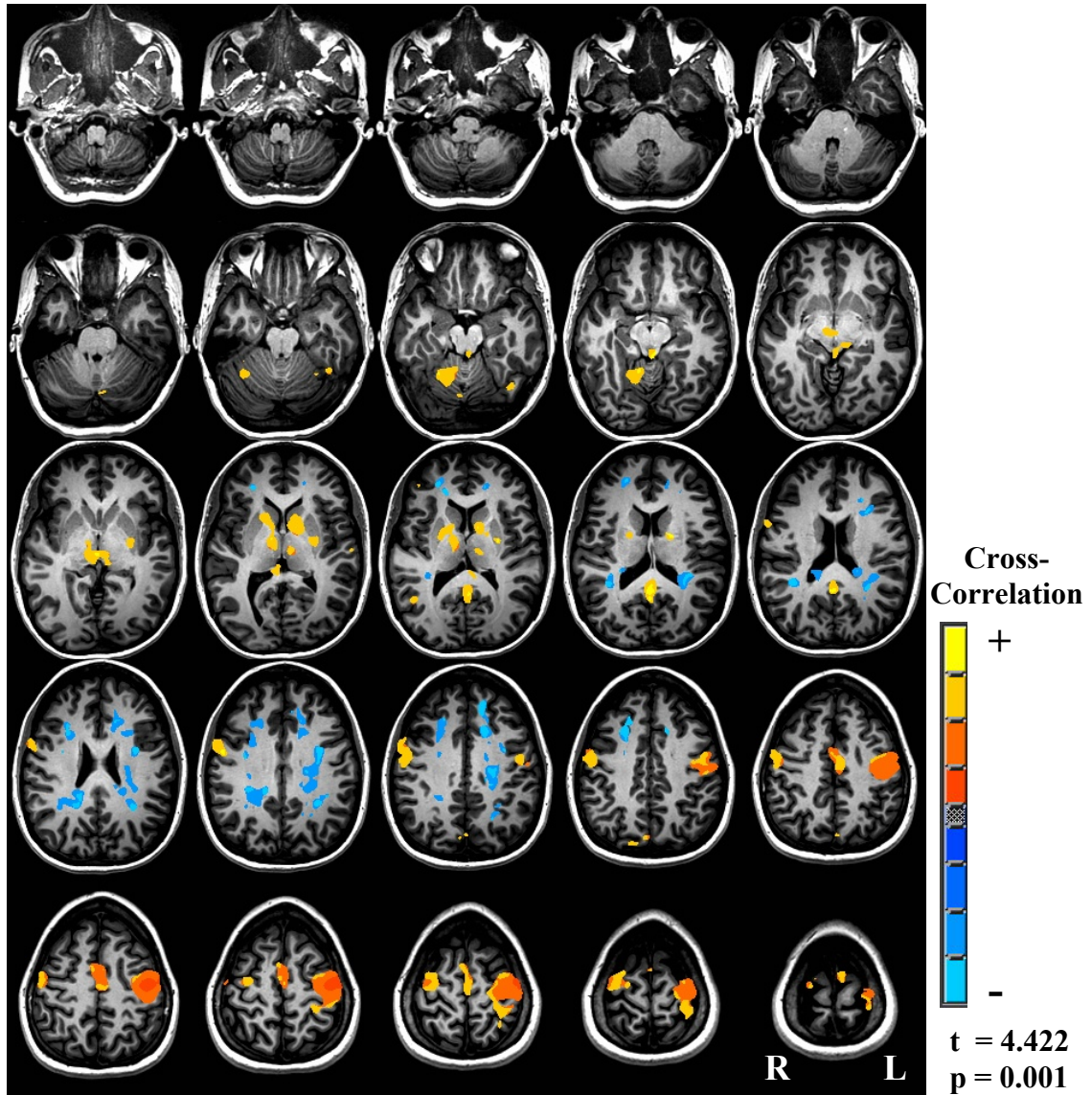


Figure 40 Seed voxel cross-correlation (Bin 2) for the Left primary motor cortex ($p < 0.001$)

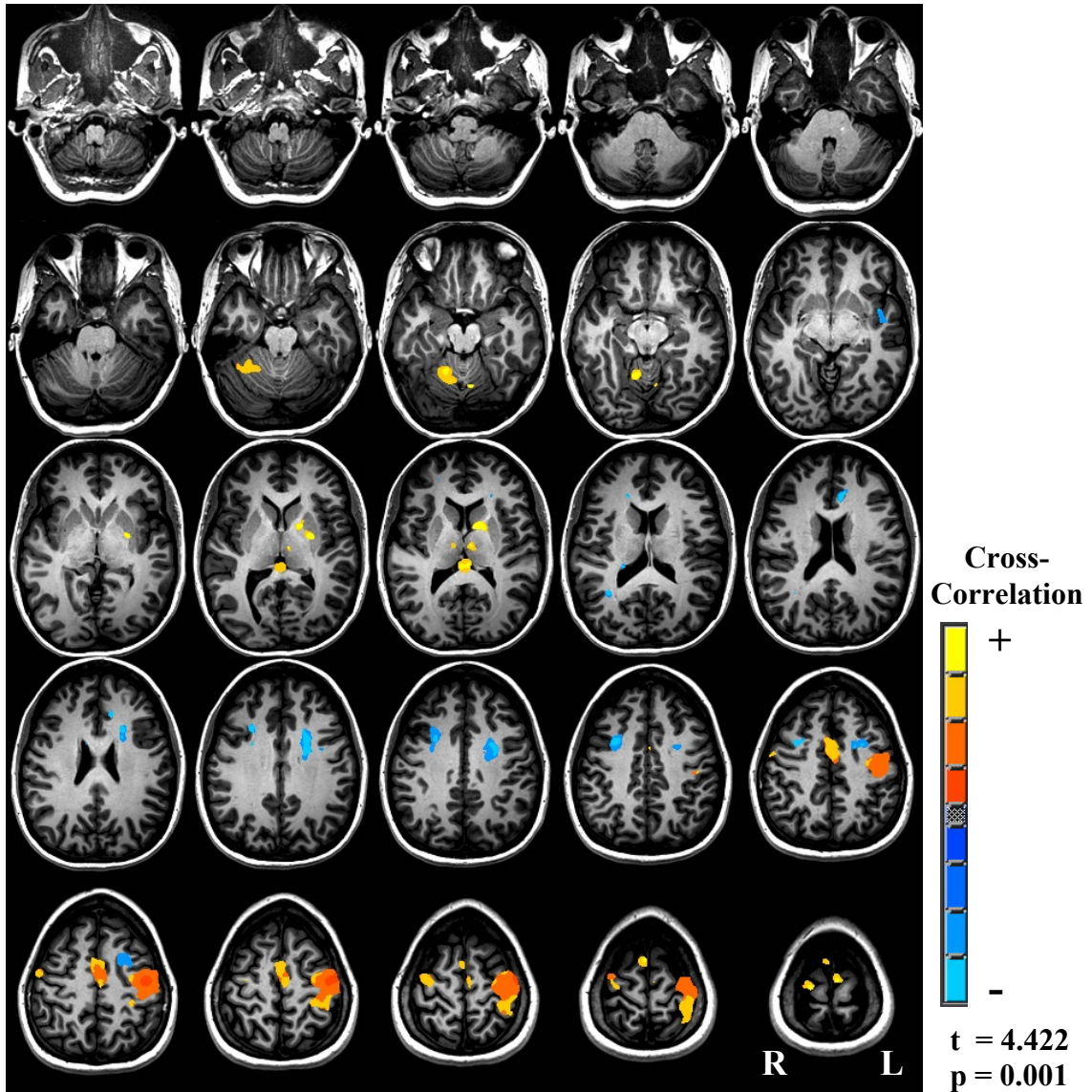


Figure 41 Bin Seed voxel cross-correlation (Bin 3) for the Left primary motor cortex (p<0.001)

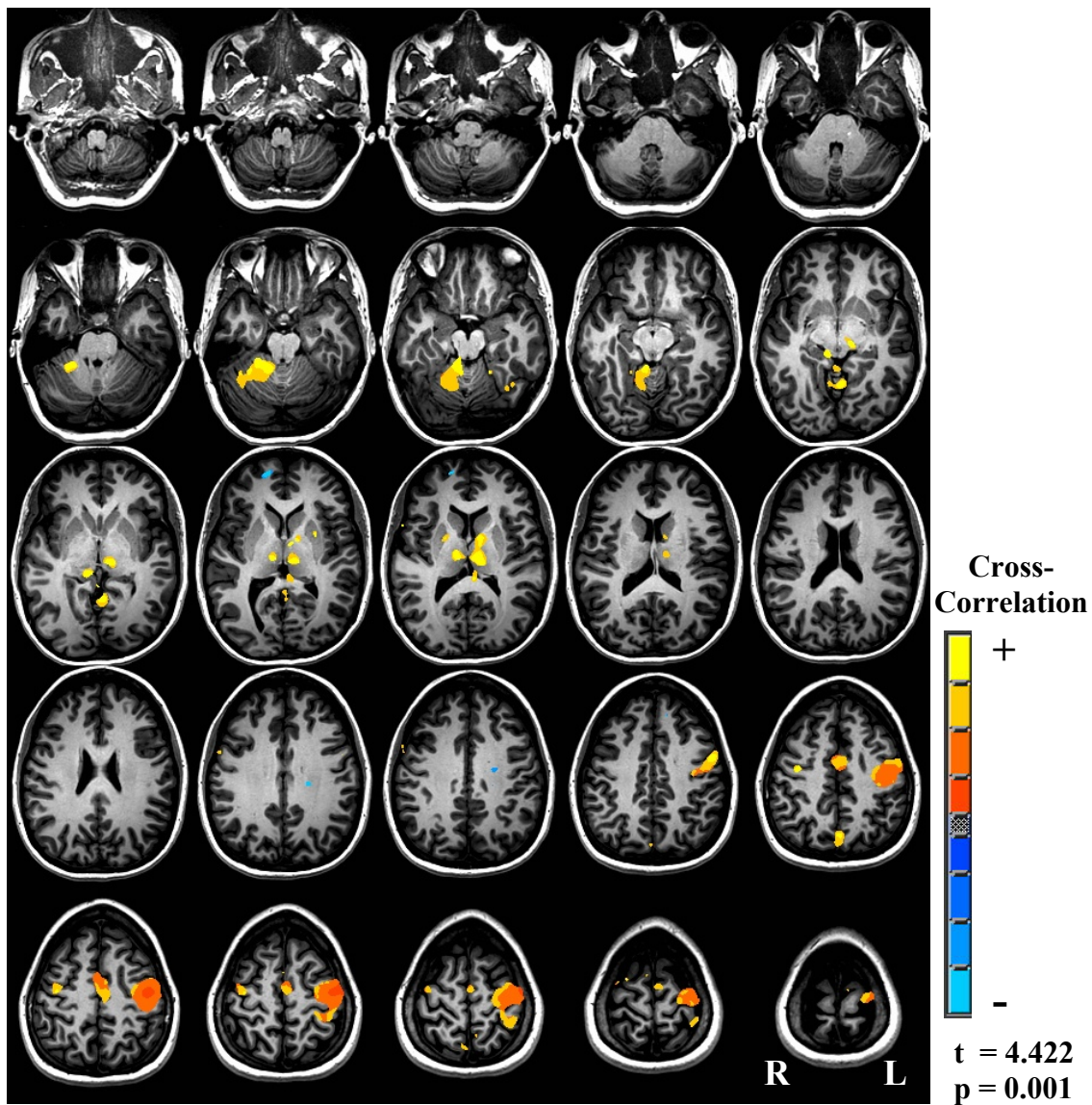


Figure 42 Bin Seed voxel cross-correlation (Bin 4) for the Left primary motor cortex (p<0.001)

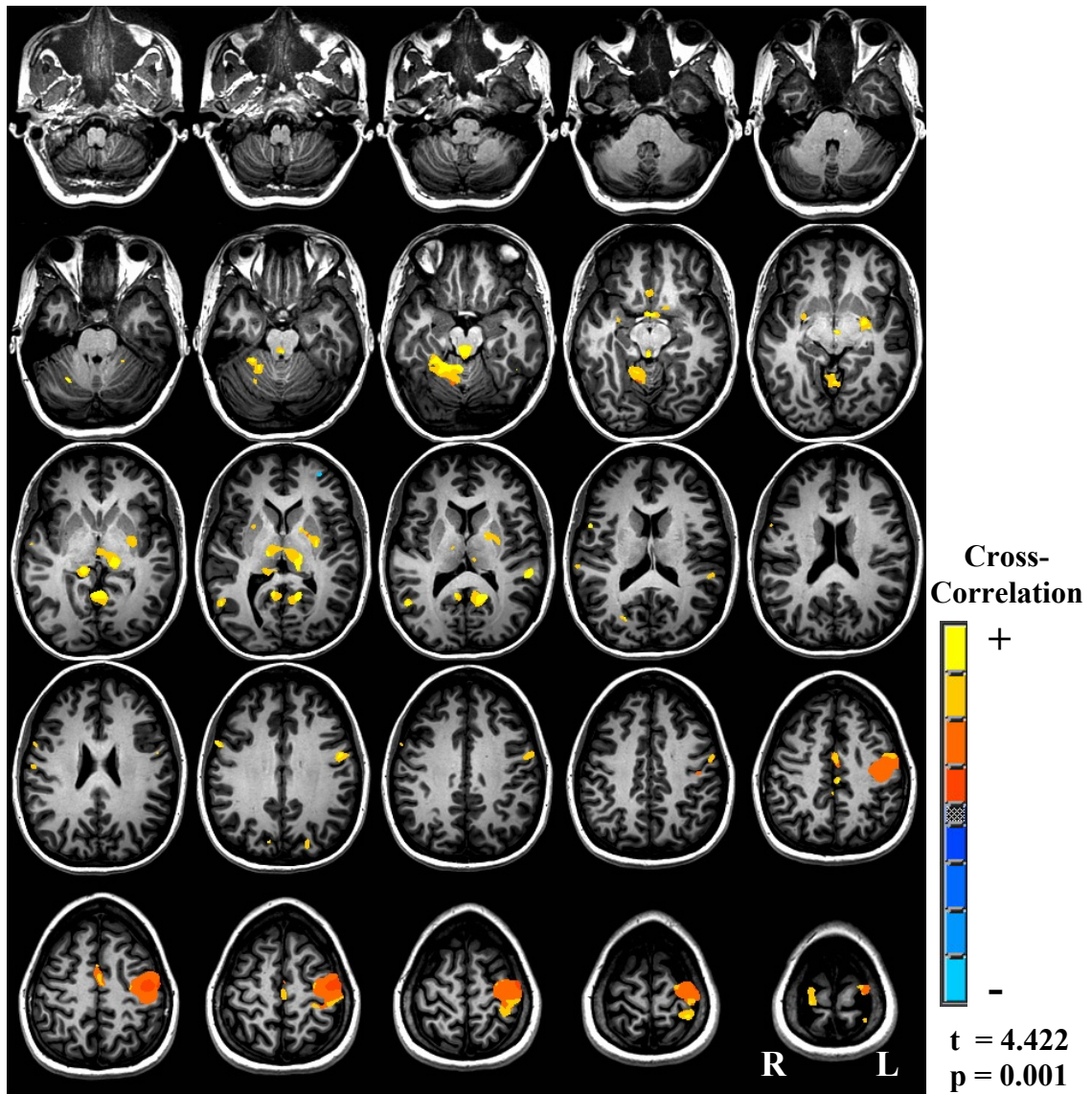


Figure 43 Seed voxel cross-correlation (Bin 5) for the Left primary motor cortex ($p < 0.001$)

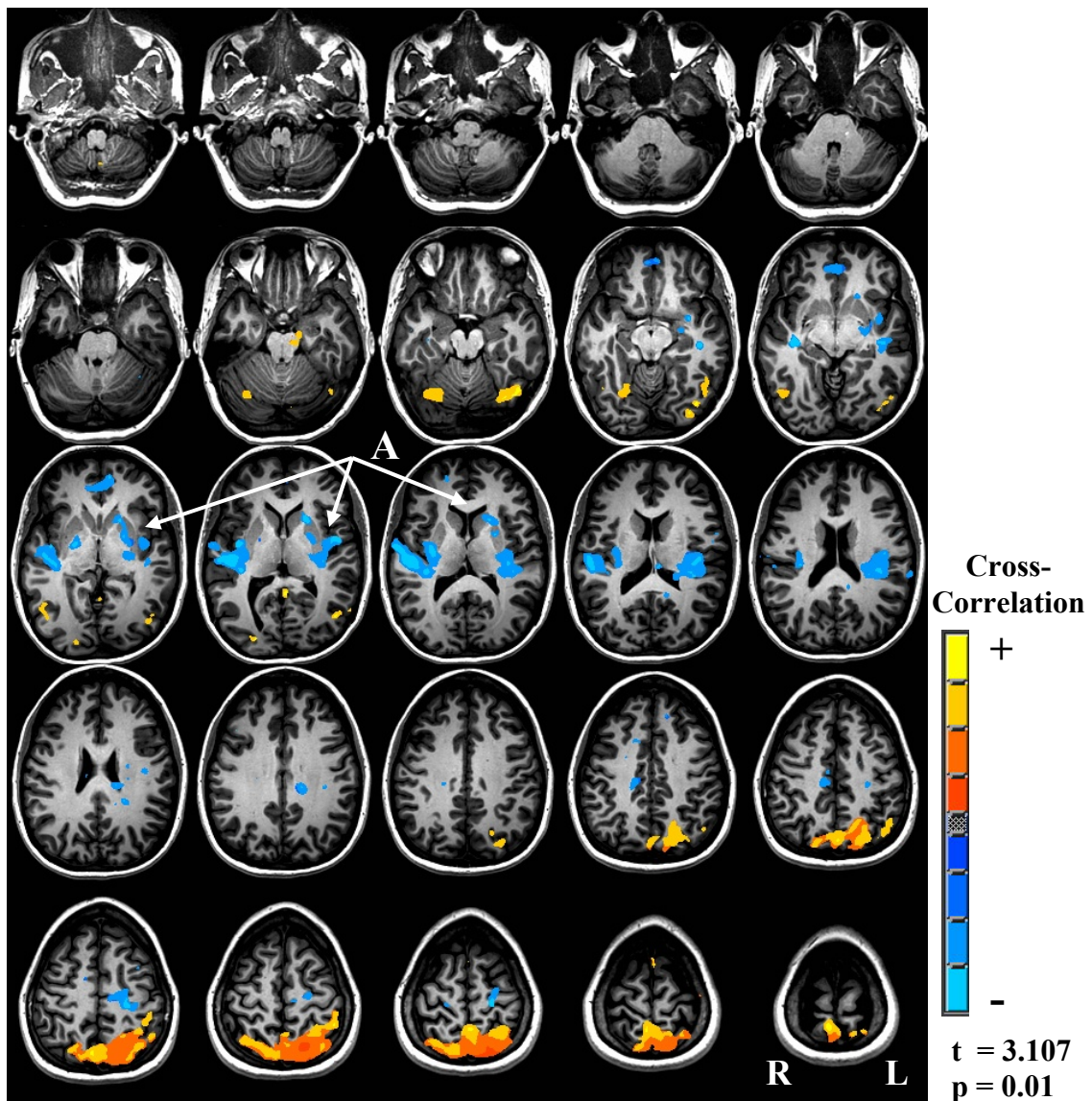


Figure 44 Seed voxel cross-correlation (Bin 1) for the left superior parietal lobule ($p < 0.01$). A. The negative cross-correlation between the left superior parietal lobule and the left head of caudate nucleus, anterior, middle, and posterior putamen.

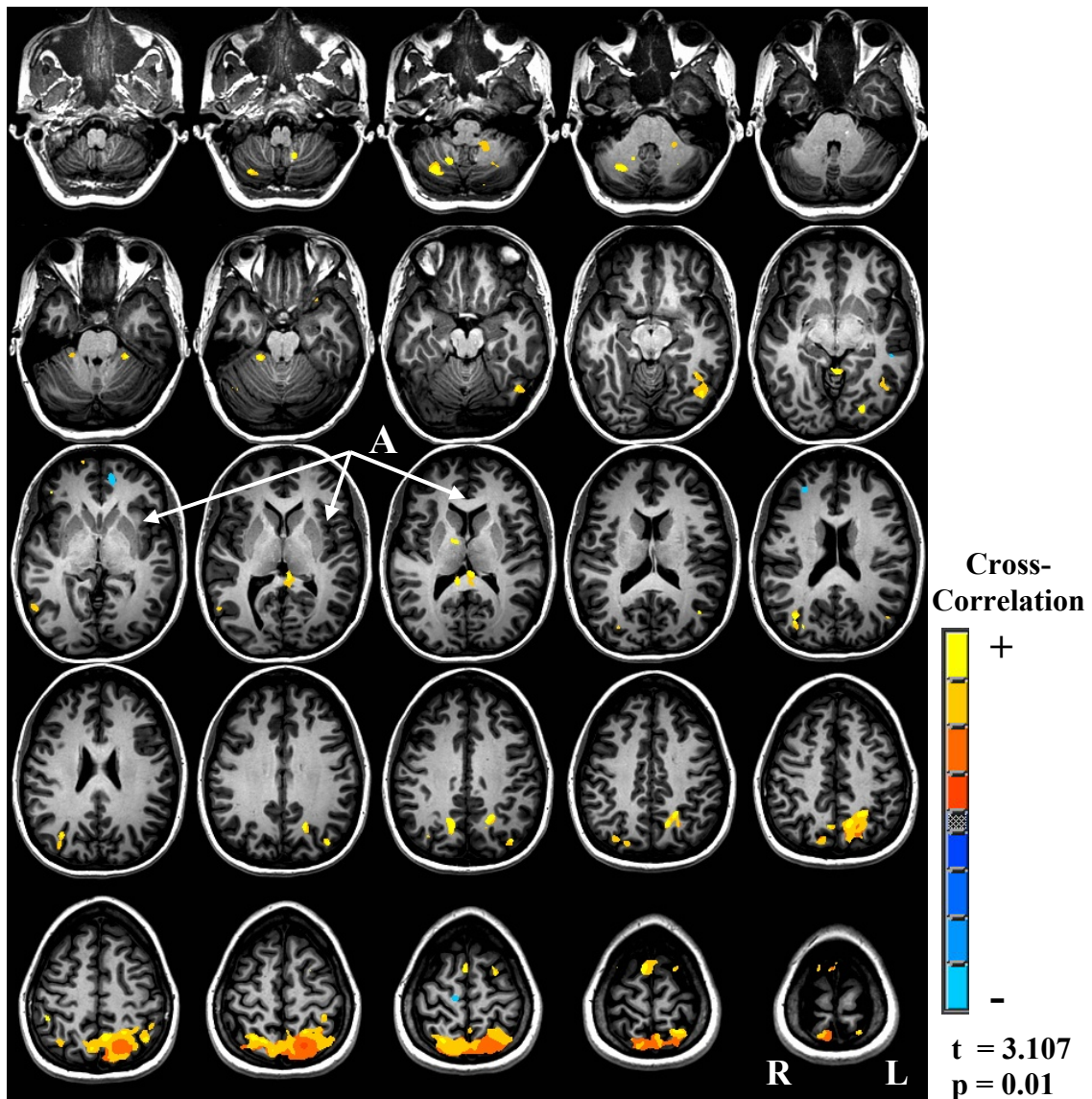


Figure 45 Seed voxel cross-correlation (Bin 2) for the left superior parietal lobule ($p < 0.01$). A. Note the decrease in negative cross-correlation between the left superior parietal lobule and the left head of caudate nucleus, anterior, middle, and posterior putamen from bin 1.

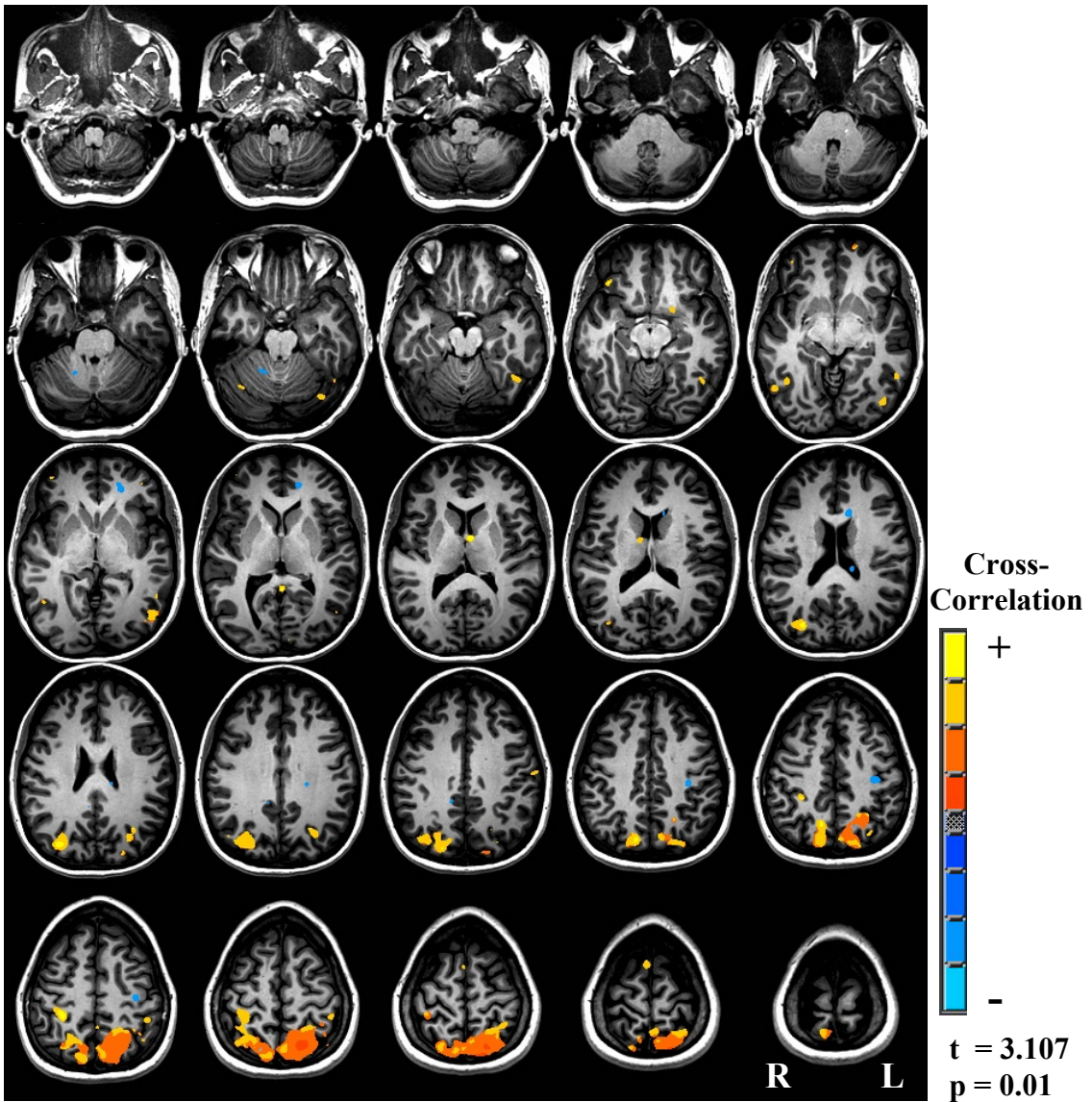


Figure 46 Seed voxel cross-correlation (Bin 3) for the left superior parietal lobule ($p < 0.01$)

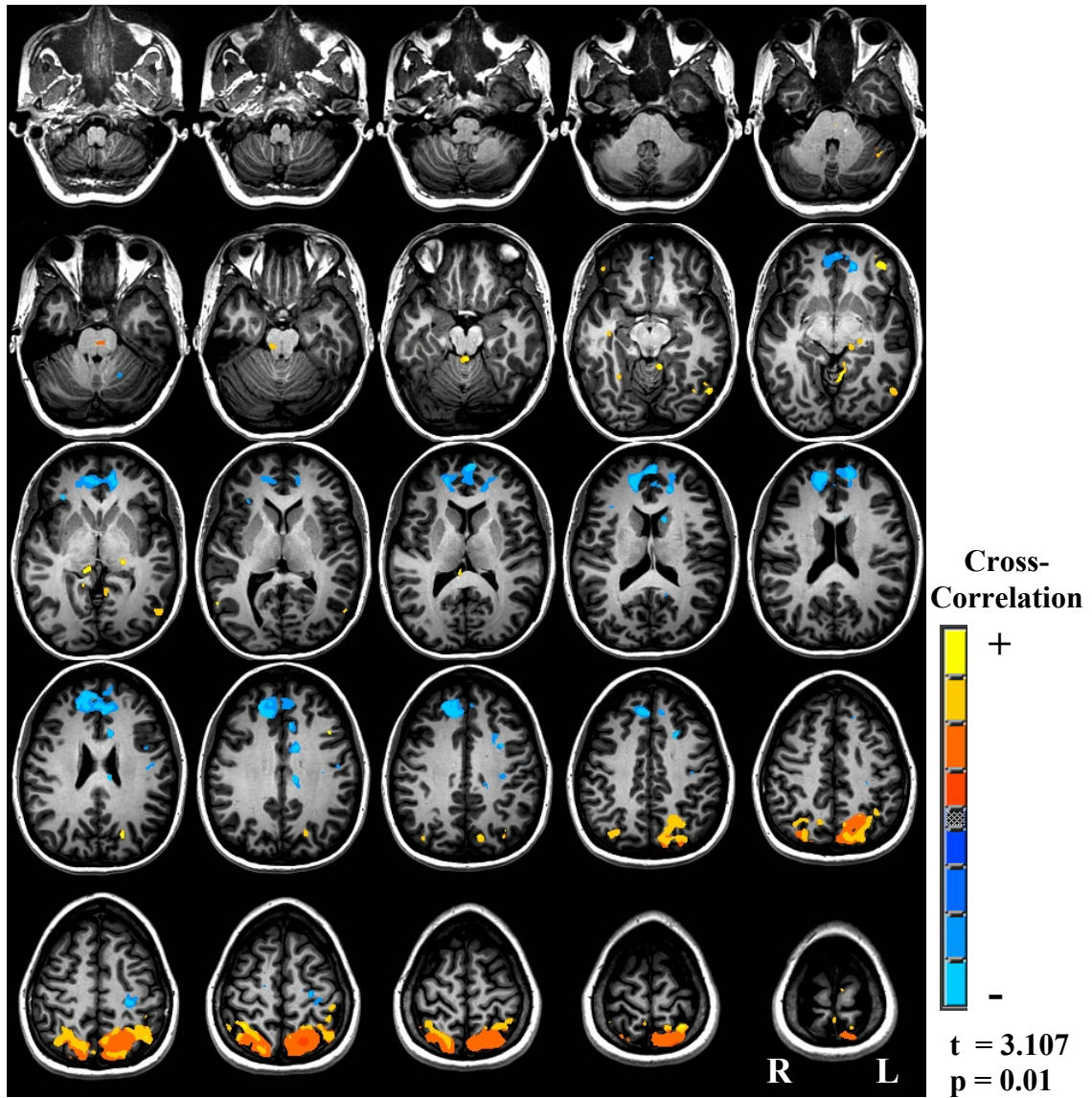


Figure 47 Seed voxel cross-correlation (Bin 4) for the left superior parietal lobule ($p < 0.01$)

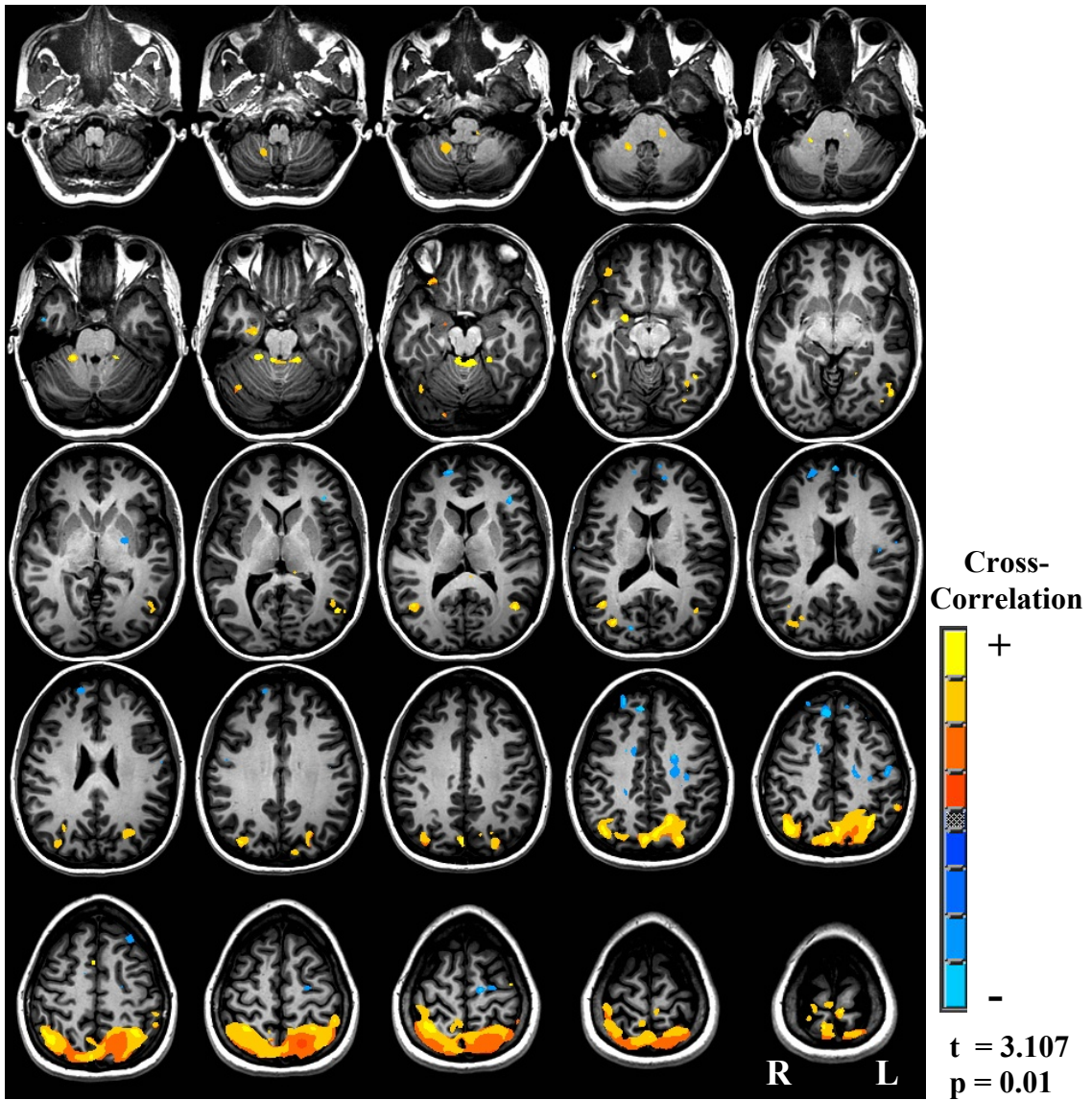
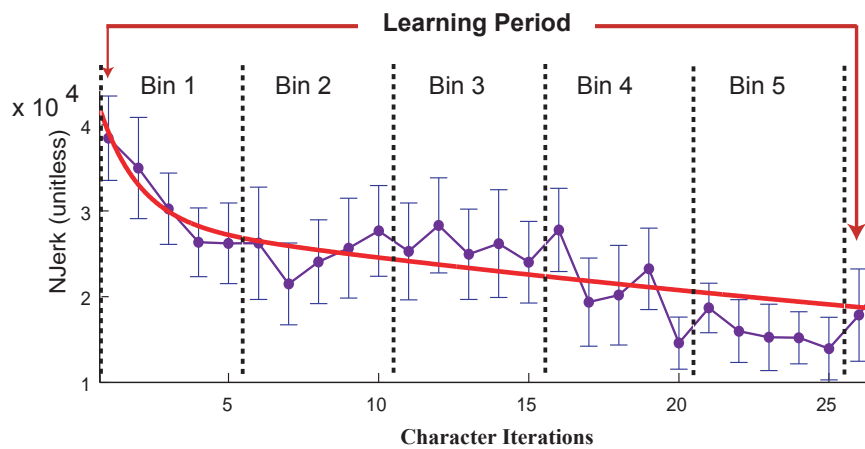


Figure 48 Seed voxel cross-correlation (Bin 5) for the left superior parietal lobule ($p < 0.01$)



Task Process:

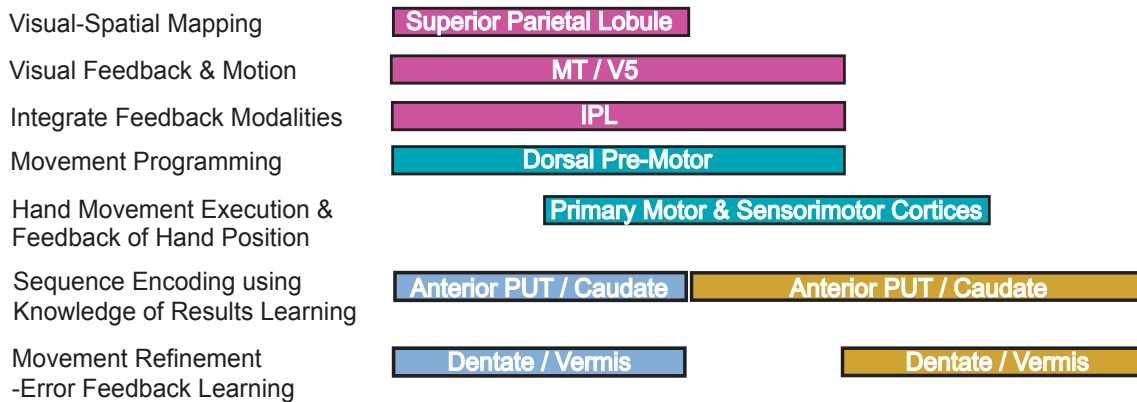


Figure 49 A model of graphomotor sequence learning, combining the task processes identified from the task analysis; the timing and participation of the regions of interest; and the kinematic (normalized jerk) learning curve

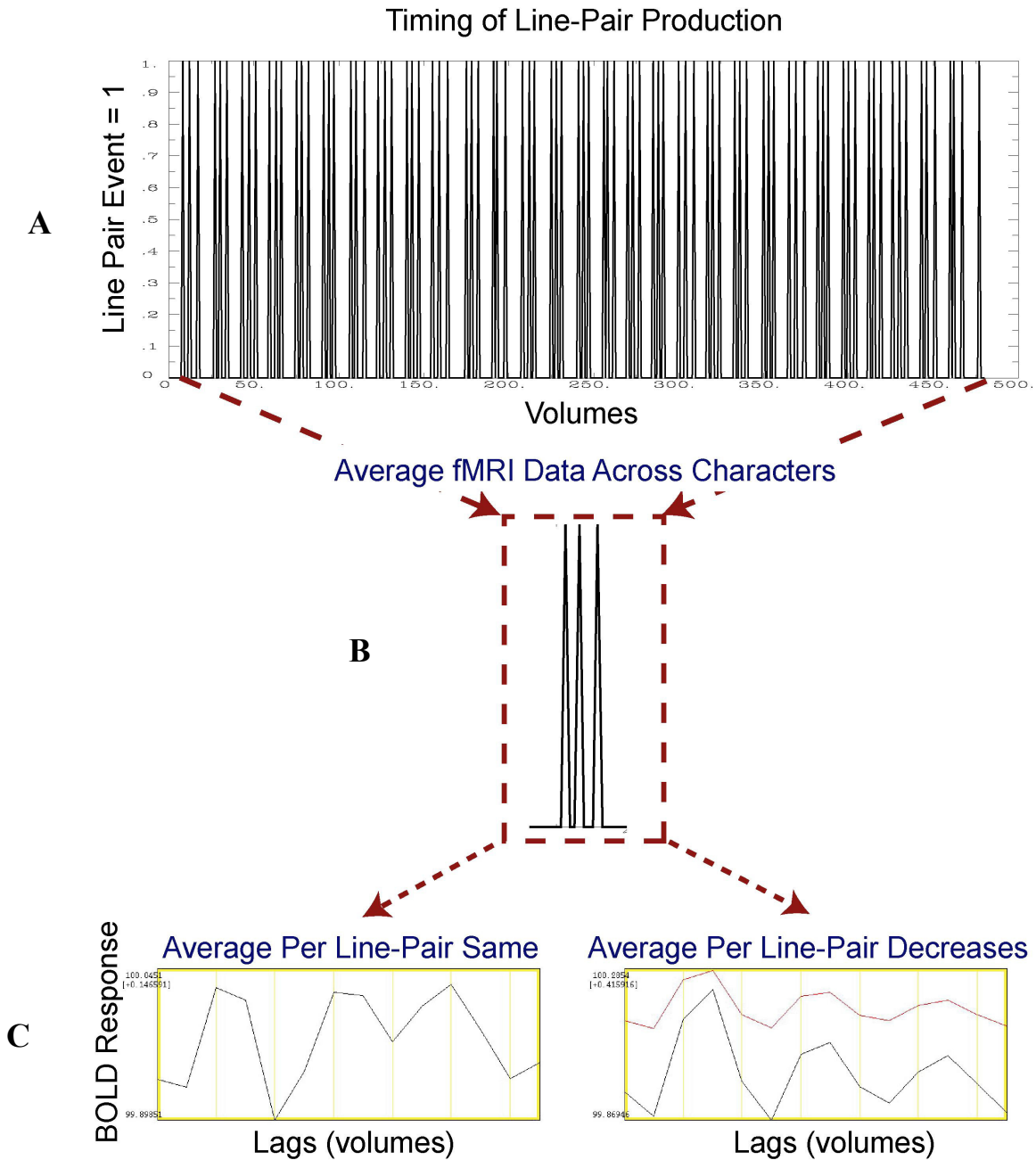


Figure 50A-C A. The writing times for each of the first line-pairs were used to segment the dataset, using a 36 second (18 TR or lag) window. B. The windows are then averaged over all characters produced within a time-bin (the three spikes each represent the predicted BOLD response for a line-pair). The resulting average BOLD signal (averaged across all subjects and all characters within the time bin) shows the response per voxel for each line-pair within each time-bin

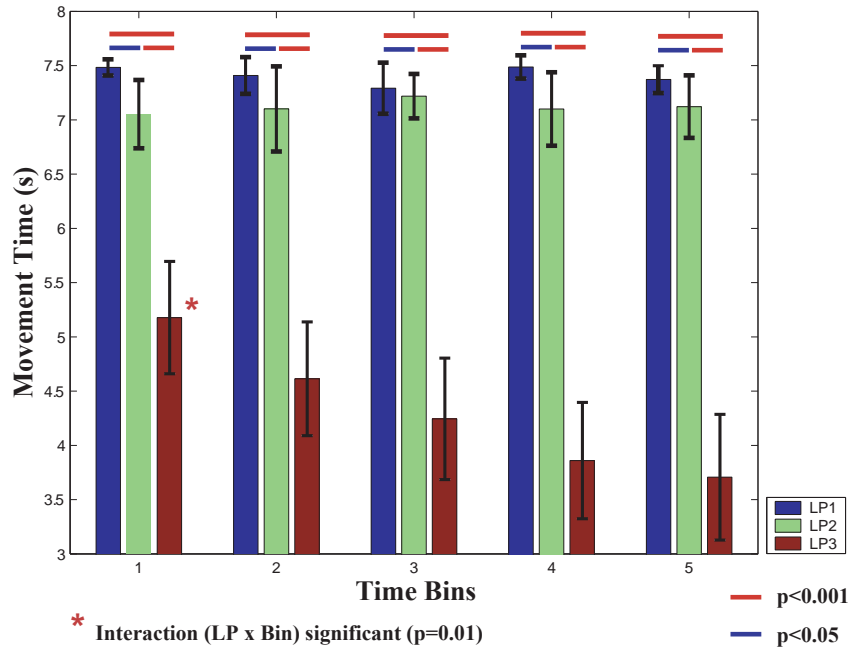


Figure 51 Average movement time (MT) per line-pair during graphomotor sequence learning. Errorbars are standard errors

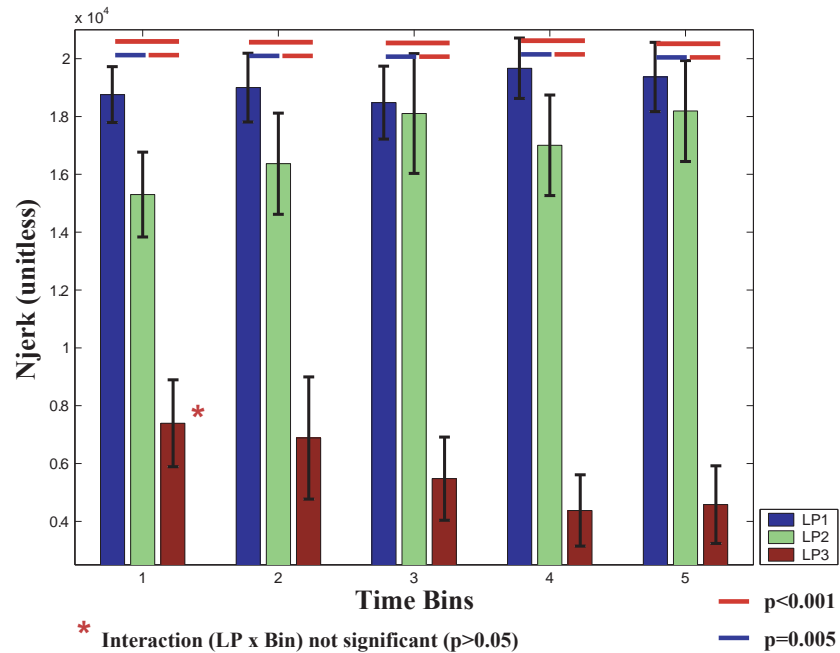


Figure 52 Average normalized jerk (Njerk) per line-pair during graphomotor sequence learning. Errorbars are standard errors

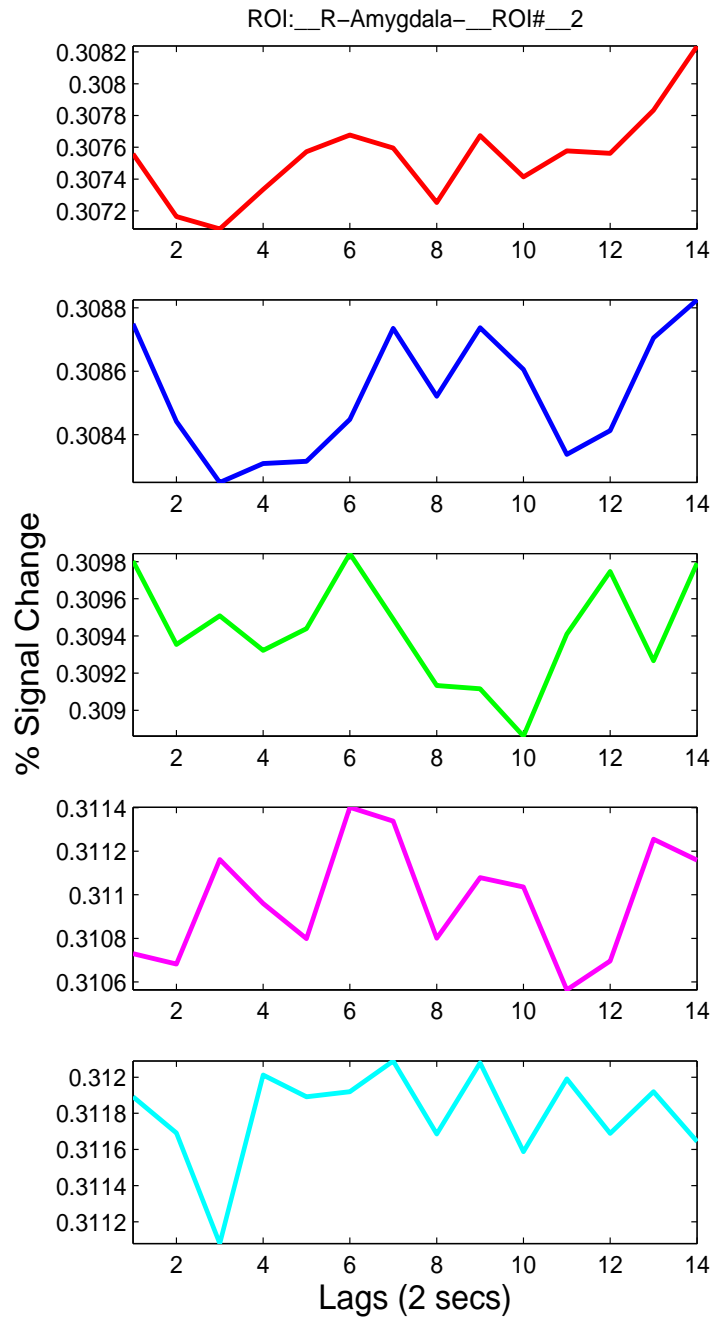


Figure 53 The average line-pair analysis for the right amygdala, over all 5 time bins. This regions serves as a control, as differences between line-pairs during sequence learning is not expected. No pattern of line-pair related changes in BOLD activation are present

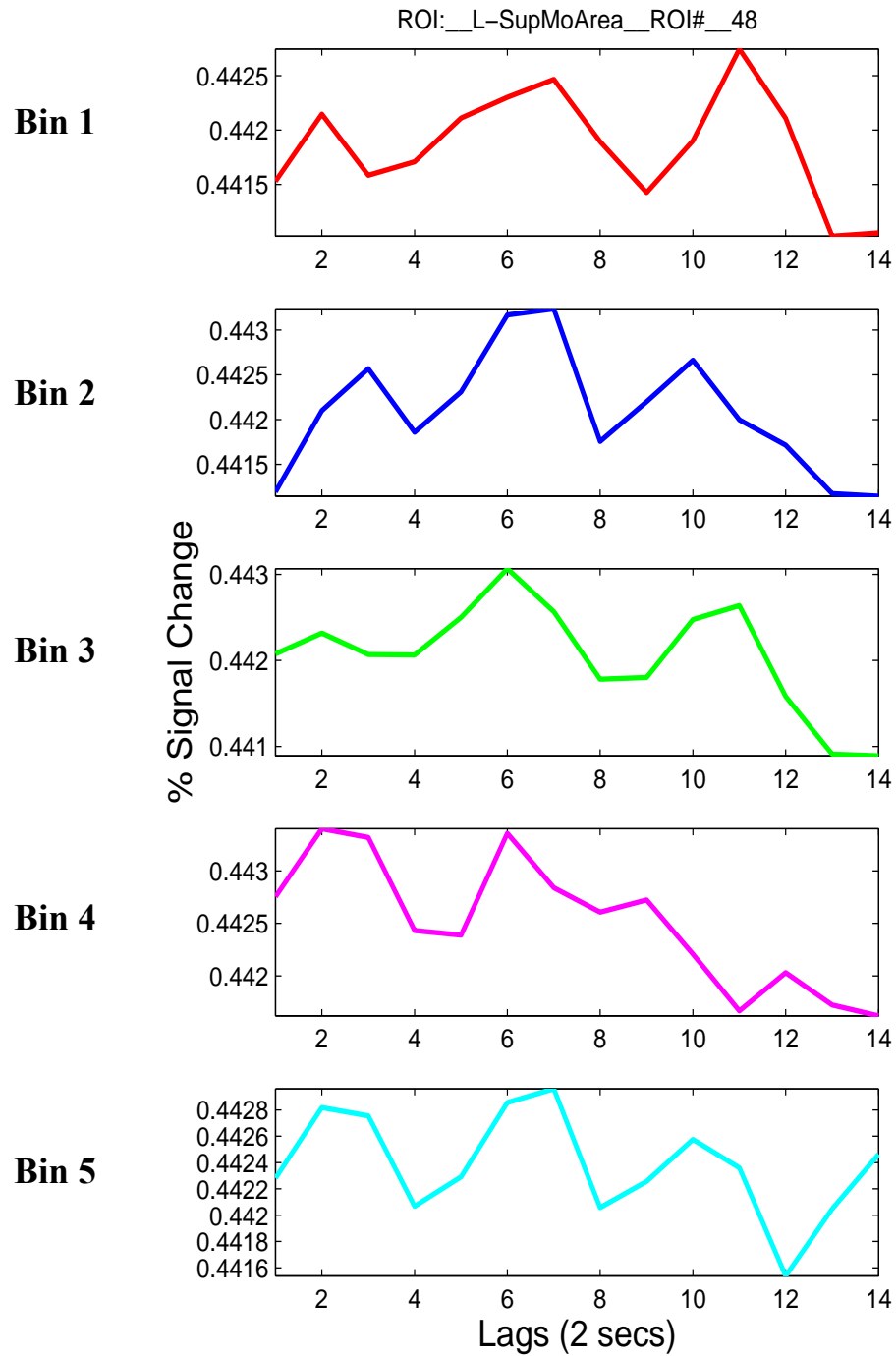


Figure 54 The average line-pair analysis for the left supplementary motor area, over all 5 time bins. A distinct pattern of line-pair related changes in BOLD activation is present

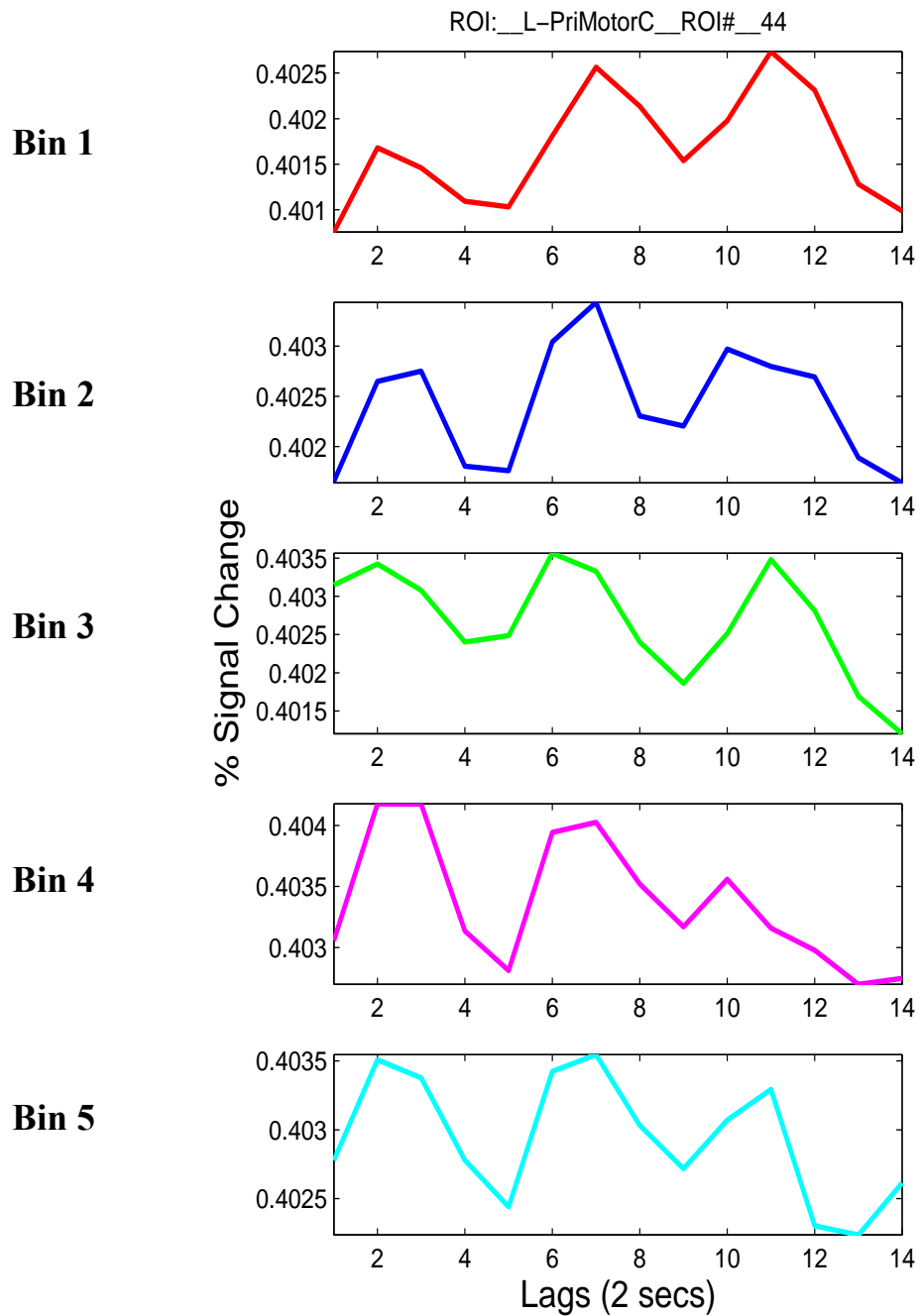


Figure 55 The average line-pair analysis for the left primary motor area, over all 5 time bins. The line-pair related changes in BOLD activation appear to be similar to the left and right supplementary motor area patterns

Appendices

APPENDIX A: Preliminary Experiments

Experiment A

Subjects

Six, right-handed subjects (age 37.5 (12.1); MMSE ≥ 28) participated in the study, after giving informed consent. Of the six subjects, four were naïve, age-matched controls (C); two were “expert controls” (XC). Expert control subjects had learned “Simplified” Chinese Characters (Cowie, 1986) as their primary written language. C subjects had no such prior experience. The C subjects included persons of approximately the same age as the two XC subjects. Subjects were evenly distributed in between those who did T&E, then EFL, and those who did EFL, then T&E.

Data Collection

Kinematic data was acquired using a non-ferromagnetic, digitizing tablet (TouchScreen, Inc.), sampling $\{x\ y\}$ coordinates at 66 Hz (see Figure 1C).

Procedures

Experiment A was a behavioral study, examining how individual movement units are combined into a movement sequence, or “chunk,” using a novel, graphomotor task – learning to write the sequence of line segments which comprise Chinese characters (see Figure 1A). (Seitz et al., 1994; Seitz et al., 1997) The experiment compared two forms of graphomotor sequence learning: Error Feedback Learning (EFL) and Trial & Error Learning (T&E). In the EFL condition, subjects were shown an example of how to draw the character; learning occurred through repeated iterations of each

character, with performance feedback (speed and accuracy). The T&E condition presented the character segments to the subject without any indication of which direction to draw the line –producing a learning situation reminiscent of Hikosaka’s paradigm.(Hikosaka et al., 1999; Hikosaka et al., 2002a; Nakahara et al., 2001; Nakamura et al., 2001) The subject had to deduce the sequence by trial and error –if the subject drew the line in the wrong direction, the same character was presented again. The performance on this behavioral task by controls (C) was compared to expert controls (XC) –persons who were native Chinese writers.

Subjects were placed on a padded table, with a LCD monitor above them (see Figure 1B). Subjects had their right arm supported by a custom designed, Plexiglas© support, to constrain motion (see Figure 1C). The subjects used a stylus to write on the digitizing tablet, which was attached to the Plexiglas© support.

The experiment began with a tablet training period, during which the subjects drew random, straight lines on the digitizing tablet with the stylus. This familiarized the subjects with the mapping of their hand movements to the visual feedback on the monitor/screen, and in writing in an unusual position. After the initial practice, the EFL task started (see Figure 2). Line segments of Chinese characters (3 line, with 3 transitions, for 6 total segments), randomly chosen from the pool of ten characters, were presented in pairs (transition 1, line segment 1; transition 2, line segment 2; etc.), in order, and with direction cues in the Example window.

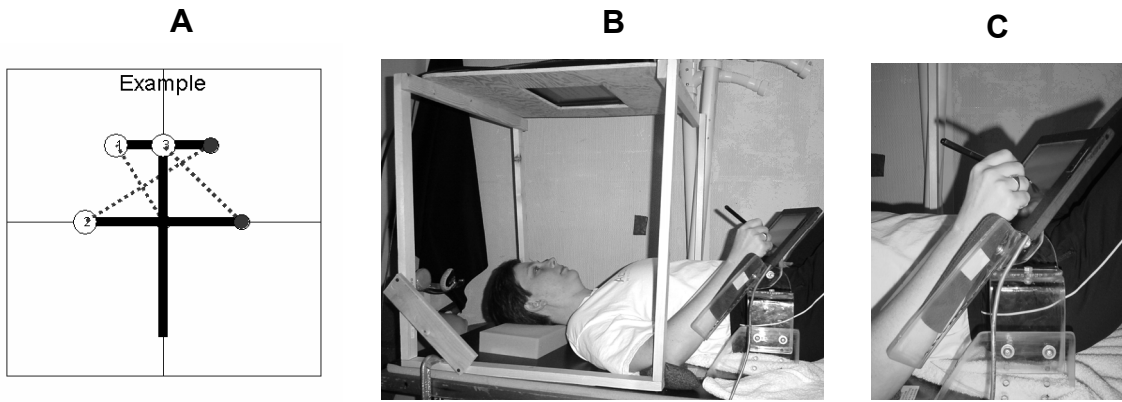


Figure 1A-C Setup for Experiment A. A. Example of a Chinese word character (starts from the center). B. Position of the subject on the table—subject views screen overhead. C. The non-ferromagnetic, digitizing tablet mounted on the holder and arm support

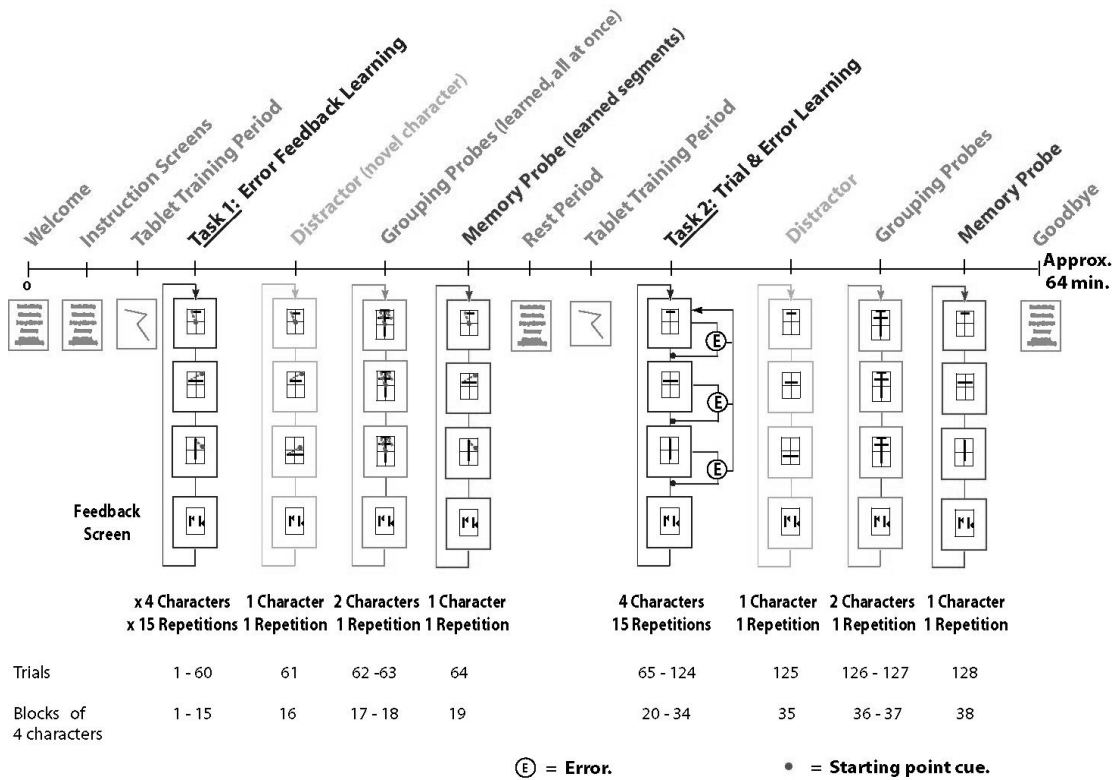


Figure 2 Behavioral time line detail for Experiment A

The sample of Chinese characters was constrained to include only characters with three straight lines. Subjects were asked to draw the segment that they were shown, as quickly and accurately as they could. The subjects were instructed to keep the pen on the tablet at all times. Kinematic data of the subject's responses was collected, and specific feedback (speed and accuracy) was given to the subject after each character. Each character had 3 sets of two line segments; four characters constituted a block; and each block was repeated 15 times. The four characters were presented in random order within each block, to avoid position effects.

During the T&E task, line segments were drawn from the same pool of Chinese characters (but were different from those learned in the EFL task) and were presented, in order, *without direction cues* in the Example window. If the subject did not draw the line segment in the correct order and direction, then the character was presented again. The data collection, feedback, repetitions, and randomization between blocks were the same as in the EFL task. Kinematic data was acquired using a non-ferromagnetic, digitizing tablet (TouchScreen, Inc.), sampling {x y} coordinates at 66 Hz.

Data Analysis

For EFL and T&E tasks, Root Mean Square Error (RMSE) was computed between each subject's data for a character, and the ideal path for that character.(Contreras-Vidal & Buch, 2003) Movement Time (MT) and Movement Length (ML) were also computed per character, with ML being compared to the ideal trajectory for each

character. In addition to RMSE, MT and ML, the T&E task produced data on the number of wrong iterations per character (WRONG) each subject made per character, before writing the sequence correctly. Results were fitted with second-order polynomials ($y = ax + bx^2 + c$) for visual inspection.

Results

Figure 4 shows descriptive images of the sequences learned, with the differences between one expert control and one naïve subject. Figure 5 depicts the differences in movement time and RMSE between expert and naïve subjects.

In Experiment A, all subjects completed the EFL task. Due to the adequate learning curves and difficulty of the T&E task for the subjects, the EFL task was used for Experiment B.

Conclusions

The Chinese character graphomotor sequence learning task is able to capture elements of the sequence learning process, and is able to differentiate between novice performers (naïve subjects) and expert performers. The two learning methods (T&E and EFL) yielded similar results, but the T& E was much more difficult for the subjects to perform.

Experiment B

Subjects

One male, right-handed subject (age 27; MMSE ≥ 28) participated, after giving informed consent. The subject was naïve to the task.

Data Collection

The neuroimaging data was collected on a 3 Tesla, GE scanner at the National Institutes of Health (see Figure 1B). Kinematic data was collected using the same non-ferromagnetic, digitizing tablet as in Experiment A.

A novel feature of the study was that the ideal HRFs were computed from the behavioral time-stamps (the times that the subject performed each task) for writing times (see Figure 3A), and kinematic measures of learning, instead of using a fitted curve or assumed learning model.

Data Analysis

Data was analyzed using AFNI (SSCC/DIRP/NIMH/National Institutes of Health). Images were corrected for motion, and masked, using AFNI 3dvolreg and 3dClipLevel commands, respectively. An ideal model hemodynamic response function (HRF) was created, using the gamma function in AFNI's waver command. This writing times-based HRF was weighted by the subjects' RMSE scores (see Figure 3B). The impact of learning (RMSE as indicator of learning) was regressed from the writing values, to produce an ideal HRF for learning only (see Figure 3C),

using the equation $S_{fit} = (R'(R'R)^{-1})R'S$ (Buchel & Friston, 1997; Buchel et al., 1998), where R =the effect of writing (without learning); and S =the effect of learning (RMSE). The residual = $R - S_{fit}$. The fMRI data was then deconvolved with this ideal, learning-only HRF, using AFNI's 3dDeconvolve function, after accounting for baseline differences and drift through the use of the fixation data. This produced t-test maps per voxel, which was evaluated for significance, using a Write vs. Learning contrast.

Results

Figure 8 shows initial fMRI BOLD activations related to the predicted HRF created from the subject's kinematic data (timing of writing movements for each line-pair). Significant deactivations in the medial pre-SMA and L IPL were noted, as were significant activations of the left SPL that were related to the sequence learning process. These activations demonstrated that the kinematic timing data could be used effectively to create a predictive HRF, in order to capture neural responses (as measured by the change in BOLD signal) related to graphomotor sequence learning.

Conclusions

The purpose of this study was to translate the behavioral task into the fMRI setting, to see if neuroimages could be collected contemporaneously with kinematic data of the sequence learning process. The neuroimaging data demonstrated that this dual data collection process was effective.

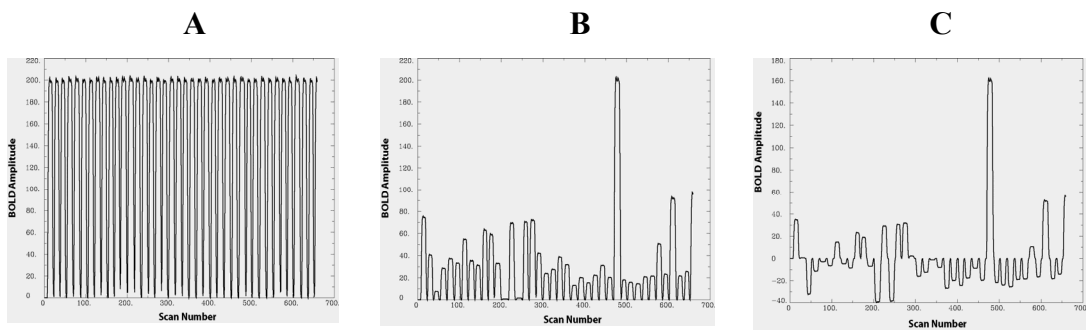


Figure 3A-C Ideal HRFs for Experiment B. A. Write times convolved with HRF. B. HRF-convolved Write times weighted by RMSE scores. C. Effects of learning regressed from Write and RMSE HRF

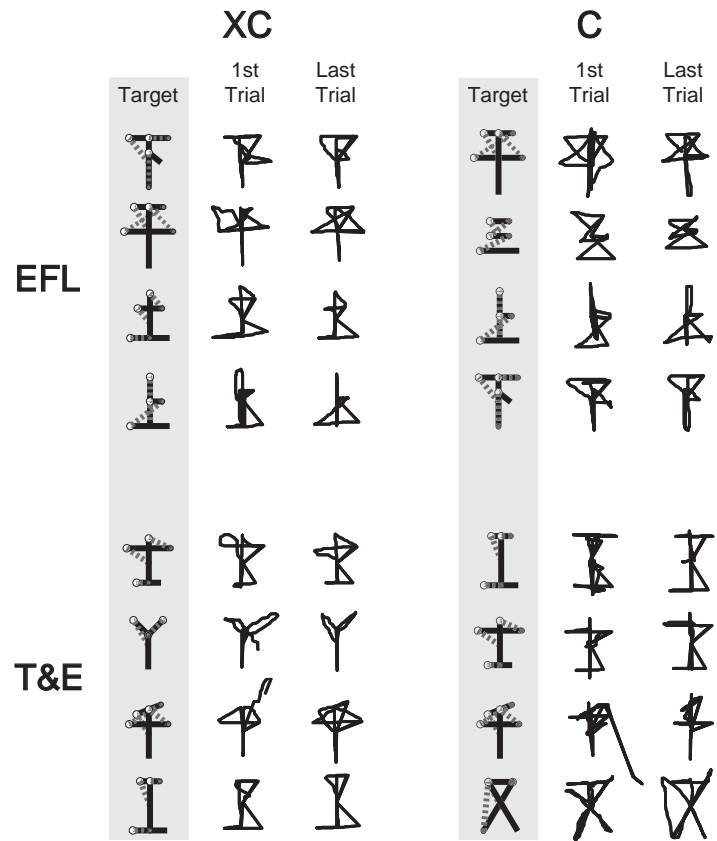


Figure 4 Examples of kinematic learning in Error Feedback (EFL) and Trial & Error (T&E) conditions

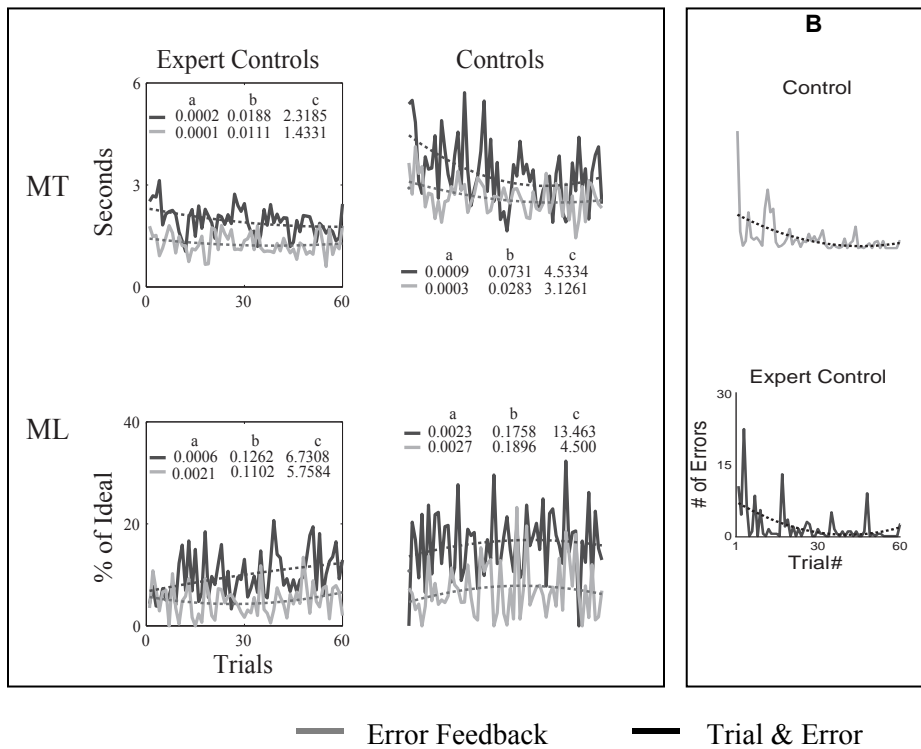


Figure 5 A-B A. Differences in Movement Time (MT) & Movement Length (ML) for Expert Controls and naïve Controls. Dotted lines are the fitted, second order polynomials ($y = ax + bx^2 + c$) for each condition. B. The number wrong per trial for Trial & Error Learning

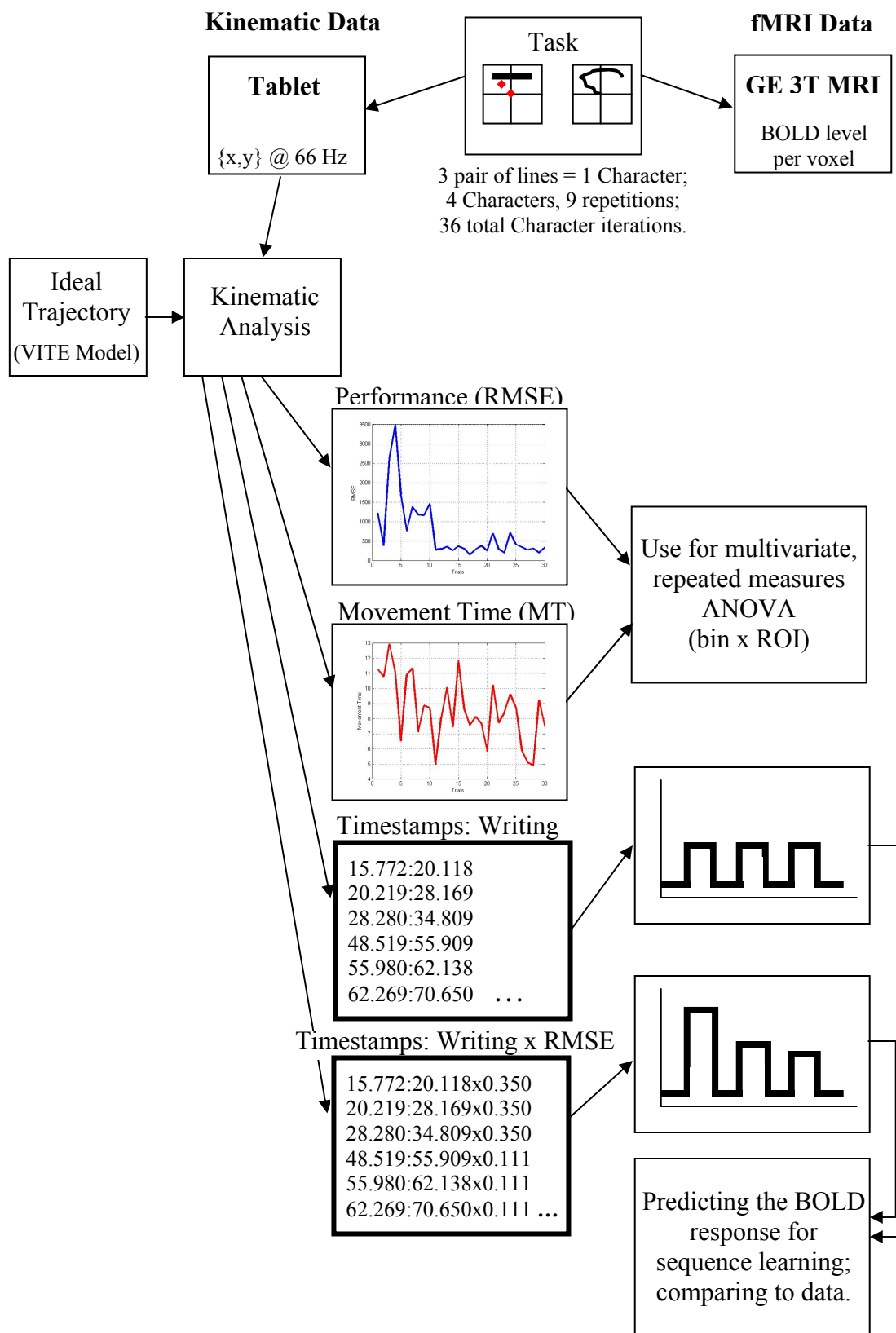


Figure 6 Kinematic data capture and statistical analysis, and collection of behavioral data for formulation of the predicted HRF

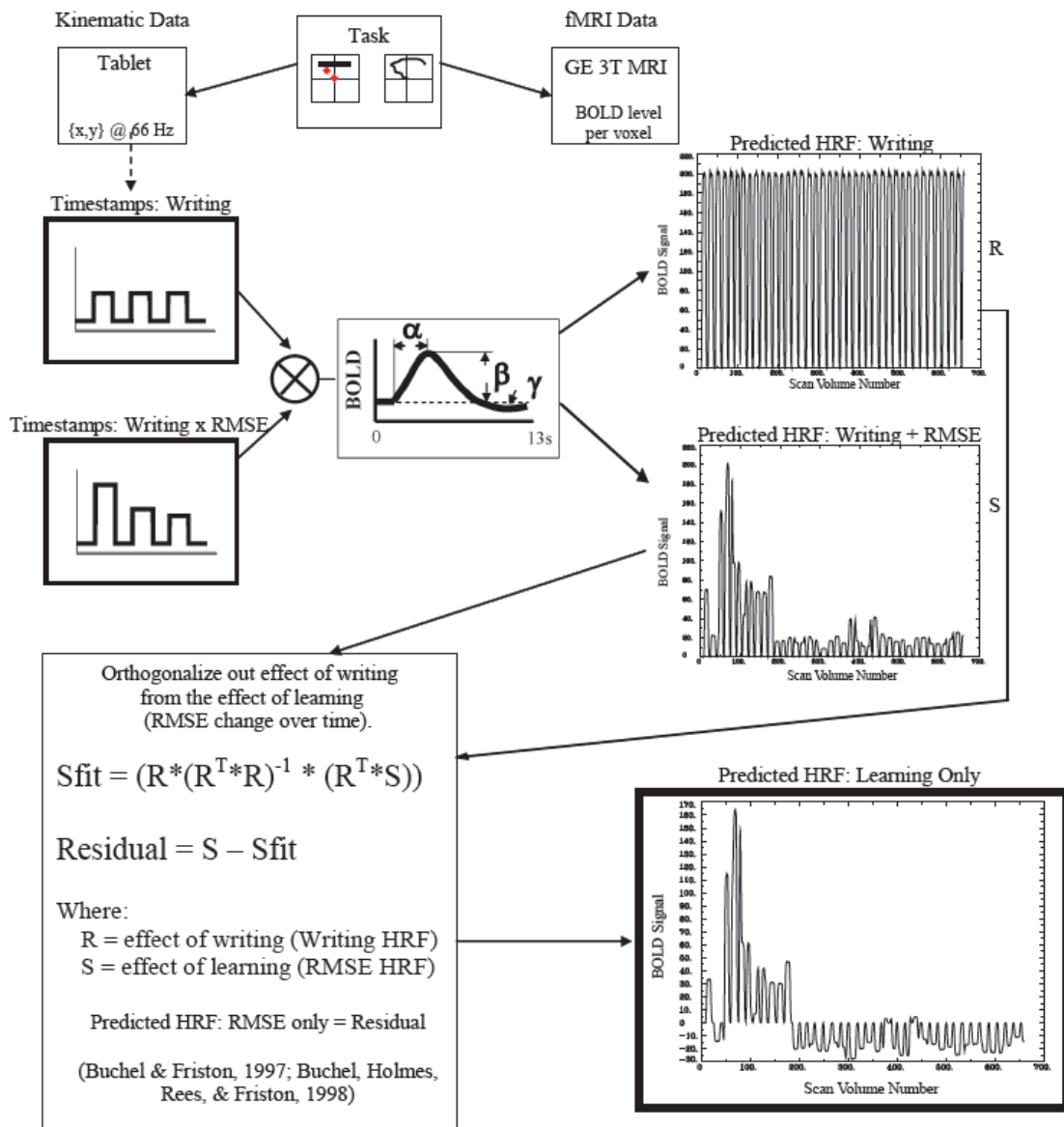


Figure 7 Development of the learning-only HRF model from the kinematic data

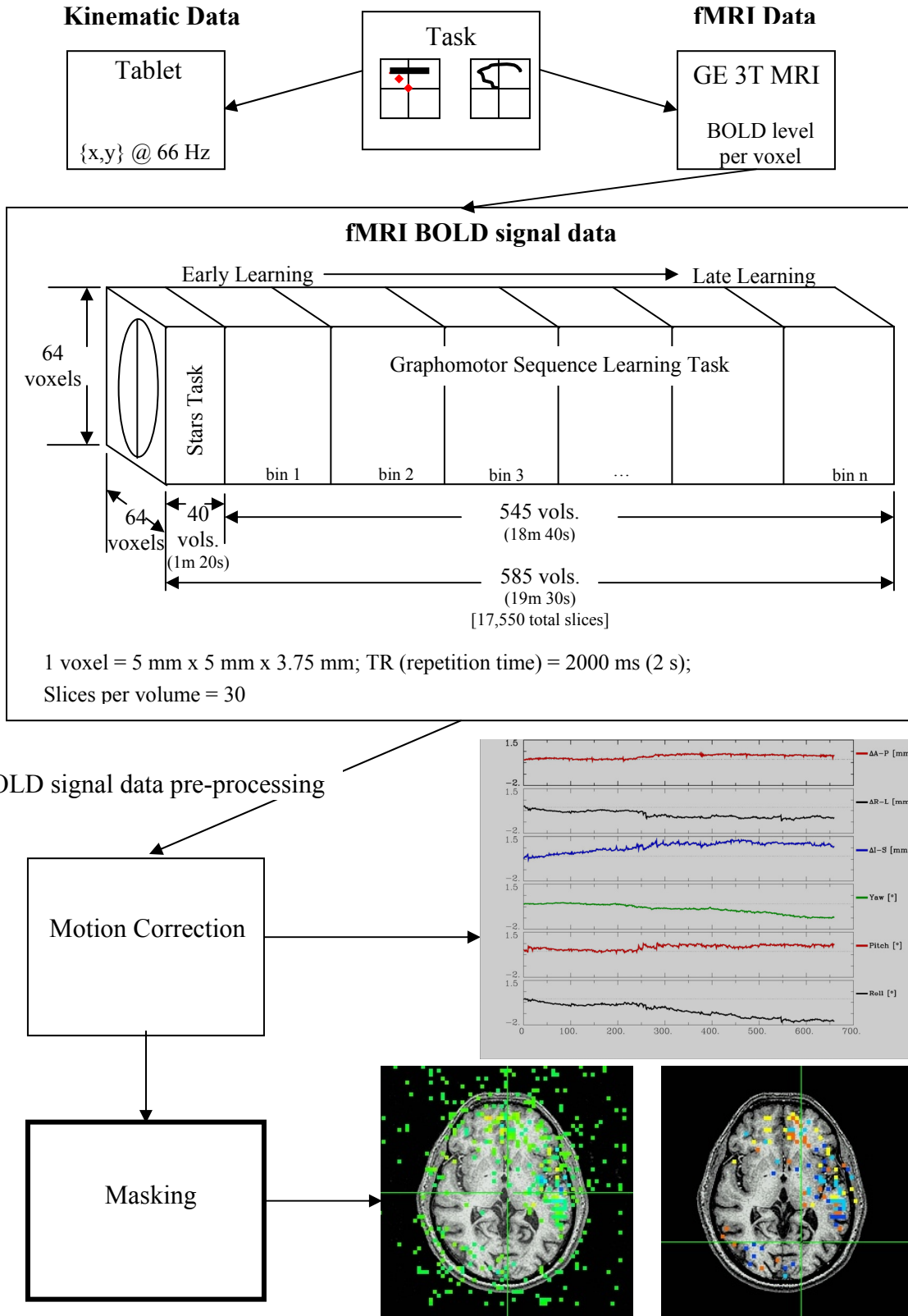


Figure 8 fMRI data collection parameters and pre-processing steps

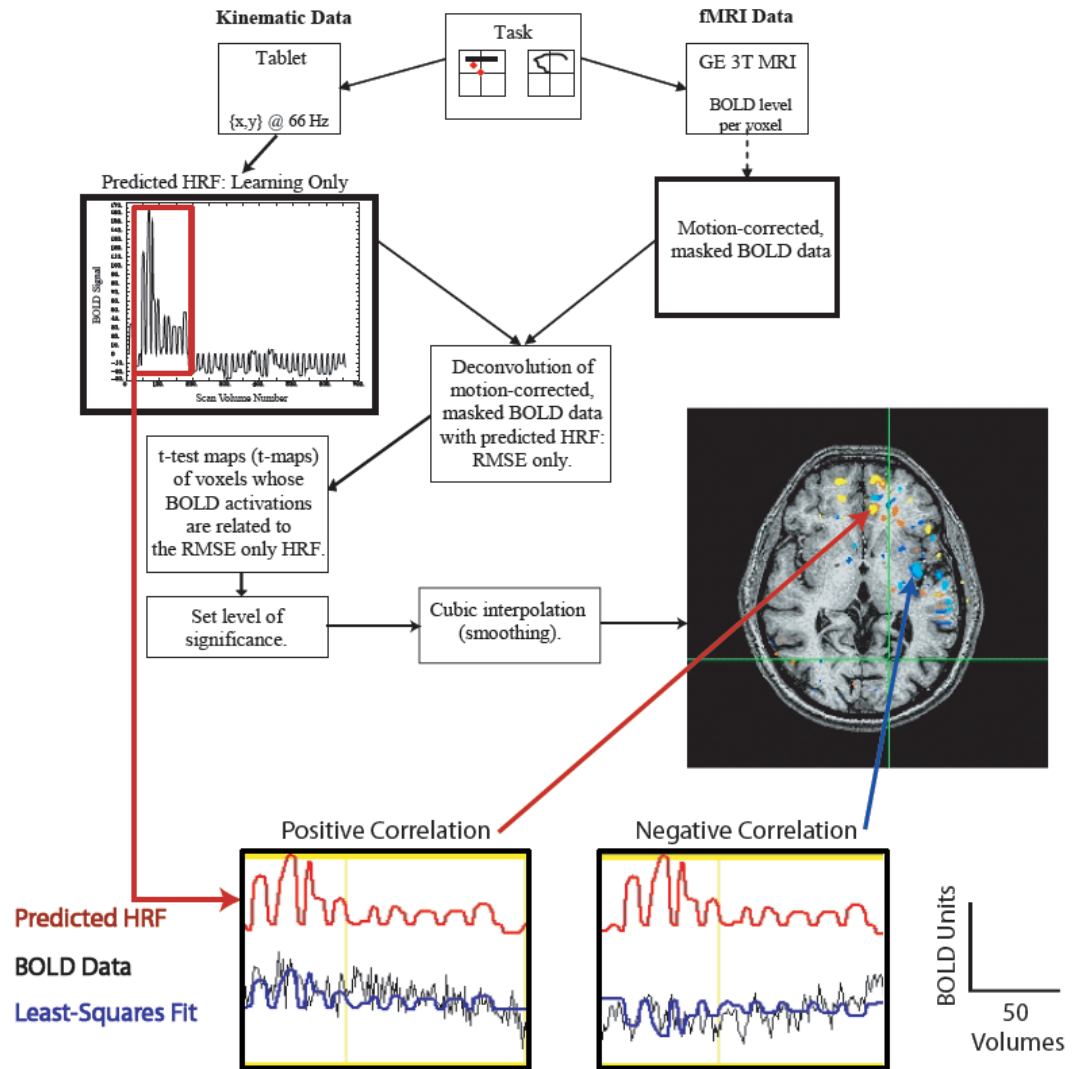


Figure 9 Use of the predicted, learning-only HRF to determine which voxel activations in the fMRI data are significantly related to motor sequence learning

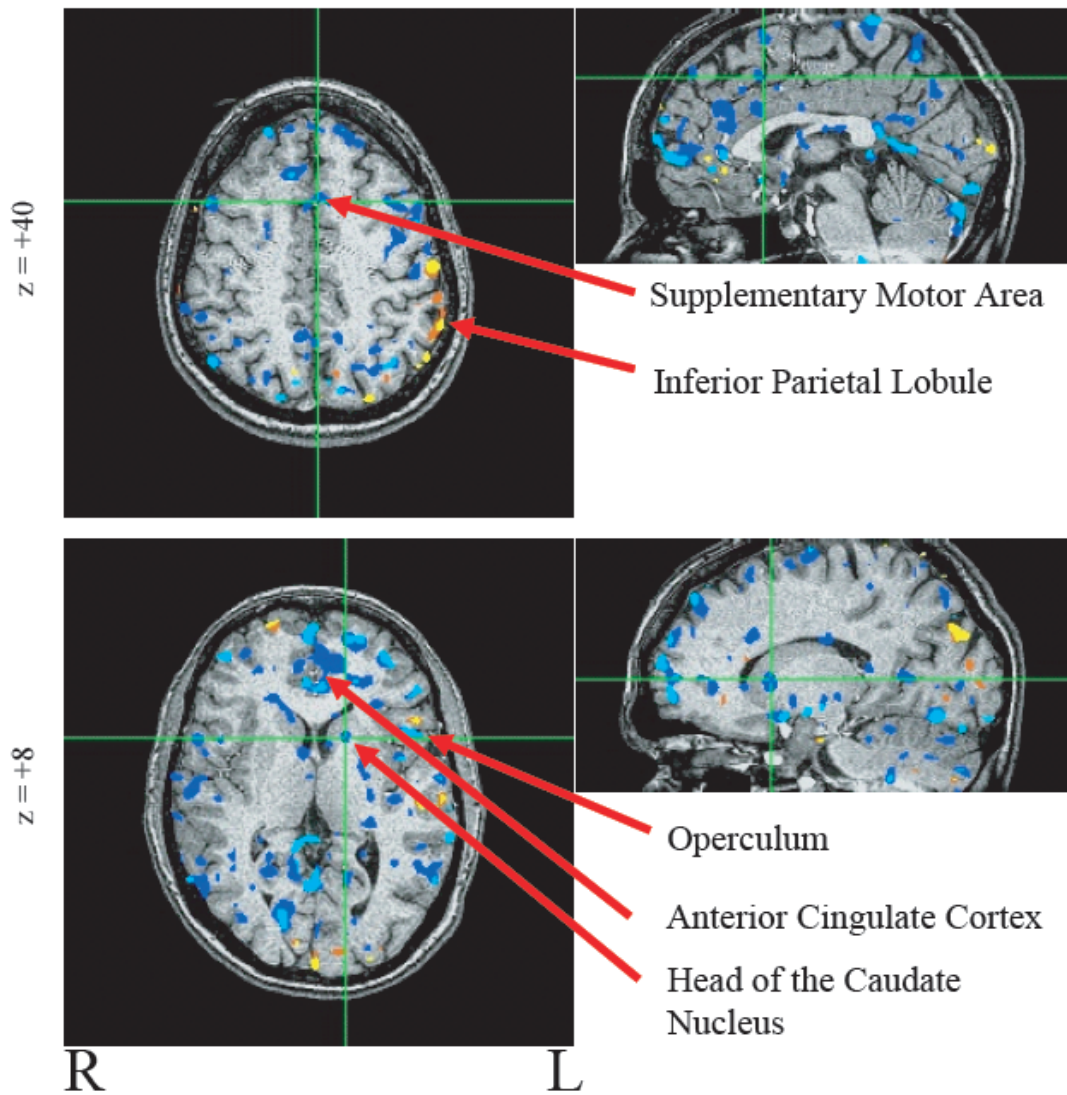


Figure 10 Functional magnetic resonance images overlaid on anatomical scans for one control subject. Activations are significantly related to the learning-only, predicted hemodynamic response function ($t=2.57$, $p=0.0104$). Yellow regions indicate voxels with a significant, positive relationship with error reduction (a measure of sequence learning); activation goes up as errors go up. Blue indicates a significant, negative relationship (activation goes up as errors go down). Images are in radiological convention (left=right)

Bibliography

- Alexander, G. E., DeLong, M. R., & Strick, P. L. (1986). Parallel organization of functionally segregated circuits linking basal ganglia and cortex. *Annu.Rev.Neurosci.*, *9*, 357-381.
- Andersen, R. A. (1997). Multimodal integration for the representation of space in the posterior parietal cortex. *Phil.Trans.R Soc.Lon.*, *352*, 1421-1428.
- Arunachalam, R., Weerasinghe, V. S., & Mills, K. R. (2005). Motor control of rapid sequential finger tapping in humans. *J Neurophysiol.*, *94*, 2162-2170.
- Battaglia-Mayer, A., Caminiti, R., Lacquaniti, F., & Zago, M. (2003a). Multiple levels of representation of reaching in the parieto-frontal network. *Cereb.Cortex*, *13*, 1009-1022.
- Battaglia-Mayer, A., Caminiti, R., Lacquaniti, F., & Zago, M. (2003b). Multiple levels of representation of reaching in the parieto-frontal network. *Cereb.Cortex*, *13*, 1009-1022.
- Battaglia-Mayer, A., Ferraina, S., Genovesio, A., Marconi, B., Squatrito, S., Molinari, M. et al. (2001). Eye-hand coordination during reaching. II. An analysis of the relationships between visuomanual signals in parietal cortex and parieto-frontal association projections. *Cereb.Cortex*, *11*, 528-544.

- Battaglia-Mayer, A., Mascaro, M., & Caminiti, R. (2006). Temporal Evolution and Strength of Neural Activity in Parietal Cortex during Eye and Hand Movements. *Cereb.Cortex*.
- Bengtsson, S. L., Ehrsson, H. H., Forssberg, H., & Ullen, F. (2004). Dissociating brain regions controlling the temporal and ordinal structure of learned movement sequences. *Eur.J Neurosci.*, *19*, 2591-2602.
- Brown, R. G., Redondo-Verge, L., Chacon, J. R., Lucas, M. L., & Channon, S. (2001). Dissociation between intentional and incidental sequence learning in Huntington's disease. *Brain*, *124*, 2188-2202.
- Buchel, C. & Friston, K. (1997). Modulation of connectivity in visual pathways by attention: Cortical interactions evaluated with structural equation modeling and fMRI. *Cereb.Cortex, Cerebral Cortex*, 768-778.
- Buchel, C., Holmes, A. P., Rees, G., & Friston, K. (1998). Characterizing stimulus-response functions using nonlinear regressors in parametric fMRI experiments. *Neuroimage*, *8*, 148.
- Bullock, D., Cisek, P., & Grossberg, S. (1998). Cortical networks for control of voluntary arm movements under variable force conditions. *Cereb.Cortex*, *8*, 48-62.
- Bullock, D. & Grossberg, S. (1988). Neural dynamics of planned arm movements: emergent invariants and speed-accuracy properties during trajectory formation. *Psychol Rev.*, *95*, 49-90.

- Burnod, Y., Baraduc, P., Battaglia-Mayer, A., Guigon, E., Koechlin, E., Ferraina, S. et al. (1999). Parieto-frontal coding of reaching: an integrated framework. *Exp.Brain Res.*, *129*, 325-346.
- Burnod, Y., Grandguillaume, P., Otto, I., Ferraina, S., Johnson, P. B., & Caminiti, R. (1992). Visuomotor transformations underlying arm movements toward visual targets: a neural network model of cerebral cortical operations. *J Neurosci.*, *12*, 1435-1453.
- Caminiti, R., Ferraina, S., & Johnson, P. B. (1996). The sources of visual information to the primate frontal lobe: a novel role for the superior parietal lobule. *Cereb.Cortex*, *6*, 319-328.
- Caminiti, R., Ferraina, S., & Mayer, A. B. (1998). Visuomotor transformations: early cortical mechanisms of reaching. *Curr.Opin.Neurobiol.*, *8*, 753-761.
- Caminiti, R., Genovesio, A., Marconi, B., Mayer, A. B., Onorati, P., Ferraina, S. et al. (1999). Early coding of reaching: frontal and parietal association connections of parieto-occipital cortex. *Eur.J Neurosci.*, *11*, 3339-3345.
- Caminiti, R. & Johnson, P. B. (1992). Internal representations of movement in the cerebral cortex as revealed by the analysis of reaching. *Cereb.Cortex*, *2*, 269-276.
- Carbon, M. & Eidelberg, D. (2006). Functional imaging of sequence learning in Parkinson's disease. *J.Neurol.Sci.*, *248*, 72-77.

- Carbon, M., Ma, Y., Barnes, A., Dhawan, V., Chaly, T., Ghilardi, M. F. et al. (2004). Caudate nucleus: influence of dopaminergic input on sequence learning and brain activation in Parkinsonism. *Neuroimage*, *21*, 1497-1507.
- Carey, J. R., Greer, K. R., Grunewald, T. K., Steele, J. L., Wiemiller, J. W., Bhatt, E. et al. (2006). Primary motor area activation during precision-demanding versus simple finger movement. *Neurorehabil. Neural Repair*, *20*, 361-370.
- Cohen, M. & Grossberg, S. (1986). Neural dynamics of speech and language coding: developmental programs, perceptual grouping, and competition for short-term memory. *Hum. Neurobiol.*, *5*, 1-22.
- Contreras-Vidal, J. L. & Buch, E. R. (2003). Effects of Parkinson's disease on visuomotor adaptation. *Exp. Brain Res.*, *150*, 25-32.
- Contreras-Vidal, J. L. & Stelmach, G. E. (1995). A neural model of basal ganglia-thalamocortical relations in normal and parkinsonian movement. *Biol. Cybern.*, *73*, 467-476.
- Contreras-Vidal, J. L., Teulings, H. L., & Stelmach, G. E. (1998). Elderly subjects are impaired in spatial coordination in fine motor control. *Acta Psychol. (Amst)*, *100*, 25-35.
- Cowie, A. P. (1986). *Concise English-Chinese, Chinese-English Dictionary*. The Commercial Press, Oxford University Press.

- Dale, A. M. & Buckner, R. L. (1997). Selective averaging of rapidly presented individual trials using fMRI. *Hum.Brain Mapp.*, 5, 329-340.
- Doyon, J. & Benali, H. (2005). Reorganization and plasticity in the adult brain during learning of motor skills. *Curr.Opin.Neurobiol.*, 15, 161-167.
- Doyon, J., Owen, A. M., Petrides, M., Sziklas, V., & Evans, A. C. (1996a). Functional anatomy of visuomotor skill learning in human subjects examined with positron emission tomography. *Eur.J.Neurosci.*, 8, 637-648.
- Doyon, J., Owen, A. M., Petrides, M., Sziklas, V., & Evans, A. C. (1996b). Functional anatomy of visuomotor skill learning in human subjects examined with positron emission tomography. *Eur.J Neurosci.*, 8, 637-648.
- Doyon, J., Penhune, V., & Ungerleider, L. G. (2003). Distinct contribution of the cortico-striatal and cortico-cerebellar systems to motor skill learning. *Neuropsychologia*, 41, 252-262.
- Doyon, J., Song, A. W., Karni, A., Lalonde, F., Adams, M. M., & Ungerleider, L. G. (2002). Experience-dependent changes in cerebellar contributions to motor sequence learning. *Proc.Natl.Acad.Sci U.S.A.*, 99, 1017-1022.
- Eliassen, J. C., Souza, T., & Sanes, J. N. (2001). Human brain activation accompanying explicitly directed movement sequence learning. *Exp.Brain Res.*, 141, 269-280.

- Elsinger, C. L., Harrington, D. L., & Rao, S. M. (2006). From preparation to online control: reappraisal of neural circuitry mediating internally generated and externally guided actions. *Neuroimage.*, *31*, 1177-1187.
- Ferraina, S., Garasto, M. R., Battaglia-Mayer, A., Ferraresi, P., Johnson, P. B., Lacquaniti, F. et al. (1997). Visual control of hand-reaching movement: activity in parietal area 7m. *Eur.J Neurosci.*, *9*, 1090-1095.
- Floyer-Lea, A. & Matthews, P. M. (2004). Changing brain networks for visuomotor control with increased movement automaticity. *J Neurophysiol.*, *92*, 2405-2412.
- Fox, M. D., Snyder, A. Z., Zacks, J. M., & Raichle, M. E. (2006). Coherent spontaneous activity accounts for trial-to-trial variability in human evoked brain responses. *Nat.Neurosci.*, *9*, 23-25.
- Friedman, L. & Glover, G. H. (2006). Report on a multicenter fMRI quality assurance protocol. *J Magn Reson.Imaging*, *23*, 827-839.
- Fujii, N. & Graybiel, A. M. (2003). Representation of action sequence boundaries by macaque prefrontal cortical neurons. *Science*, *301*, 1246-1249.
- Fujii, N. & Graybiel, A. M. (2005). Time-varying covariance of neural activities recorded in striatum and frontal cortex as monkeys perform sequential-saccade tasks. *Proc.Natl.Acad.Sci U.S.A.*

- Gardner, E. P., Babu, K. S., Reitzen, S. D., Ghosh, S., Brown, A. M., Chen, J. et al. (2006). Neurophysiology of prehension: I. Posterior parietal cortex and object-oriented hand behaviors. *J.Neurophysiol.*
- Georgopoulos, A. P. (1996). Arm movements in monkeys: behavior and neurophysiology. *J Comp Physiol [A]*, 179, 603-612.
- Georgopoulos, A. P. (1998). Online visual control of the arm. *Novartis.Found.Symp.*, 218, 147-164.
- Georgopoulos, A. P. (2000). Neural aspects of cognitive motor control. *Curr.Opin.Neurobiol.*, 10, 238-241.
- Georgopoulos, A. P., Pellizzer, G., Poliakov, A. V., & Schieber, M. H. (1999). Neural coding of finger and wrist movements. *J Comput.Neurosci.*, 6, 279-288.
- Ghilardi, M. F., Feigin, A. S., Battaglia, F., Silvestri, G., Mattis, P., Eidelberg, D. et al. (2006). L-Dopa infusion does not improve explicit sequence learning in Parkinson's disease. *Parkinsonism.Relat Disord.*
- Graybiel, A. M. (2001). Neural networks: neural systems V: basal ganglia. *Am.J Psychiatry*, 158, 21.
- Graybiel, A. M. (2004). Network-level neuroplasticity in cortico-basal ganglia pathways. *Parkinsonism.Relat Disord.*, 10, 293-296.
- Graybiel, A. M., Aosaki, T., Flaherty, A. W., & Kimura, M. (1994). The basal ganglia and adaptive motor control. *Science*, 265, 1826-1831.

- Greicius, M. D., Krasnow, B., Reiss, A. L., & Menon, V. (2003). Functional connectivity in the resting brain: a network analysis of the default mode hypothesis. *Proc.Natl.Acad.Sci.U.S.A*, *100*, 253-258.
- Greicius, M. D. & Menon, V. (2004). Default-mode activity during a passive sensory task: uncoupled from deactivation but impacting activation. *J.Cogn Neurosci.*, *16*, 1484-1492.
- Greicius, M. D., Srivastava, G., Reiss, A. L., & Menon, V. (2004). Default-mode network activity distinguishes Alzheimer's disease from healthy aging: evidence from functional MRI. *Proc.Natl.Acad.Sci.U.S.A*, *101*, 4637-4642.
- Grossberg, S. (1978). Behavioral contrast in short-term memory: serial binary memory models or parallel continuous memory models? *Journal of Mathematical Psychology.*, *17*, 219.
- Grossberg, S. & Gutowski, W. E. (1987). Neural dynamics of decision making under risk: affective balance and cognitive-emotional interactions. *Psychol Rev.*, *94*, 300-318.
- Grossberg, S. & Paine, R. W. (2000). A neural model of cortico-cerebellar interactions during attentive imitation and predictive learning of sequential handwriting movements. *Neural Netw.*, *13*, 999-1046.
- Hamzei, F., Dettmers, C., Rijntjes, M., Glauche, V., Kiebel, S., Weber, B. et al. (2002). Visuomotor control within a distributed parieto-frontal network. *Exp.Brain Res.*, *146*, 273-281.

- Hikosaka, O., Miyashita, K., Miyachi, S., Sakai, K., & Lu, X. (1998). Differential roles of the frontal cortex, basal ganglia, and cerebellum in visuomotor sequence learning. *Neurobiol.Learn.Mem.*, *70*, 137-149.
- Hikosaka, O., Nakahara, H., Rand, M. K., Sakai, K., Lu, X., Nakamura, K. et al. (1999). Parallel neural networks for learning sequential procedures. *Trends Neurosci.*, *22*, 464-471.
- Hikosaka, O., Nakamura, K., Sakai, K., & Nakahara, H. (2002a). Central mechanisms of motor skill learning. *Curr.Opin.Neurobiol.*, *12*, 217-222.
- Hikosaka, O., Rand, M. K., Nakamura, K., Miyachi, S., Kitaguchi, K., Sakai, K. et al. (2002b). Long-term retention of motor skill in macaque monkeys and humans. *Exp.Brain Res.*, *147*, 494-504.
- Honda, M., Deiber, M. P., Ibanez, V., Pascual-Leone, A., Zhuang, P., & Hallett, M. (1998). Dynamic cortical involvement in implicit and explicit motor sequence learning. A PET study. *Brain*, *121 (Pt 11)*, 2159-2173.
- Hoshi, E., Trambly, L., Feger, J., Carras, P., & Strick, P. L. (2005). The cerebellum communicates with the basal ganglia. *Nature Neuroscience, Advanced Online Publication*.
- Kitazawa, S., Goto, T., & Urushihara, Y. (1993). Quantitative evaluation of reaching movements in cats with and without cerebellar lesions using normalized integral of jerk. In N.Mano, I. Hamada, & M. R. Delong (Eds.), *Role of the*

Cerebellum and Basal Ganglia in Voluntary Movement. (pp. 11-19).

Amsterdam: Elsevier.

Koch, G., Franca, M., Mochizuki, H., Marconi, B., Caltagirone, C., & Rothwell, J. C.

(2006). Interactions between pairs of transcranial magnetic stimuli over the human left dorsal premotor cortex differ from those seen in primary motor cortex. *J Physiol.*

Lacquaniti, F., Guigon, E., Bianchi, L., Ferraina, S., & Caminiti, R. (1995).

Representing spatial information for limb movement: role of area 5 in the monkey. *Cereb.Cortex*, 5, 391-409.

Lashley, K. S. (1951). The problem of serial order in behavior. In L.A.Jeffress (Ed.),

Cerebral Mechanisms in behavior. (New York: Wiley.

Lee, J. H. & van Donkelaar, P. (2006). The human dorsal premotor cortex generates

on-line error corrections during sensorimotor adaptation. *J Neurosci.*, 26, 3330-3334.

Lehericy, S., Bardinet, E., Tremblay, L., Van de Moortele, P. F., Pochon, J. B.,

Dormont, D. et al. (2005a). Motor control in basal ganglia circuits using fMRI and brain atlas approaches. *Cereb.Cortex.*

Lehericy, S., Benali, H., Van de Moortele, P. F., Pelegriani-Issac, M., Waechter, T.,

Ugurbil, K. et al. (2005b). Distinct basal ganglia territories are engaged in early and advanced motor sequence learning. *Proc.Natl.Acad.Sci U.S.A*, 102, 12566-12571.

- Lehericy, S., Ducros, M., Krainik, A., Francois, C., Van de Moortele, P. F., Ugurbil, K. et al. (2004a). 3-D diffusion tensor axonal tracking shows distinct SMA and pre-SMA projections to the human striatum. *Cereb.Cortex*, *14*, 1302-1309.
- Lehericy, S., Ducros, M., Van de Moortele, P. F., Francois, C., Thivard, L., Poupon, C. et al. (2004b). Diffusion tensor fiber tracking shows distinct corticostriatal circuits in humans. *Ann.Neurol.*, *55*, 522-529.
- Lehericy, S. & Gerardin, E. (2002). Normal functional imaging of the basal ganglia. *Epileptic.Disord.*, *4 Suppl 3*, S23-S30.
- Marconi, B., Genovesio, A., Battaglia-Mayer, A., Ferraina, S., Squatrito, S., Molinari, M. et al. (2001). Eye-hand coordination during reaching. I. Anatomical relationships between parietal and frontal cortex. *Cereb.Cortex*, *11*, 513-527.
- Mascaro, M., Battaglia-Mayer, A., Nasi, L., Amit, D. J., & Caminiti, R. (2003). The eye and the hand: neural mechanisms and network models for oculomanual coordination in parietal cortex. *Cereb.Cortex*, *13*, 1276-1286.
- Middleton, F. A. & Strick, P. L. (1994). Anatomical evidence for cerebellar and basal ganglia involvement in higher cognitive function. *Science*, *266*, 458-461.
- Middleton, F. A. & Strick, P. L. (1997a). Cerebellar output channels. *Int Rev.Neurobiol.*, *41*, 61-82.

- Middleton, F. A. & Strick, P. L. (1997b). Dentate output channels: motor and cognitive components. *Prog.Brain Res.*, 114, 553-566.
- Middleton, F. A. & Strick, P. L. (1997c). New concepts about the organization of basal ganglia output. *Adv.Neurol.*, 74, 57-68.
- Middleton, F. A. & Strick, P. L. (1998). The cerebellum: an overview. *Trends Neurosci.*, 21, 367-369.
- Middleton, F. A. & Strick, P. L. (2000a). Basal ganglia and cerebellar loops: motor and cognitive circuits. *Brain Res.Brain Res.Rev.*, 31, 236-250.
- Middleton, F. A. & Strick, P. L. (2000b). Basal ganglia output and cognition: evidence from anatomical, behavioral, and clinical studies. *Brain Cogn*, 42, 183-200.
- Middleton, F. A. & Strick, P. L. (2001). Cerebellar projections to the prefrontal cortex of the primate. *J Neurosci.*, 21, 700-712.
- Middleton, F. A. & Strick, P. L. (2002). Basal-ganglia 'projections' to the prefrontal cortex of the primate. *Cereb.Cortex*, 12, 926-935.
- Miyachi, S., Hikosaka, O., & Lu, X. (2002). Differential activation of monkey striatal neurons in the early and late stages of procedural learning. *Exp.Brain Res.*, 146, 122-126.

- Miyachi, S., Hikosaka, O., Miyashita, K., Karadi, Z., & Rand, M. K. (1997). Differential roles of monkey striatum in learning of sequential hand movement. *Exp. Brain Res.*, *115*, 1-5.
- Muller, R. A., Kleinhans, N., Pierce, K., Kemmotsu, N., & Courchesne, E. (2002). Functional MRI of motor sequence acquisition: effects of learning stage and performance. *Brain Res. Cogn Brain Res.*, *14*, 277-293.
- Naito, E. & Ehrsson, H. H. (2006). Somatic sensation of hand-object interactive movement is associated with activity in the left inferior parietal cortex. *J. Neurosci.*, *26*, 3783-3790.
- Nakahara, H., Doya, K., & Hikosaka, O. (2001). Parallel cortico-basal ganglia mechanisms for acquisition and execution of visuomotor sequences - a computational approach. *J Cogn Neurosci.*, *13*, 626-647.
- Nakamura, K., Sakai, K., & Hikosaka, O. (1998). Neuronal activity in medial frontal cortex during learning of sequential procedures. *J Neurophysiol.*, *80*, 2671-2687.
- Nakamura, K., Sakai, K., & Hikosaka, O. (1999). Effects of local inactivation of monkey medial frontal cortex in learning of sequential procedures. *J Neurophysiol.*, *82*, 1063-1068.
- Nakamura, T., Ghilardi, M. F., Mentis, M., Dhawan, V., Fukuda, M., Hacking, A. et al. (2001). Functional networks in motor sequence learning: abnormal topographies in Parkinson's disease. *Hum. Brain Mapp.*, *12*, 42-60.

- Oreja-Guevara, C., Kleiser, R., Paulus, W., Kruse, W., Seitz, R. J., & Hoffmann, K. P. (2004). The role of V5 (hMT+) in visually guided hand movements: an fMRI study. *Eur.J.Neurosci.*, *19*, 3113-3120.
- Paine, R. W., Grossberg, S., & Van Gemmert, A. W. (2004). A quantitative evaluation of the AVITEWRITE model of handwriting learning. *Hum.Mov Sci.*, *23*, 837-860.
- Pohl, P. S., McDowd, J. M., Filion, D. L., Richards, L. G., & Stiers, W. (2001). Implicit learning of a perceptual-motor skill after stroke. *Phys.Ther.*, *81*, 1780-1789.
- Rhodes, B. J., Bullock, D., Verwey, W. B., Averbeck, B. B., & Page, M. P. (2004). Learning and production of movement sequences: behavioral, neurophysiological, and modeling perspectives. *Hum.Mov Sci.*, *23*, 699-746.
- Sakai, K., Hikosaka, O., Miyauchi, S., Takino, R., Sasaki, Y., & Putz, B. (1998). Transition of brain activation from frontal to parietal areas in visuomotor sequence learning. *J Neurosci.*, *18*, 1827-1840.
- Sakai, K., Hikosaka, O., & Nakamura, K. (2004). Emergence of rhythm during motor learning. *Trends Cogn Sci*, *8*, 547-553.
- Sakai, K., Hikosaka, O., Takino, R., Miyauchi, S., Nielsen, M., & Tamada, T. (2000). What and when: parallel and convergent processing in motor control. *J Neurosci.*, *20*, 2691-2700.

- Sakai, K., Kitaguchi, K., & Hikosaka, O. (2003). Chunking during human visuomotor sequence learning. *Exp. Brain Res.*, *152*, 229-242.
- Sakai, K., Ramnani, N., & Passingham, R. E. (2002). Learning of sequences of finger movements and timing: frontal lobe and action-oriented representation. *J Neurophysiol.*, *88*, 2035-2046.
- Schluter, N. D., Rushworth, M. F., Mills, K. R., & Passingham, R. E. (1999). Signal-, set-, and movement-related activity in the human premotor cortex. *Neuropsychologia*, *37*, 233-243.
- Seitz, R. J., Canavan, A. G., Yaguez, L., Herzog, H., Tellmann, L., Knorr, U. et al. (1994). Successive roles of the cerebellum and premotor cortices in trajectorial learning. *Neuroreport*, *5*, 2541-2544.
- Seitz, R. J., Canavan, A. G., Yaguez, L., Herzog, H., Tellmann, L., Knorr, U. et al. (1997). Representations of graphomotor trajectories in the human parietal cortex: evidence for controlled processing and automatic performance. *Eur. J Neurosci.*, *9*, 378-389.
- Siegert, R. J., Taylor, K. D., Weatherall, M., & Abernethy, D. A. (2006). Is implicit sequence learning impaired in Parkinson's disease? A meta-analysis. *Neuropsychology.*, *20*, 490-495.
- Smith, E. E., Jonides, J., & Koeppel, R. A. (1996). Dissociating verbal and spatial working memory using PET. *Cereb. Cortex*, *6*, 11-20.

- Smith, J. G. & McDowall, J. (2005). The implicit sequence learning deficit in patients with Parkinson's disease: A matter of impaired sequence integration? *Neuropsychologia*.
- Strick, P. L., Dum, R. P., & Mushiake, H. (1995). Basal ganglia 'loops' with the cerebral cortex. In M. Kimura & A. M. Graybiel (Eds.), *Functions of the Cortico-Basal Ganglia Loop*. (pp. 106-124). Tokyo: Springer.
- Strick, P. L., Hoover, J. E., & Mushiake, H. (1993). Evidence for "output channels" in the basal ganglia and cerebellum. In N. Mano, I. Hamada, & M. R. DeLong (Eds.), *Role of the Cerebellum and Basal Ganglia in Voluntary Movement*. (pp. 171-180). New York: Elsevier.
- Tanji, J. (2001). Sequential organization of multiple movements: involvement of cortical motor areas. *Annu.Rev.Neurosci.*, 24, 631-651.
- Tanji, J., Shima, K., Matsuzaka, Y., & Halsband, U. (1995). Neuronal activity in the supplementary, presupplementary, and premotor cortex of monkey. In M. Kimura & A. M. Graybiel (Eds.), *Functions of the Cortico-Basal Ganglia Loop*. (pp. 154-165). Tokyo: Springer.
- Teulings, H. L., Contreras-Vidal, J. L., Stelmach, G. E., & Adler, C. H. (1997). Parkinsonism reduces coordination of fingers, wrist, and arm in fine motor control. *Exp.Neurol.*, 146, 159-170.
- Ullen, F. & Bengtsson, S. L. (2003). Independent processing of the temporal and ordinal structure of movement sequences. *J Neurophysiol.*, 90, 3725-3735.

- Ullén, F., Bengtsson, S. L., Ehrsson, H. H., & Forssberg, H. (2005). Neural control of rhythmic sequences. *Ann.N.Y.Acad.Sci.*, *1060*, 368-376.
- Verwey, W. B. (2001). Concatenating familiar movement sequences: the versatile cognitive processor. *Acta Psychol.(Amst)*, *106*, 69-95.
- Verwey, W. B. (2003a). Effect of sequence length on the execution of familiar keying sequences: lasting segmentation and preparation? *J.Mot.Behav.*, *35*, 343-354.
- Verwey, W. B. (2003b). Processing modes and parallel processors in producing familiar keying sequences. *Psychol.Res.*, *67*, 106-122.
- Verwey, W. B. & Clegg, B. A. (2005). Effector dependent sequence learning in the serial RT task. *Psychol.Res.*, *69*, 242-251.
- Verwey, W. B. & Dronkert, Y. (1996). Practicing a Structured Continuous Key-Pressing Task: Motor Chunking or Rhythm Consolidation? *J.Mot.Behav.*, *28*, 71-79.
- Verwey, W. B. & Eikelboom, T. (2003). Evidence for lasting sequence segmentation in the discrete sequence-production task. *J.Mot.Behav.*, *35*, 171-181.
- Verwey, W. B. & Wright, D. L. (2004). Effector-independent and effector-dependent learning in the discrete sequence production task. *Psychol.Res.*, *68*, 64-70.
- Webster, W. G. (1989). Sequence initiation performance by stutterers under conditions of response competition. *Brain Lang*, *36*, 286-300.

Wise, S. P., Boussaoud, D., Johnson, P. B., & Caminiti, R. (1997). Premotor and parietal cortex: corticocortical connectivity and combinatorial computations. *Annu.Rev.Neurosci.*, 20, 25-42.

Wise, S. P., Murray, E. A., & Gerfen, C. R. (1996). The frontal cortex-basal ganglia system in primates. *Crit Rev.Neurobiol.*, 10, 317-356.